BELLCOMM, INC.
Washington, D. C. 20024

TR-69-310-1

ENTRY MONITORING SYSTEM STUDY

September 26, 1969

I. Bogner
G. Duncan
C. H. Eley, III
D. S. Lopez
S. B. Watson

Work performed for the Office of Manned Space Flight, National Aeronautics and Space Administration under Contract NASW-417.

ABSTRACT

This document reports on Phases 2 and 3 of an evaluation of the Apollo Entry Monitoring System (EMS) and supplements a prior report on Phase 1. Approximately 100 simulated Apollo entries were made by each of three pilots on Bellcomm's EMS hybrid simulator. Entry parameters consisted of various combinations of (1) five entry speeds from 36,210.fps to 40,000.fps, (2) shallow, nominal, and steep entry angles, and (3) five ranges to splashdown from 1200.nm to 2500.nm.

Phase 2 evaluated manual guidance using the EMS display to (1) maintain a safe entry with respect to skip-out and excessive g boundaries and (2) regulate the Command Module range potential by modulating the left vector so as to achieve splashdown at a specified range. The down-range errors markedly increased with range; they were primarily dependent upon range and largely independent of speed and entry angle. Generally, there was no difficulty in achieving safe and accurate manual entries to ranges up to 1700.nm, beyond which the ranges were substantially under-shot. Ranges less than 1350.nm required excessive g's and are not recommended for initial velocities greater than 38,000.fps. High speed entries are readily controllable but do require special techniques for both guided and manual entries to offset guidance anomalies. The monitoring of both primary and manual guidance can be enhanced by the use of a plot of the anticipated entry trace.

Phase 3 presented the pilots with random primary guidance malfunctions interspersed with nominal guidance over a spectrum of entry conditions and evaluated their ability to (1) diagnose failures using the EMS and (2) takeover control in the event of a failure and complete the entry. The guidance failures, introduced by means of a + or -50.% scaling error in sensed acceleration, were readily detectable in time to complete a safe entry. There were 8 false take-overs in 61 opportunities, 6 of them arising from the some-what alarming behavior of the primary guidance seen on the high speed entries.

SYNOPSIS

To evaluate the performance of the Entry Monitoring System, approximately 100 entries were flown on the Bellcomm Hybrid Entry Simulator by each of three members of the Technical Staff, who were former military test pilots.

Parameters included combinations of the following:

Velocity: 36,210., 37,000., 38,500., 40,000.fps
Flight-path Angle: -5.6°, -6.49°, -7.0°
Range: 1200., 1350., 1600., 2000., 2500.nm

Discussed in a separate memorandum, and limited to eleven entries per pilot, Phase 1 of the study provided timely support to the F Mission (Apollo 10). Entry speeds were either 36,210. or 40,000.fps; range and flight-path angle were for the most part nominal. Phase 1 type simulations were repeated as part of Phase 2 and all important findings are included as part of the Phase 2 discussion.

In Phase 2 the primary (automatic) entry guidance was assumed failed and the pilot used the Entry Monitoring System and the spacecraft Stabilization Control System to fly the complete entry. In Phase 3 the primary guidance controlled the spacecraft and the pilot observed the entry on the Entry Monitoring System and G-meter. When the pilot detected a failure in the primary guidance he assumed control and, in the same manner as in Phase 2, flew the remainder of the trajectory to the landing site. Failures -- scaling sensed acceleration by 0.5 and 1.5 -- were randomly inserted among good guided entries.

The following pertain to the Entry Monitoring System as the primary entry guidance:

1. For nominal lunar return entries -- 36,210.fps, -6.49°, 1350.nm -- the probable landing area was an ellipse centered 23.nm short and 66.nm cross-range of the target. The semimajor and semiminor axes were 33.nm and 20.nm yielding a 75.% probable landing area of 2115. sq. nm.

2. Mean down-range miss was found to be independent of velocity and flight-path angle but strongly dependent upon range for the longer ranges. For ranges of 1200. to 1600.nm, the mean down-range

miss varied from approximately 15.nm short to 35.nm short. For the 2000. and 2500.nm ranges mean down-range misses were 178.nm short and 542.nm short.

3. Mean cross-range miss, varying from 65.nm to 85.nm showed no dependence upon velocity, flight-path angle or range.

4. In no case did peak acceleration exceed 9.g.

5. Pilot violation of prescribed ground rules -- permitting an excessive g-rate or too low a minimum g -- occurred only when the pilot tried to reach the longer ranges.

6. Probable landing area increased markedly with range for the longer ranges:

Range, nm:	1200.	1350.	1600.	2000.	2500.
75.% Probable Landing Area, sq. nm:	1139.	2115.	2953.	22,458.	61,188.

The following pertain to the Entry Monitoring System as the Monitor and Backup Guidance:

1. Failures of the type simulated -- ±50.% scaling in sensed acceleration -- were readily detectable in time to complete a safe entry.

2. Following takeover, landing point control increased in difficulty with range. The frequency of cases having a down-range miss of 50.nm or more increased from 11.% to 18.% to 40.% as the range increased from 1350. to 1600. to 2000.nm.

3. Regardless of speed, in the range of 36,210. to 40,000.fps, making the 2000.nm range appeared possible only as the result of a fortunate skip or a low g, hence an unsafe trajectory.

4. False takeover in 8 of 61 good guided entries resulted from lack of pilot familiarity with the primary guidance coupled with a basic difference in guidance philosophy between the primary guidance and manual guidance using the Entry Monitoring System. There was no difficulty in satisfactorily completing the entries.

It is suggested that:

1. Range to the target be less than 1700.nm to avoid large misses during manually controlled EMS entries.

2. To avoid excessive g during the higher speed entries, a range greater than 1350.nm is desirable.

3. Spacecraft response to variations in lift at entry speeds greater than 36,210.fps is sufficiently different from nominal lunar return entries to warrant attention in astronaut training.

4. Furnishing the flight crew with a plot of anticipated entry acceleration versus velocity is advisable for higher speed entries (e.g., greater than 37,000.fps).

5. The incompatibility between the primary and backup system merits attention. Manual override during the short period where the two systems differ is an acceptable interim solution.

TABLE OF CONTENTS

TABLE OF CONTENTS (CONTINUED)

LIST OF TABLES

LIST OF ILLUSTRATIONS

PREFACE

The material presented in this document and the document covering Phase 1 represents the final reports of the Entry Monitoring System Study. The work was performed at Bellcomm using the Bellcomm Digital Entry Simulator and at Electronics Associates, Inc., Rockville, Maryland, under contract number 105,994 using the Hybrid Entry Simulator.

Considering the operational EMS man-machine system, it is to be recognized that the information developed in this and the preceeding Phase 1 report is derived from pilot performance in a simulator under laboratory fixed-base conditions. However, MSC experience indicates good correlation between pilot EMS performance under unstressed, 1-g conditions and that demonstrated during centrifuge and flight conditions.

ENTRY MONITORING SYSTEM STUDY PHASE 2 AND 3

1.0 INTRODUCTION

Based upon a real-time hybrid computer simulation, the Entry Monitoring System Study examines system performance with respect to:

1. in-flight pilot monitoring of the primary entry guidance.

2. pilot-executed entry in the event of primary guidance failure.

The work considers the nominal lunar-return speed of 36,210.fps, however emphasis is on emergency abort speeds up to 40,000.fps. *

Discussed in a separate memorandum (1) and limited to eleven entries per pilot, Phase 1 of the study provided timely support to the F Mission (Apollo 10). Entry speeds were either 36,210. or 40,000.fps; range and flight-path angle were for the most part nominal. Phase 1 type simulations were repeated as part of Phase 2 and all the important findings are included as part of the Phase 2 discussion.

Phase 2, concerned with a broad spectrum of initial conditions, and Phase 3, with failure detection, are described in this report. A sketch of the entry guidance problem, a description of the existing primary and backup guidance, and a description of the Hybrid Entry Simulation are presented in Appendix 1.

2.0 STUDY OBJECTIVES

It was the purpose of the Bellcomm Study to provide an independent assessment of performance of the EMS in the light of its tasks (2).

1. When the EMS is the primary means of entry guidance, how well does the system perform in accomplishing a safe entry? How close does the spacecraft come to the landing site?

2. Using the EMS as a monitor, can the pilot recognize failures soon enough to achieve a safe entry close to the target?

---

*In the remainder of this memorandum, the term "high speed" refers to entries with an initial velocity of 37,000.fps or greater.

3. Does the display, based upon a simplified model and only one accelerometer, mislead the pilot into assuming control when there is no failure in the primary system? If yes, what are the consequences?

To find answers, a study was performed which made use of a real-time hybrid computer simulation of Apollo entry. Included in the simulation were the programming, spacecraft mockup, and entry displays necessary to execute both automatic and manual entries. A description of the simulation appears in Appendix 1.

The material which follows discusses pilot background, the test plan, procedures, and a presentation of the results. The memo closes with a summary and conclusions.

3.0 PERSONNEL AND TRAINING

Taken from the Bellcomm Staff, pilots were selected on the basis of appropriate background.

Pilot 1 Former Naval Aviator.
1800 hours jet time.
Experience in aircraft and guided missile testing.

Pilot 2 Retired Air Force Pilot.
4800 hours pilot time, 1800 hours jet time.
Graduate of Air Force Test Pilot School.
Fighter test pilot for 5 years.

Pilot 3 Retired Naval Aviator.
3700 hours pilot time, 800 hours jet time.
Fighter weapons system test pilot for 4 years.

Following a briefing on backup guidance philosophy, the pilots trained themselves flying SCS/EMS entries.

The training period is summarized as follows:

Pilot 1: 32 entries over a 1 1/2 day period, spread over 2 days.

Pilot 2: 57 entries over a 2 day period, spread over 3 days.

Pilot 3: 50 entries over a 1 1/2 day period, spread over 3 days.

The pilots determined when they were prepared to take data.

4.0 PROCEDURES

During the Apollo CM return, the ground transmits, via voice communication, data which the Command Pilot uses in preparing for and monitoring the entry. Known as the Entry Pad, the information is recorded by hand on a form identical to that in Figure 1 except that in the flight pad, time to 100,000. ft is replaced by the time to drogue chute deployment.

Under flight conditions all pad data is generated at Mission Control by means of a digital simulation of the entry trajectory. For the study all pad data was generated on the Bellcomm Digital Entry Simulator. Each pilot was provided a notebook containing approximately 120 pad data sheets, referred to by case number, representing 60 different entries.

In Phase 2 of the study, those cases where the primary guidance was assumed failed and a manual SCS/EMS entry was to take place from the start, the pilot applied the following procedure:

1. Always roll North.
2. Roll the lift vector to the orientation designated on the pad. (All simulations were initialized lift up.)
3. At 1.5g roll lift to conform to the EMS g-onset and g-offset constraints.
4. Following pullout i.e. g decreasing, attempt to achieve a descreasing g-rate.
5. Where feasible attempt to cross the VSAT (25,500.fps) line at $2.0 \leq g \leq 5.0$.
6. At or shortly before VSAT compare range-to-go with the range potential and modulate the lift vector to null the difference.
7. For long ranges, where steps (4), (5) and (6) are not readily applicable, attempt to keep the minimum g level to greater than 0.2.

In Phase 3 of the study, those cases where the pilot was unaware of a failure in the primary guidance, the pilot monitored the G-V display, the g-meter and the two roll indicators. He assumed control only when:

1. an onset or offset violation occurred, and

2. the lift was in other than the correct direction (up or down ±15.°) depending on the type of violation.

Following takeover, he applied the procedured for a manual SCS/EMS entry.

The simulation procedure was as follows:

1. The pilot was informed of the simulation case number, thus identifying one of his Entry Pad sheets.

2. Computer and EMS initialization was performed by computer operators.

3. Because for this study the pilot performed no function prior to 0.05g, the simulations were initialized to the 0.05g state.

4. The pilot monitored the guided entry or flew an SCS/EMS entry to termination.

5. The simulation was terminated at an altitude of 100,000. ft.

6. Termination data was recorded and the pilot documented his impressions of the flight.

Drogue chute deployment occurs at approximately 25,000. ft. However, simulation aerodynamics are inaccurate at the low speeds corresponding to termination altitudes of less than 100,000. ft. In addition, the range executed below 100,000. ft. is quite small - on the order of 15.nm.

Prior to making any production runs on a given day two check cases were run. These consisted of one full lift up trajectory and one spinning entry. The hybrid simulations were accepted if the terminal latitude and longitude were within ±0.2° of a similar digital simulation for the full lift up case and within ±0.02° and ±0.1° respectively for the spinning entry. The following are the initial and terminal conditions of the digital runs:

Initial Conditions	Spinning	Full Lift Up
Altitude (ft)	399,722.	399,722.
Latitude (deg)	-18.315	-18.315
Longitude (deg)	0.0	0.0
Azimuth (deg)	98.562	98.562
Flight-Path Angle (deg)	-6.49	-1.60
Velocity (fps)	36,210.494	25,700.

Terminal Conditions	Spinning	Full Lift Up
Altitude (ft)	100,000.	100,000.
Latitude (deg)	-19.598	-19.715
Longitude (deg)	11.061	35.341
Total Range Executed (nm)	632.3	2,002.9

The mean and associated standard deviation of the Hybrid down-range miss, cross-range miss and total miss are tabulated below. Here the difference between the terminal data for hybrid and digital entries is called a miss.

Means	Spinning (21 simulations)	Full Lift Up (24 simulations)
Down-range Miss	3.075nm Short	8.871nm Short
Cross-range Miss	0.200nm North	5.439nm North
Total Miss	3.085nm	11.813nm
Standard Deviations		
Down-range Miss	1.111nm	1.128nm
Cross-range Miss	0.097nm	6.098nm
Total Miss	1.105nm	2.681nm

5.0 TEST PLAN

All entry initial conditions had the following variables fixed:

Vehicle location and heading

Latitude:	0.°
Longitude:	0.°
Azimuth:	90.°
Altitude:	400,000. ft.

Target Location

Longitude:	a function of down-range.
Latitude:	0.2° North, chosen instead of 0.° to avoid permitting computation noise to establish the initial roll direction in the primary guidance.

5.1 INPUT DATA FOR PHASE 2 - THE EMS AS THE PRIMARY MODE OF ENTRY

Table 1 is a summary of the 60 entries flown by each pilot. Summarized, the parameters at the entry interface were:

Velocity (fps): 36,210., 37,000., 38,500., 40,000.

Range (nm): 1200., 1350., 1600., 2000., 2500.

Flight-path Angle (°): Shallow (-5.6)*, Nominal (-6.49), Steep (-7.0)

The selection of sequence of cases was based upon minimizing initialization time.

Range: First parameter varied.

Flight-path Angle: Second parameter varied.

Velocity: Third parameter varied.

Except for running 1350.nm (nominal) before 1200.nm, the ranges were simulated in increasing order. Flight-path angles were simulated in the order of shallow, nominal, steep. Velocities were taken in no specific order other than nominal (36,210.fps) first.

5.2 INPUT DATA FOR PHASE 3 - THE EMS AS A MONITOR. TAKEOVER WHEN NECESSARY

Failure in the primary guidance was simulated by scaling sensed acceleration by factors of 0.5 and 1.5. While one of these factors was in the simulation from the start, the pilot was unaware that a failure existed. This was accomplished by interspersing good guided entries in the sequence. The parameters included:

Velocity (fps): 36,210., 37,000., 38,500., 40,000.

Range (nm): 1350., 1600., 2000.

Flight-path Angle (°): -6.49

Scaled sensed acceleration: 1.

1.5 (+50.% scaling)

0.5 (-50.% scaling)

Prior to each range sequence involving a velocity and flight-path angle, the pilot observed three good guided entries: one for each range. Thus prior to the data runs he became aware of the G-V profile and associated roll history he would experience provided the guidance were not failed. Table 2 presents the nominal run sequence for this phase.

*The PGNCS, for 40,000.fps, -5.6°, 1200.nm, overshot the target by approximately 90.nm.

5.3 RECORDED DATA

1. Pilot comments on Entry Pad.
2. Termination latitude and longitude as read from the digital printout.
3. Key accelerations read by an operator from the analog during the run:
   - -peak g.
   - -g at satellite velocity.
   - -minimum g.
4. EMS G-V trace with takeover point noted. A pip appeared on the trace automatically when the pilot switched from the primary guidance to the SCS.
5. EMS range-to-go at termination.
6. Strip chart recordings as a function of time:
   - -altitude.
   - -latitude.
   - -longitude.
   - -dynamic pressure.
   - -3 aerodynamic angles.
   - -3 Euler angles.
   - -body roll rate and yaw rate.
   - -roll about the velocity vector.
   - -point of takeover via a step on the chart.

6.0 THE EMS AS THE PRIMARY ENTRY GUIDANCE: PHASE 2 RESULTS

Data is discussed from two points of view: miss distances statistics associated with velocity, flight-path angle and range as the parameters, and pilot performance with respect to safety. In all the work that follows, a positive down-range miss or error is an overshoot; a positive cross-range miss means the spacecraft is South of the target.

6.1 EMS LANDING AREA STATISTICS*

Among the parameters -- velocity, flight-path angle and range -- down-range miss was least dependent upon velocity. The data was therefore divided into the 15 groups in Table 3, each group having a common range and flight-path angle.

*The work on statistical tests here and in Appendix 4 was performed with the assistance of H. J. Bixhorn.

Values of the cross-range and down-range miss in each group were tested for normality using the Kolmogorov-Smirnov statistic. In each case the hypothesis that the data came from a normal population with mean and variance equal respectively to the $\bar{x}$ and σ^2 obtained from the data was accepted. Because of the small number of data points in each sample (12 points in 14 groups, 9 points in one group), it is possible that deviations from normality exist but go undetected. However, until data from further simulations give evidence to the contrary, down-range and cross-range miss are each assumed to be normally distributed.

The data can be examined as a function of only one variable: velocity, flight-path angle or range. In this form, the data tabulated in Tables 4, 5 and 6, is plotted in Figures 2, 3 and 4.

Note however that in Table 5 and Figure 3, where flight-path angle is the parameter, data for the two long ranges -- 2000. and 2500.nm -- are tabulated and plotted separately. This was necessary because miss was so range dependent for the long ranges. Ignoring any changes less than 10.nm Tables 4, 5 and 6 and Figures 2, 3 and 4 may be summarized as follows:

Parameter	Magnitude of Mean Miss (nm)		
	Total	Down-range (Short)	Cross-range (North)
V_{fps}			
36,210. - 40,000.	$\approx$200.	155. - 170.	65. - 85.
$\gamma°$			
-5.6 - -7.0			
a	$\approx$80.	15. - 30.	70. - 80.
b	295. - 480.	265. - 470.	70. - 90.
R_{nm}			
1200. - 2500.	70. - 550.	15. - 540.	70. - 85.

a based upon 1200., 1350., and 1600.nm.

b based upon 2000. and 2500.nm.

Tests were performed to determine how down-range miss varied with range and flight-path angle. Cross-range miss was not tested since the indication of a relationship between it and any of the parameters was quite weak. Results from the Wilcoxon test gave strong indication that down-range miss increased by more than 10.nm when range was increased from 1600. to 2000.nm and from 2000. to 2500.nm. There was no indication that the miss increased by more than 10.nm for other pairs of values of range or for any pair of flight-path angles.

In summary the graphical data suggests that miss increases only with range. Statistical testing supports this hypothesis, but only for the longer ranges.

The probability of landing within an ellipse is found by noting that:

$$\frac{X^2}{\sigma_x^2} + \frac{Y^2}{\sigma_y^2}$$

is distributed as χ_2^2 if X (down-range miss) and Y (cross-range miss) are independently normally distributed with zero mean. Making this assumption, the probability of falling within the ellipse:

$$\frac{X^2}{\sigma_x^2} + \frac{Y^2}{\sigma_y^2} \leq 2.773$$

is 0.75.*

The impact areas based on these figures are plotted in Figure 5 for the three flight-path angles and given ranges. The data is from Table 3.

The ellipses of Figure 5 illustrate:

1. the difficulty in reaching the long range targets, and
2. the difficulty in locating the spacecraft for these ranges.

*The corresponding numbers for .50 and .995 are 1.356 and 10.597.

A study was recently completed at MSC(3) in which one goal was to establish the landing area for entries when the EMS was used as the primary entry guidance. The model and initial conditions of that study and this one were similar enough to suggest a comparison. Table 7 presents results from the two simulations. Note that the Bellcomm results combine four speeds while the MSC study is based on the one nominal lunar return speed.

Consider the ratio of each of the nine pairs of down-range and cross-range means. For example for Case 1 the down-range ratio is 1.62; the cross-range ratio is 0.87. The average ratio for the nine down-range cases is 1.66; for the cross-range cases, 0.73. The corresponding standard deviations are 1.11 and 0.23. One can infer only that the two simulations produce results of similar magnitudes.

In summary, for the nominal case: 36,210.fps, -6.49°, 1350.nm, the 75. percent probable landing area is an ellipse centered at -23.nm down-range and 66.nm North of the target. The semimajor and semiminor axes are 33.nm and 20.nm, yielding a 75. percent probable landing area of 2115. sq. nm. With range as the parameter and increasing, the ellipse center falls increasingly short of the target but remains at about the same cross-range. The probable landing area increases markedly as the range increases beyond 1600.nm.

There still remains the question of how safe were the SCS/EMS entries of Phase 2.

A study of the G-V traces and trajectory data summaries was made to determine the following:

1. Did the peak acceleration exceed 10.g?
2. Did the minimum g equal or fall below 0.2?
3. Under what circumstances did offset tangencies occur?

For no entry did the acceleration exceed 9.g.

In 17 entries minimum g equal to or less than 0.2g occurred in the skip portion below VSAT. In all but three cases the reason was pilot desire to make the 2000.nm or 2500.nm range. Exceptions were as follows:

1. Case 19: 36,210.fps, -6.49°, 1600.nm

   The pilot permitted himself too much range potential which he later unloaded.

2. Case 22: 36,210.fps, -7.0°, 1350.nm

3. Case 24: 36,210.fps, -7.0°, 1600.nm

   The pilots wanted range potential to overcome the loss of range capability: a situation resulting from the steep entry into the high g region.

There were a number of offset tangencies, all grouped into one of two areas:

1. Tangencies in the higher g region, shortly after pullout. There was a failure to roll down soon enough. This permitted greater range potential. (31 entries)
2. Tangencies in the low g region below VSAT. The intent was to gain range potential. (16 entries)

In summary:

1. High g was no problem.
2. Low g, and offset tangencies in the low g region, were due to pilot effort to make long ranges. Sensitivity of the landing point to the exit conditions resulted in a large probable landing area.
3. An offset tangency in the high g region, due to a desire to make range, was not of itself dangerous. With lift down as confirmed by the reverse curvature of the G-V trace, skip was not impending.
4. A few of the low g trajectories and offset tangencies were due to:
   a. a lapse in pilot skill.
   b. pilot urge to experiment, even while generating data.

7.0 THE EMS AS A MONITOR AND AS THE BACKUP GUIDANCE: PHASE 3 RESULTS

Appendix 3 contains the G-V traces, trajectory data and pilot comments for each of 44 entries flown by the pilots. The +50.% and -50.% failures indicate the PGNCS roll commands were based upon a sensed acceleration which was 1.5 times or 0.5 times the true sensed acceleration. The ±50.% figure, frequently used in simulated entry guidance failures, results in an entry which is distinguishably different from a normal guided entry.

The pilot detected failures with the aid of the G-Meter, the EMS and his PAD data sheet. For those entries requiring an initial lift down, early detection was possible:

1. Roll reversal to lift up -- nominally at 1.5g -- occurred earlier (+50.%) or later (-50.%).

2. The change in roll reversal timing resulted in a peak g which was higher (-50.%) or lower (+50.%) than the PAD figure.

For entries with initial roll full up, the failure became evident at or following pullout:

1. A -50.% failure for the high velocity cases resulted in a sustained negative roll command at pullout. For the lower velocity cases, the constant drag phase following pullout maintained a g level higher than the PAD reference drag level.

2. A +50.% failure produced an offset tangency following pullout. Confirmation was obtained by the large excess range potential prior to VSAT.

A review of Table 8, the summary of terminal miss data of Appendix 3, reveals the extremes in terminal miss. The large variations in down-range miss indicate that the data is not from a homogeneous population; a computed mean or standard deviation is therefore of questionable value.

A more useful approach is to consider the percent of all cases in which the down-range miss exceeds a specific value. Consider the following:

	RANGE		
	1350.nm	1600.nm	2000.nm
Number of Entries	27	28	25
Down-range miss > 50.nm	3 (11.%)	5 (18.%)	10 (40.%)
Down-range miss >100.nm	1 (4.%)	4 (14.%)	7 (28.%)

The inference is that miss increases with range. This becomes obvious as the range steps from 1600.nm to 2000.nm. Now consider velocity as the parameter:

VELOCITY

	36,210.fps	37,000.fps	38,500.fps	40,000.fps
Number of Entries	20	18	19	23
Down-range miss > 50.nm	9 (45.%)	3 (17.%)	1 (5.%)	5 (22.%)
Down-range miss >100.nm	7 (35.%)	2 (11.%)	1 (5.%)	2 (9.%)

The figures suggest that landing point control is somewhat easier at the higher speeds.

When we consider the misses by failure, there appears to be little difference between the two types.

	-50% Failure	+50% Failure
Number of Entries	36	36
Down-range error > 50.nm	10 (28.%)	8 (22.%)
Down-range error >100.nm	6 (17.%)	6 (17.%)

Acceleration data in Table 8 shows that in no case did the peak acceleration exceed 9.g. Minimum g equal to or less than 0.2 occurred in 11 cases. Almost all were by design; the pilot wanted to make a 1600. or 2000.nm range.

The termination and trajectory data of Table 8, the G-V trace, and the pilot comments for each case were studied in an effort to generate a pattern. The results, presented in Table 9, represent a summary which combines related cases under the following categories:

a. Indication of Failure

b. Safety

c. Landing Point Control

Salient points are as follows:

1. Failures of the type simulated were readily detectable in time to execute a safe entry.

2. Following a detected failure, landing point control increased in difficulty with an increase in range.

3. For failures at speeds of 36,210.fps and 37,000.fps, the 2000.nm range was not made accurately except as the result of a fortunate skip.

4. For failures at speeds of 38,500.fps and 40,000.fps it appeared easier to make the 2000.nm range. Pilot philosophy -- more or less conservative -- and pilot skill were important factors.

5. The -50% failures led to an early loss in range capability. This resulted in a predominance of large undershoots for combinations of lower speeds and longer ranges.

6. The +50% failures resulted in an early excess range capability. Large overshoots occurred for the two shorter ranges. For the 2000.nm range there were a significant number of large undershoots due to conservative guidance technique.

7. There were 8 false takeovers in a total of 61 good guided entries. These resulted from a lack of experience with the PGNCS coupled with a basic incompatibility between the PGNCS and the EMS. Following takeover there was no difficulty in completing a safe entry to the target area.

8.0 PILOT TECHNIQUE FOR HIGH SPEED SCS/EMS ENTRIES

Pilot technique for EMS entries at velocities greater than 37,000.fps varied with each pilot, depending upon his philosophy. However, in all cases the technique differed from what the pilot used during entry at nominal velocities. This is not to imply that the degree of difficulty increased with velocity, but it was found that a straightforward SCS/EMS procedure permitted a safe, smooth transition from the start of the entry to VSAT.

As the entry velocity increased so did the effectiveness of the spacecraft L/D, hence the ability to control g loads increased. Simulator experience indicated control increased markedly above 38,000.fps; furthermore, so did the risk of over-controlling -- a pitfall which had to be avoided to accomplish a smooth, safe SCS/EMS entry.

To keep from over-controlling the pilot avoided large changes in bank angle, particularly prior to VSAT. Full lift up or full lift down were not used where control reversals were expected. For inertial flight-path angles equal to or steeper than -6.49°, a good technique prior to VSAT is the following "one-two" procedure:

1. Hold initial lift vector at full lift up from the start of entry to maximum g.

2. At peak g execute a crisp roll to 105.° - 115.°, using ±10.° for minor corrections; maintain this attitude to VSAT.

If the roll is performed correctly, the g load decreases from pullout to VSAT at a smooth and managable rate, crossing VSAT at 3.-4.g. The procedure is easy to follow but note that the roll to 105.° - 115.° must come as soon as maximum g is reached. Regardless of the magnitude of the bank angle, the maximum permissible delay in rolling down is 3 or 4 seconds. Hesitating any longer, the pilot stands a good chance of skipping out -- even with full lift down. A 4 second delay in rolling down produces low g's (0.8 to 1.8) in the region of 28,500. to 27,000.fps, a state which can give the pilot a few anxious moments.

For inertial flight-path angles more shallow than -6.49°, the initial lift vector may be down instead of up. The shallower the angle, the longer the lift down attitude is held in order to reach the proper g loading. At 3.g a roll to 90.° - 95.° bank angle, using ±10.° corrections, will maintain a smooth 3.-4.g to VSAT.

Simulator experience showed that except for entries at shallow flight-path angles, higher than nominal entry velocities did not necessarily result in greater range capability. As with nominal entry velocities, the ability to consistently range to greater than 1700.nm depended upon pilot technique and good fortune. The important factor in ranging was the slope of the EMS trace approaching VSAT. For ranges of 1500.nm or greater, independent of the initial flight-path angle, the EMS trace should approach VSAT at a constant g, or preferably a decreasing but safe g rate. To do this, pull up can be initiated at 26,500.fps. However, to avoid the danger of going exo-atmospheric the G-V trace should cross VSAT at 2.5g or greater.

High-speed short-range entries using PGNCS or SCS/EMS control may be physically uncomfortable due to the relatively high g load required for much of the entry. To range to 1200.nm from an initial velocity of 38,500.fps, one must maintain 4.5 to 6.5g until velocity decreases to 11,000.fps. Longer range targets reduce or eliminate the problem.

Summarizing, due to the increase in response, the pilot will find high-speed SCS/EMS entries easier than nominal entries only if changes in bank angle are kept to a minimum, roll reversals are avoided, and the range is 1350.nm or greater.

9.0 PGNCS-EMS INCOMPATIBILITY

The Constant Drag guidance of the PGNCS, described in Appendix 1, Section A2.1.2.7 and flow-charted in Figure A1-13, is the source of the PGNCS-EMS incompatibility. Following pullout, the PGNCS inhibits lift down, calling instead for a 90.° roll until the deceleration reduces to less than 5.44g. For high speed entries, with pullout accelerations up to 8.g, some time elapses before 5.44g is reached. The combination of the resulting offset tangency and roll held at 90.° for a few seconds is enough incentive for the pilot to take over. Table 10 lists the guided entries in Phase 2 which exhibited the 90.° hold.

There are a number of ways of coping with the problem:

1. The pilot can be educated to wait out the delay in rolling full down.

2. A less unnerving approach is that the pilot override the PGNCS using the SCS and roll full down for the short period between pullout and 5.44g.

3. Modification of the EMS offset pattern is possible, and should be evaluated.

4. Modification of the PGNCS is a possibility.

Along the lines of modifying the PGNCS, one approach is to increase the lift down threshold to greater than 5.44g. Another, the subject of an investigation by the authors of this paper, is to consider drag rate in the decision to lift down. Figure 6 presents the flow diagram for a possible Constant Drag logic.

Drag rate is computed as:

$$\frac{dD}{dt} = -\frac{D}{HS}\dot{R} - \frac{2D^2}{V}$$

D = Drag, fps^2.

HS = Atmospheric Scale Height, 28,500.ft.

$\dot{R}$ = Altitude Rate, fps.

V = Inertial Velocity, fps.

Lift down is permitted only if the drag rate is sufficiently negative. Figure 7 contains the G-V traces and roll histories for one of the cases simulated: 38,500.fps, -6.49°, 1350.nm. The G-V trace is improved -- though not spectacularly -- but most important, the roll decreases smoothly to 180.°. The matrix of initial conditions of Phase 2,

Velocity: 36,210., 37,000., 38,500., 40,000.fps

Flight-path angle: -5.7°, -6.49°, -7.0°

Range: 1200., 1350., 1600., 2000., 2500.nm

were used in connection with the following models and environments:

L/D: 0.25, 0.291, 0.33

Atmosphere: 1962 Standard.
July 60.° N Warm.
January 60.° N Cold.

to compare COLOSSUS 2 with the suggested revision. The 1,080 entries were evaluated, and all indications were that the suggested revision alleviated the incompatibility without adversely affecting performance.

10.0 SUMMARY AND CONCLUSIONS

10.1 PHASE 2 - THE EMS AS THE PRIMARY ENTRY GUIDANCE

1. For nominal lunar return entries -- 36,210.fps, -6.49°. 1350.nm -- the probable landing area was an ellipse centered 23.nm short and 66.nm cross-range of the target. The semimajor and semiminor axes were 33.nm and 20.nm, yielding a 75.% probable landing area of 2115.sq.nm.

2. Mean down-range miss for all ranges considered collectively appeared independent of velocity, varying from 170.nm to 155.nm (short) as the velocity increased from 36,210.fps to 40,000.fps.

3. Mean down-range miss for the short ranges (1200. to 1600.nm), was essentially independent of flight-path angle, varying from 15. to 30.nm short as the flight-path angle varied from -5.6° to -7.0°. For the two long ranges (2000. to 2500.nm) the mean down-range miss varied from 265. to 470.nm short for the same span of flight-path angles.

4. Mean down-range miss increased from 15.nm to 540.nm (short) as the range increased from 1200. to 2500.nm.

5. Mean cross-range miss, varying from 65.nm to 85.nm, showed no dependence upon velocity, flight-path angle, or range.

6. In no case did the peak acceleration exceed 9.g.

7. Offset tangencies and low acceleration levels -- between 0.2 and 0.0g -- occurred only when the pilots were trying to reach the longer range targets.

8. For ranges greater than 1600.nm the probable landing area increased markedly with range:

Range, nm:	1200.	1350.	1600.	2000.	2500.
75.% Probable Landing Area, sq. nm:	1139.	2115.	2953.	22,458.	61,188.

10.2 PHASE 3 - THE EMS AS THE MONITOR AND BACKUP GUIDANCE

1. Failures of the type simulated -- ±50.% scaling in sensed acceleration -- were readily detectable in time to complete a safe entry.

2. Following takeover, landing point control increased in difficulty as the range increased. The percent of which the down-range miss was 50.nm or greater increased from 11.% to 18.% to 40.% as the range increased from 1350. to 1600. to 2000.nm.

3. At 36,210. and 37,000.fps, making the 2000.nm range was possible only as the result of a fortunate skip trajectory.

4. It appeared easier to make the 2000.nm range at entry speeds of 38,500. and 40,000.fps, provided the pilot flew a less than conservative trajectory, i.e. low g's after VSAT.

5. While -50.% scaling failure led to early loss in range capability and the +50.% failure led to early excess range capability, there was no clear indication that one was easier to handle than was the other.

6. False takeover occurred in 8 of 61 good guided entries. Takeover resulted from a lack of pilot experience with the PGNCS coupled with a basic incompatibility between the PGNCS and the EMS. There was no difficulty in completing a safe entry to the target area.

11.0 RECOMMENDATIONS

1. Range to the target be less than 1700.nm to avoid large misses during manually controlled EMS entries.

2. To keep the acceleration time history within reasonable limits during high speed entries, ranges greater than 1350.nm are desirable.

3. Spacecraft response to variations of lift during high speed entries are sufficiently different from nominal lunar return entries to warrant attention in astronaut training. The approach described in the Pilot Techniques section is a suggested procedure for manual entry guidance.

4. Furnishing the flight crew with a plot of anticipated acceleration versus velocity is advisable for both automatic and manually controlled entries at speeds greater than 37,000.fps.

5. The PGNCS-EMS incompatibility is a problem which merits attention. Manual/SCS override during the PGNCS 90.° hold following pullout is an acceptable interim solution.

I. Bogner

G. Duncan

C. H. Eley, III

D. S. Lopez

S. B. Watson

1034-IB
1024-GD
2032-CHE-bsb
1024-DSL
2014-SBW

Attachments

REFERENCES

Bogner, I., G. Duncan, C. H. Eley, III, D. S. Lopez, and S. B. Watson, Entry Monitoring System Study Phase 1, Bellcomm Technical Memorandum, TM-69-2014-7, June 26, 1969.

Bogner, I., and S. B. Watson, Entry Monitoring System Simulation Study Plan, Bellcomm Internal Document B69 03075, March 21, 1969.

Ferland, R., and R. Edwards, Reentry Trajectory Control Using the Entry Monitoring System, NASA/MSC Internal Note Number 69-FM-146, May 15, 1969.

TABLE 1

PHASE 2 PARAMETERS

	Velocity (fps)	Range (nm)	Initial Flight-path Angle (deg) Shallow	Nominal	Steep
1.	36,210.	1350.	-5.6	-6.49	-7.0
2.	36,210.	1200.	-5.6	-6.49	-7.0
3.	36,210.	1600.	-5.6	-6.49	-7.0
4.	36,210.	2000.	-5.6	-6.49	-7.0
5.	36,210	2500.	-5.6	-6.49	-7.0
6.	37,000.	1350.	-5.6	-6.49	-7.0
7.	37,000.	1200.	-5,6	-6.49	-7.0
8.	37,000.	1600.	-5.6	-6.49	-7.0
9.	37,000.	2000.	-5.6	-6.49	-7.0
10.	37,000.	2500.	-5.6	-6.49	-7.0
11.	38,500.	1350.	-5.6	-6.49	-7.0
12.	38,500.	1200.	-5.6	-6.49	-7.0
13.	38,500.	1600.	-5.6	-6.49	-7.0
14.	38,500.	2000.	-5.6	-6.49	-7.0
15.	38,500.	2500.	-5.6	-6.49	-7.0
16.	40,000.	1350.	-5.6	-6.49	-7.0
17.	40,000.	1200.	-5.6	-6.49	-7.0
18.	40,000.	1600.	-5.6	-6.49	-7.0
19.	40,000.	2000.	-5.6	-6.49	-7.0
20.	40,000.	2500.	-5.6	-6.49	-7.0

TABLE 2

NOMINAL RUN SEQUENCE FOR PHASE 3

Velocity = 36,210.fps

	Range (nm)	Failure
1)	1350.	+50.%
2)	2000.	no failure
3)	1600.	-50.%
4)	1600.	no failure
5)	2000.	+50.%
6)	1600.	no failure
7)	2000.	-50.%
8)	1350.	no failure
9)	1600.	+50.%
10)	1350.	-50.%

Velocity = 37,000.fps

	Range (nm)	Failure
1)	2000.	+50.%
2)	1600.	no failure
3)	1350.	no failure
4)	1350.	-50.%
5)	2000.	no failure
6)	1600.	-50.%
7)	1600.	+50.%
8)	2000.	-50.%
9)	1350.	no failure
10)	1600.	no failure
11)	1350.	+50.%
12)	1350.	no failure

Velocity = 38,500.fps

	Range (nm)	Failure
1)	1600.	-50.%
2)	1350.	+50.%
3)	2000.	-50.%
4)	1600.	no failure
5)	1350.	-50.%
6)	2000.	no failure
7)	1600.	no failure
8)	2000.	+50.%
9)	1350.	no failure
10)	1600.	+50.%
11)	1350.	no failure

Velocity = 40,000.fps

	Range (nm)	Failure
1)	2000.	+50.%
2)	1600.	-50.%
3)	1600.	no failure
4)	1350.	-50.%
5)	2000.	no failure
6)	1350.	no failure
7)	1600.	+50.%
8)	2000.	-50.%
9)	1350.	+50.%
10)	1600.	no failure
11)	1350.	no failure

TABLE 3

RANGE AND FLIGHT-PATH ANGLE EFFECTS ON MEANS
AND STANDARD DEVIATION OF MISSES

Range nm	Flight-path Angle deg.	Number of Runs	Total Miss		Down-range Miss		Cross-range Miss	
			Mean nm	Standard Deviation nm	Mean nm	Standard Deviation nm	Mean nm	Standard Deviation nm
1200.	-5.60	9*	66.1	9.8	-5.6	15.0	-64.1	9.8
1200.	-6.49	12	69.7	11.4	-11.4	12.0	-67.8	10.9
1200.	-7.00	12	74.7	13.4	-21.6	13.9	-70.3	12.4
1350.	-5.60	12	74.9	18.8	-15.3	16.7	-71.8	17.3
1350.	-6.49	12	72.0	15.0	-23.1	19.9	-65.8	12.2
1350.	-7.00	12	77.1	16.1	-18.6	12.7	-73.9	15.2
1600.	-5.60	12	97.0	14.7	-28.7	17.4	-91.1	14.2
1600.	-6.49	12	96.2	22.5	-34.0	16.7	-89.0	20.3
1600.	-7.00	12	89.3	33.5	-41.3	30.8	-76.4	24.5
2000.	-5.60	12	142.4	44.6	-90.3	63.8	-97.8	22.4
2000.	-6.49	12	208.9	100.2	-175.8	121.6	-87.0	21.2
2000.	-7.00	12	286.0	107.4	-272.6	117.6	-65.7	30.2
2500.	-5.60	12	453.4	175.0	-441.7	179.2	-92.9	24.0
2500.	-6.49	12	530.0	222.8	-523.1	224.4	-76.3	31.3
2500.	-7.00	12	668.2	235.0	-661.8	238.1	-80.3	30.6

*Omitted are three 40,000.fps entries where the EMS range to-go number was based on a PGNCS entry which overflew the target.

TABLE 4

VELOCITY EFFECTS ON MEANS AND STANDARD DEVIATIONS OF MISSES

Velocity fps	Number of Runs	Total Miss		Down-range Miss		Cross-range Miss	
		Mean nm	Standard Deviation nm	Mean nm	Standard Deviation nm	Mean nm	Standard Deviation nm
36,210.	45	202.1	244.1	-169.0	260.0	-64.5	16.9
37,000.	45	207.9	212.9	-164.8	234.9	-76.7	19.8
38,500.	45	201.0	212.2	-153.1	232.7	-86.5	20.5
40,000.	42	199.5	192.4	-153.7	212.1	-86.9	28.2

TABLE 5

FLIGHT-PATH ANGLE EFFECTS ON MEANS
AND STANDARD DEVIATIONS OF MISSES

Flight-path Angle deg.	Number of Runs	Total Miss		Down-range Miss		Cross-range Miss	
		Mean nm	Standard Deviation nm	Mean nm	Standard Deviation nm	Mean nm	Standard Deviation nm
(a) Data Based on 1200., 1350., and 1600.nm Entries.							
-5.60	33	80.5	20.0	-17.5	19.0	-76.7	18.3
-6.49	36	79.3	20.7	-22.8	18.9	-74.2	18.3
-7.00	36	80.3	23.7	-27.2	23.1	-73.5	18.3
(b) Data Based on 2000. and 2500.nm Entries.							
-5.60	24	297.9	201.2	-266.0	221.3	-95.3	23.3
-6.49	24	369.5	235.8	-349.5	250.4	-81.6	27.2
-7.00	24	477.1	264.4	-467.2	270.4	-73.0	31.2

TABLE 6

RANGE EFFECTS ON MEANS AND STANDARD DEVIATIONS OF MISSES

Range nm	Number of Runs	Total Miss		Down-range Miss		Cross-range Miss	
		Mean nm	Standard Deviation nm	Mean nm	Standard Deviation nm	Mean nm	Standard Deviation nm
1200.	33	70.5	12.2	-13.5	15.1	-67.7	11.5
1350.	36	74.7	16.8	-19.0	17.0	-70.5	15.4
1600.	36	94.1	25.0	-34.7	23.1	-85.5	21.1
2000.	36	210.7	107.2	-177.9	128.8	-82.9	28.5
2500.	36	550.5	230.4	-542.2	233.8	-83.2	29.6

TABLE 7

COMPARISON OF LANDING POINTS AND DISPERSIONS

Case	Range nm	γ deg.	Number of Runs	Down-range Mean nm	Down-range σ nm	Cross-range Mean nm	Cross-range σ nm
1 a)	1350.	-5.75	10	-24.79	9.77	-62.17	16.41
b)	1350.	-5.60	12	-15.3	16.7	-71.8	17.3
2 a)	1350.	-6.49	10	-38.37	7.22	-66.99	14.03
b)	1350.	-6.49	12	-23.1	19.9	-65.8	12.2
3 a)	1350.	-7.10	10	-26.28	6.86	-45.97	10.44
b)	1350.	-7.00	12	-18.6	12.7	-73.9	15.2
4 a)	1180.	-5.75	10	-23.56	8.46	-67.06	12.34
b)	1200.	-5.60	9	-5.6	15.0	-64.1	9.8
5 a)	1180.	-6.49	10	-31.11	7.36	-58.98	10.89
b)	1200.	-6.49	12	-11.4	12.0	-67.8	10.9
6 a)	1180.	-7.10	10	-26.01	5.58	-29.01	10.22
b)	1200.	-7.00	12	-21.6	13.9	-70.3	12.4
7 a)	1519.	-5.75	10	-28.76	6.18	-70.59	17.54
b)	1600.	-5.60	12	-28.7	17.4	-91.1	14.2
8 a)	1519.	-6.49	10	-31.84	8.99	-31.07	8.35
b)	1600.	-6.49	12	-34.0	16.7	-89.0	20.3
9 a)	1519	-7.10	10	-7.49	6.52	-46.89	13.34
b)	1600.	-7.00	12	-41.3	30.8	-76.4	24.5

Data line a) From MSC Study Reference 3, Table II
line b) From Table 3

	Reference 3 Data	Bellcomm Data
Vehicle Latitude	-18.315°	0.0°
Vehicle Longitude	171.29°	0.0°
Altitude	399,720.ft	400,000.ft
Velocity	36,210.fps	36,210., 37,000., 38,500., 40,000.fps
Flight-path Angle	As indicated	As indicated
Azimuth	98.562°	90.0°
L/D	0.291	0.291

TABLE 8: PHASE 3 PERFORMANCE DATA

Range, nm	1350.		1600.		2000.		1350.		1600.		2000.	
Miss* / Velocity, fps	Down-range, nm	Cross-range, nm	Down-range, nm	Cross-range, nm	Down-range, nm	Cross-range, nm	Max g	Min g	Max g	Min g	Max g	Min g
-50.% failure	- 18.	-51.	- 51.	- 40.	-275.	- 42.	6.4	.7	6.4	.4	6.4	.2
	- 60.	-37.	-331.	- 23.	-584.	- 34.	6.4	.7	6.4	.8	6.4	.5
36,210.	- 16.	-38.	-161.	- 21.	- 37.	- 53.	6.4	.5	6.4	.5	6.4	.04
	- 2.	-66.	- 21.	- 51.	- 20.	- 70.	6.1	.8	6.1	.4	6.1	.2
	+ 14.	-36.	+ 39.	- 44.	- 77.	- 49.	6.1	.4	7.2	.1	6.1	.1
37,000.	+ 10.	-57.	- 18.	- 44.	-292.	- 36.	6.1	.6	6.1	.2	6.1	.2
	+ 20.	-85.	- 8.	- 76.	-172.	- 80.	6.2	1.6	5.8	1.2	5.9	.5
	- 8.	-76.	- 7.	- 79.	+ 11.	- 88.	6.1	1.8	6.1	.6	7.0	.3
38,500.	- 4.	-61.	- 19.	- 54.	- 7.	- 61.	5.8	2.2	5.7	1.0	6.2	.3
	+ 3.	-84.	+ 16.	-128.	+ 7.	-144.	7.9	1.8	8.8	.5	8.1	.2
	- 10.	-82.	+ 32.	- 86.	- 67.	-121.	7.6	1.7	7.9	.4	7.6	.6
40,000.	+ 22.	-26.	- 21.	- 68.	- 4.	- 99.	9.0	1.0	7.9	.9	8.9	.3
no failure	- 34.	-47.					6.4	1.2				
36,210.			- 6.	- 49.					6.4	.3		
37,000.												
38,500.			- 18.	- 57.					5.6	.6		
	- 4.	-45.	0.	- 71.			7.1	2.6	7.0	1.4		
40,000.	+ 3.	-56.	- 13.	- 76.	- 32.	- 75.	7.0	2.4	7.1	1.3	7.0	.5
+50.% failure	+ 10.	-34.	+110.	- 22.	+ 48.	- 65.	6.4	1.4	8.0	.5	6.4	.2
	+636.	-33.	- 16.	- 59.	-180.	- 38.	7.5	.1	6.4	.5	6.4	.4
36,210.	- 23.	-55.	- 7.	- 51.	- 12.	- 48.	6.4	1.7	6.4	.4	6.4	.1
	- 5.	-63.	- 10.	- 67.	-166.	- 32.	6.1	1.8	6.1	.8	6.1	.5
	+ 1.	-54.	+ 34.	- 46.	- 28.	- 49.	6.1	1.6	6.8	.4	6.1	.3
37,000.	- 14.	-55.	- 15.	- 69.	- 14.	- 47.	6.1	1.8	6.1	.7	6.1	.4
	+ 21.	-60.	+ 31.	- 53.	+ 6.	- 69.	5.6	2.2	5.6	.6	5.6	.6
	+ 17.	-52.	+ 2.	- 61.	- 8.	- 66.	5.6	2.1	5.6	1.1	5.6	.4
38,500.	+ 0.	-48.	- 9.	- 27.	- 28.	-117.	5.6	2.0	5.6	1.0	6.3	.4
	+ 5.	-88.	+ 16.	- 16.	-108.	- 34.	6.6	2.9	6.6	1.4	6.6	.5
	+ 3.	-94.	+538.	- 41.	- 74.	- 76.	6.6	2.0	7.0	.3	6.6	.4
40,000.	+ 92.	-18.	+ 3.	- 28.	- 10.	- 43.	7.7	1.3	6.6	1.0	6.6	.9

* + indicates overshoot or South
  - indicates undershoot or North

TABLE 9 PHASE 3 SUMMARY

VELOCITY, FPS		INDICATION OF FAILURE			LANDING POINT CONTROL			SAFETY			FINDINGS		
	RANGE, nm	1350.	1600.	2000.	1350.	1600.	2000.	1350.	1600.	2000.	1350.	1600.	2000.
− 50% FAILURE	36,210.	THE GUIDANCE LEVELED OFF AT AN ACCELERATION HIGHER THAN THE REFERENCE DRAG LEVEL, DO, AND CONTINUED TO HOLD LIFT DOWN.			THE PILOTS WERE UNABLE TO REACH THE TARGET AREA. MISSES RANGE FROM 25. nm TO 584. nm SHORT.						TIMING OF FAILURE DETECTION WAS NOT SOON ENOUGH TO AVOID A TRADE OFF BETWEEN MAGNITUDE OF THE MISS AND LOW MINIMUM G.		REGARDLESS OF TIMING AND TECHNIQUE IT WAS NOT POSSIBLE TO REACH THE TARGET WITHOUT A FORTUITOUS SKIP.
	37,000.								THE PILOTS REACHED A MINIMUM G OF 0.2 OR LESS. THE PEAK G WAS LESS THAN 7.				
	38,500.	THE GUIDANCE PULLED DOWN PRIOR TO PULLOUT, AT AN ACCELERATION HIGHER THAN THE REFERENCE DRAG LEVEL, DO.			WITH FEW EXCEPTIONS, THE PILOTS CAME WITHIN 30. nm DOWN RANGE OF THE TARGET AREA.			THE MINIMUM G WAS GREATER THAN 0.2 AND THE PEAK G WAS LESS THAN 9.			FAILURES WERE DETECTED EARLY ENOUGH TO COMPLETE A SAFE ENTRY TO THE TARGET AREA.		
	40,000.	FROM AN INITIAL ROLL OF 180° THE GUIDANCE FAILED TO ROLL UP AT 1.5g.											
NO FAILURE	36,210.	THE PILOTS TOOK OVER WHEN THE GUIDANCE ROLLED DOWN DURING THE CONSTANT G PHASE. 1 FALSE TAKEOVER	1 FALSE TAKEOVER								THE PILOTS' TRAINING IN MANUAL ENTRIES RESULTED IN A BIAS IN GUIDANCE PHILOSOPHY. COMBINED WITH A LACK OF EXPERIENCE ON GOOD GUIDED ENTRIES, THIS PRODUCED 3 FALSE TAKEOVERS.		
	37,000.												
	38,500.		1 FALSE TAKEOVER										
	40,000.	THE PILOT TOOK OVER IN RESPONSE TO OFFSET TANGENCIES WHILE THE ROLL COMMAND HELD AT 90° 2 FALSE TAKEOVERS	2 FALSE TAKEOVERS	1 FALSE TAKEOVER	THE PILOTS CAME WITHIN 35. nm DOWN RANGE OF THE TARGET AREA.			THERE WAS NO SAFETY PROBLEM WITH REGARD TO PEAK OR MINIMUM G.			TAKEOVER WAS DUE TO AN INCOMPATIBILITY BETWEEN THE PGNCS AND THE EMS. IN ALL CASES THE PILOT COMPLETED A SAFETY ENTRY TO THE TARGET AREA.		
+ 50% FAILURE	36,210.	TAKEOVER OCCURRED AT OFFSET TANGENCIES OR WHEN THERE WAS AN EXCESS OF RANGE CAPABILITY NEAR VSAT.			IN 20 OF THE 24 ENTRIES THE PILOTS CAME WITHIN ± 35. nm DOWNRANGE OF THE TARGET. THE OTHER 4 ENTRIES OVERSHOT BETWEEN 90. AND 640.nm.		LANDING POINT CONTROL WAS UNCERTAIN IN 8 OF THE ENTRIES. THE PILOTS LANDED WITHIN ±50 N.M. IN 4 CASES THEY WERE SHORT BETWEEN 70 AND 180 N.M.		THE PILOTS REACHED A MINIMUM G BETWEEN 0.1 and 0.5.		THE G-V TRACE ENCOUNTERED WAS IN ACCORDANCE WITH PILOT DESIRE TO GAIN RANGE POTENTIAL EARLY. IN RESPONSE TO AN EARLY TAKEOVER, THERE WAS LITTLE DIFFICULTY IN EXECUTING A SAFE ENTRY CLOSE TO TARGET; OCCASIONALLY A LATE TAKEOVER RESULTED IN AN OVERSHOOT AND/OR MUCH TIME IN THE HIGH G REGION.	EARLY FAILURE DETECTION CORRELATED WITH FLYING A MORE CONSERVATIVE TRAJECTORY. THIS RESULTED IN AVOIDING A LOW MINIMUM G AND CONSEQUENTLY FALLING SHORT BETWEEN 70. AND 180.nm. LATE DETECTION RESULTED IN EXCESS RANGE CAPABILITY WHICH CORRELATED WITH A LOW MINIMUM G AND RESULTED IN THE PILOTS' REACHING THE TARGET MORE FREQUENTLY.
	37,000.												
	38,500.							EXCEPT FOR ONE CASE OF LATE TAKEOVER, THERE WAS NO SAFETY PROBLEM WITH REFERENCE TO MINIMUM OR MAXIMUM G. IN 5 OF THE 30 ENTRIES IN THIS GROUP, CONSIDERABLE TIME WAS SPENT IN THE HIGH G REGION LATE IN THE TRAJECTORY.					
	40,000.	THERE WERE THREE PLACES TO DETECT FAILURES: 1. REVERSAL TO FULL UP PRIOR TO 1.5g. 2. LOWER THAN PREDICTED PULLOUT ACCELERATION. 3. OFFSET TANGENCIES.											

TABLE 10

PHASE 2 GUIDED ENTRIES WITH ROLL DELAY AT 90.°

			Initial Flight-path Angle (deg)		
	Velocity (fps)	Range (nm)	Shallow	Nominal	Steep
1.	36,210.	1350.	-5.6	-6.49	-7.0
2.	36,210.	1200.	-5.6	-6.49	-7.0***
3.	36,210.	1600.	-5.6	-6.49	-7.0↑↑↑
4.	36,210.	2000.	-5.6	-6.49↑	-7.0↑
5.	36,210.	2500.	-5.6↑	-6.49↑	-7.0↑
6.	37,000.	1350.	-5.6	-6.49	-7.0***
7.	37,000.	1200.	-5.6	-6.49	-7.0***
8.	37,000.	1600.	-5.6	-6.49	-7.0***
9.	37,000.	2000.	-5.6	-6.49	-7.0***
10.	37,000.	2500.	-5.6↑	-6.49**	-7.0↑
11.	38,500.	1350.	-5.6	-6.49**	-7.0****
12	38,500.	1200.	-5.6	-6.49**	-7.0****
13.	38,500.	1600.	-5.6	-6.49**	-7.0****
14.	38,500.	2000.	-5.6	-6.49*	-7.0***
15.	38,500.	2500.	-5.6↑	-6.49*	-7.0***
16.	40,000.	1350.	-5.6	-6.49*****	-7.0****
17.	40,000.	1200.	-5.6	-6.49*****	-7.0****
18.	40,000.	1600.	-5.6	-6.49*****	-7.0*****
19.	40,000.	2000.	-5.6	-6.49*****	-7.0*****
20.	40,000.	2500.	-5.6↑	-6.49*****	-7.0*****

↑ The trajectory is tangent to an offset curve in the low g region and the roll command is not full down.

* Each * represents a case in which a roll command of 90.° was held for two seconds in a high g region where the trajectory is tangent to an offset curve.

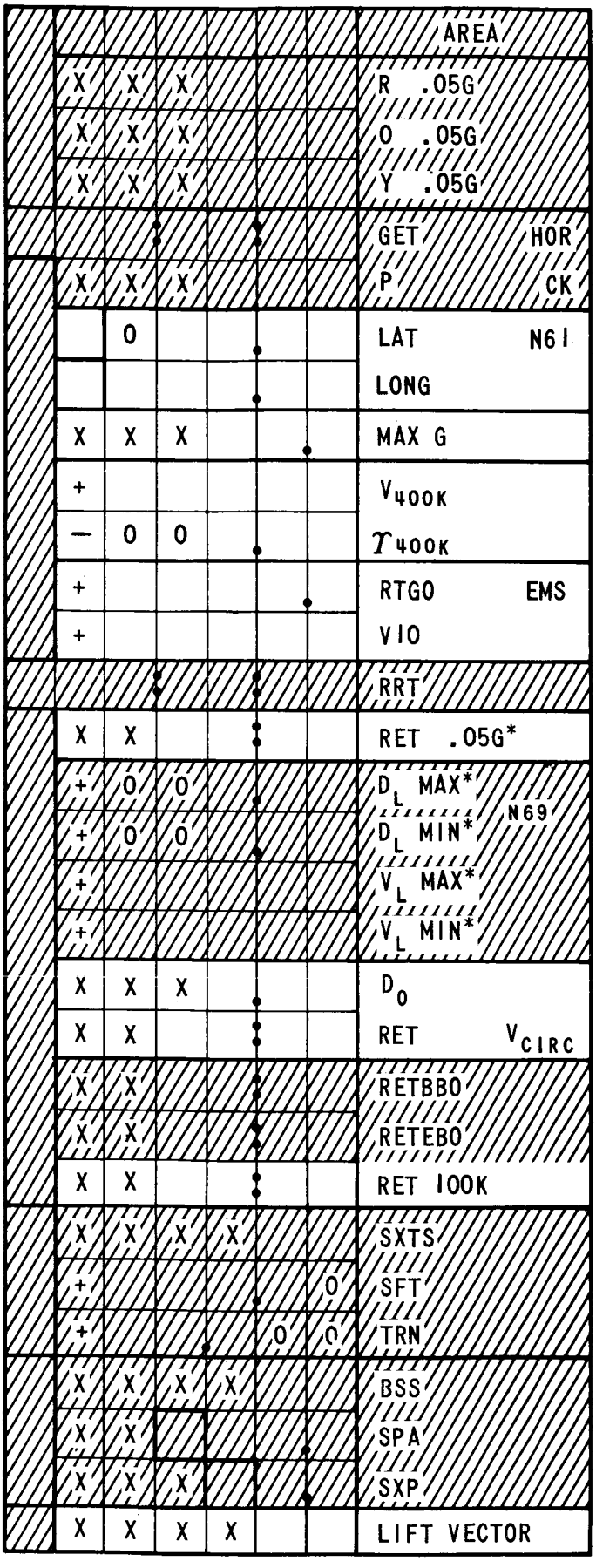

COMMENTS: _____

_____

_____

_____

_____

_____

PILOT _____

PAD NOMENCLATURE

LAT	LANDING SITE LATITUDE
LONG	LANDING SITE LONGITUDE
MAX G	GROUND COMPUTED MAXIMUM ENTRY ACCELERATION
V_{400K}	VELOCITY AT ENTRY INTERFACE (EI)
γ_{400K}	FLIGHT PATH ANGLE AT EI
RTGO EMS	RANGE AT 0.05g FOR EMS INITIALIZATION BASED ON GROUND SIMULATION OF THE GUIDED ENTRY
VIO	INERTIAL VELOCITY AT 0.05g FOR EMS INITIALIZATION
RET .05G	TIME FROM EI TO 0.05g
D_O	GROUND COMPUTED CONSTANT DRAG LEVEL USED IN THE PRIMARY GUIDANCE
RET V_{CIRC}	TIME FROM EI TO ORBITAL VELOCITY
RET 100K	TIME FROM EI TO 100,000.FT.
LIFT VECTOR	INITIAL LIFT VECTOR ORIENTATION UP OR DOWN.

FIGURE 1 - ENTRY PAD

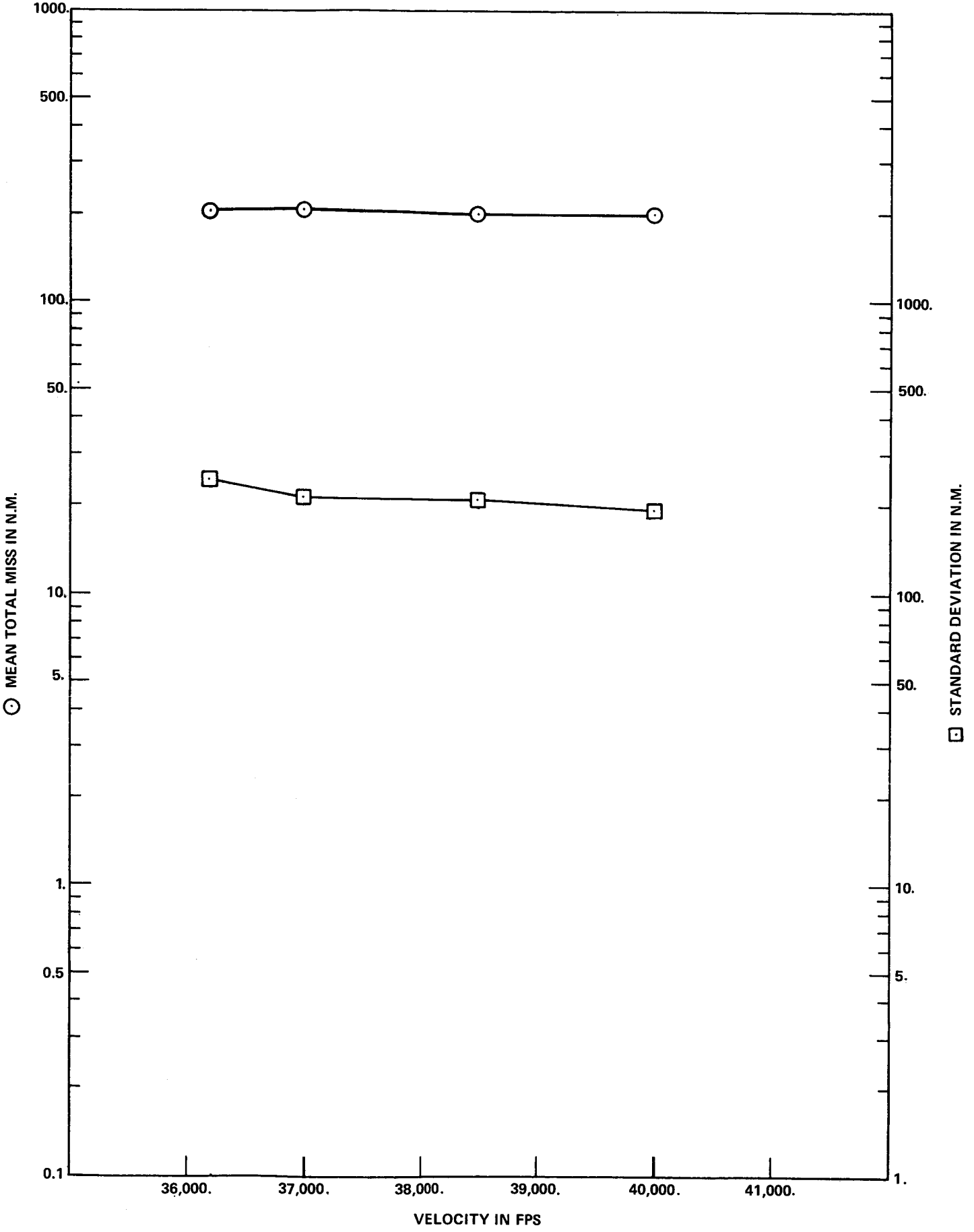

FIGURE 2a - MEAN AND STANDARD DEVIATION OF TOTAL MISS VS. VELOCITY

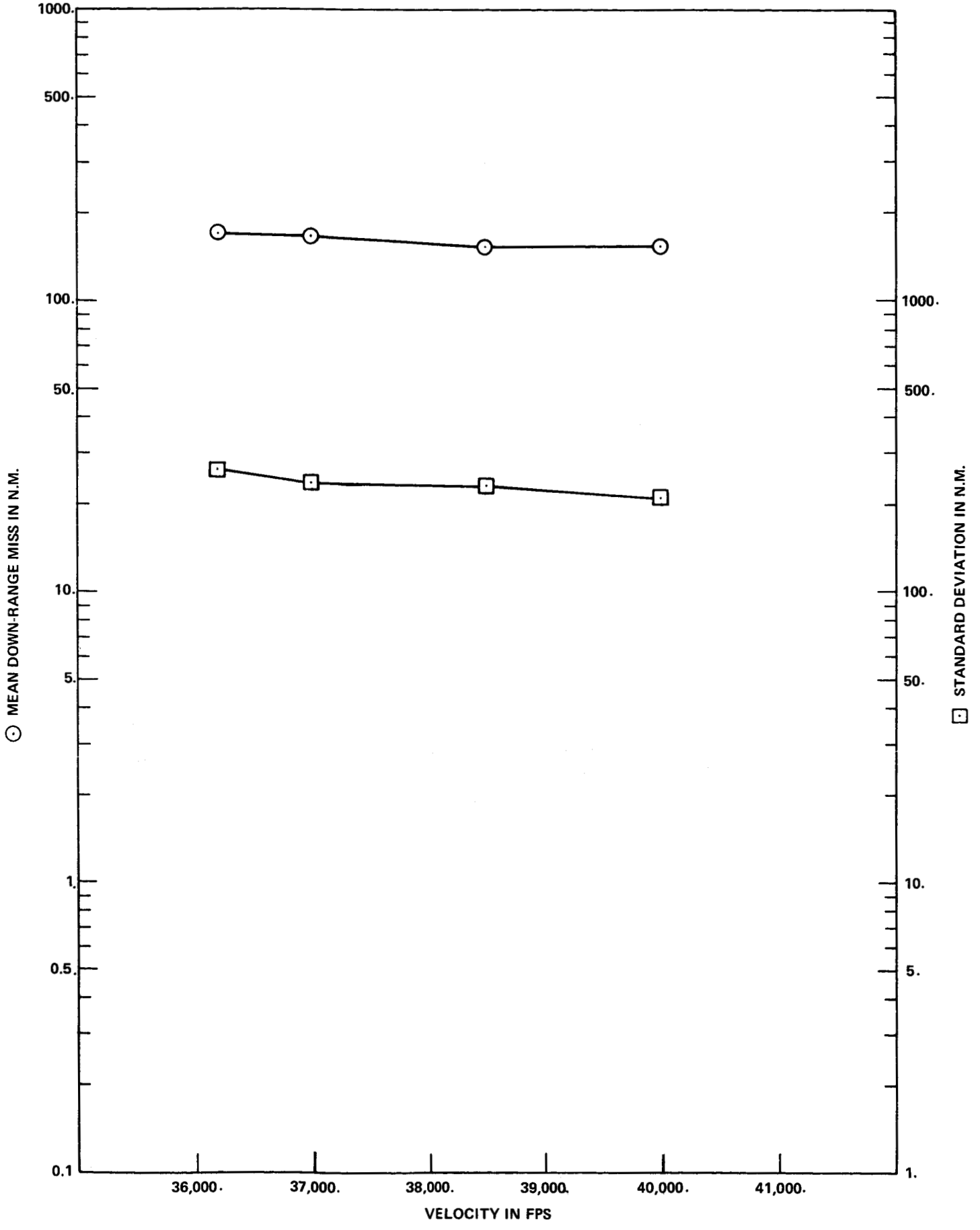

FIGURE 2b - MEAN AND STANDARD DEVIATION OF DOWN-RANGE MISS VS. VELOCITY

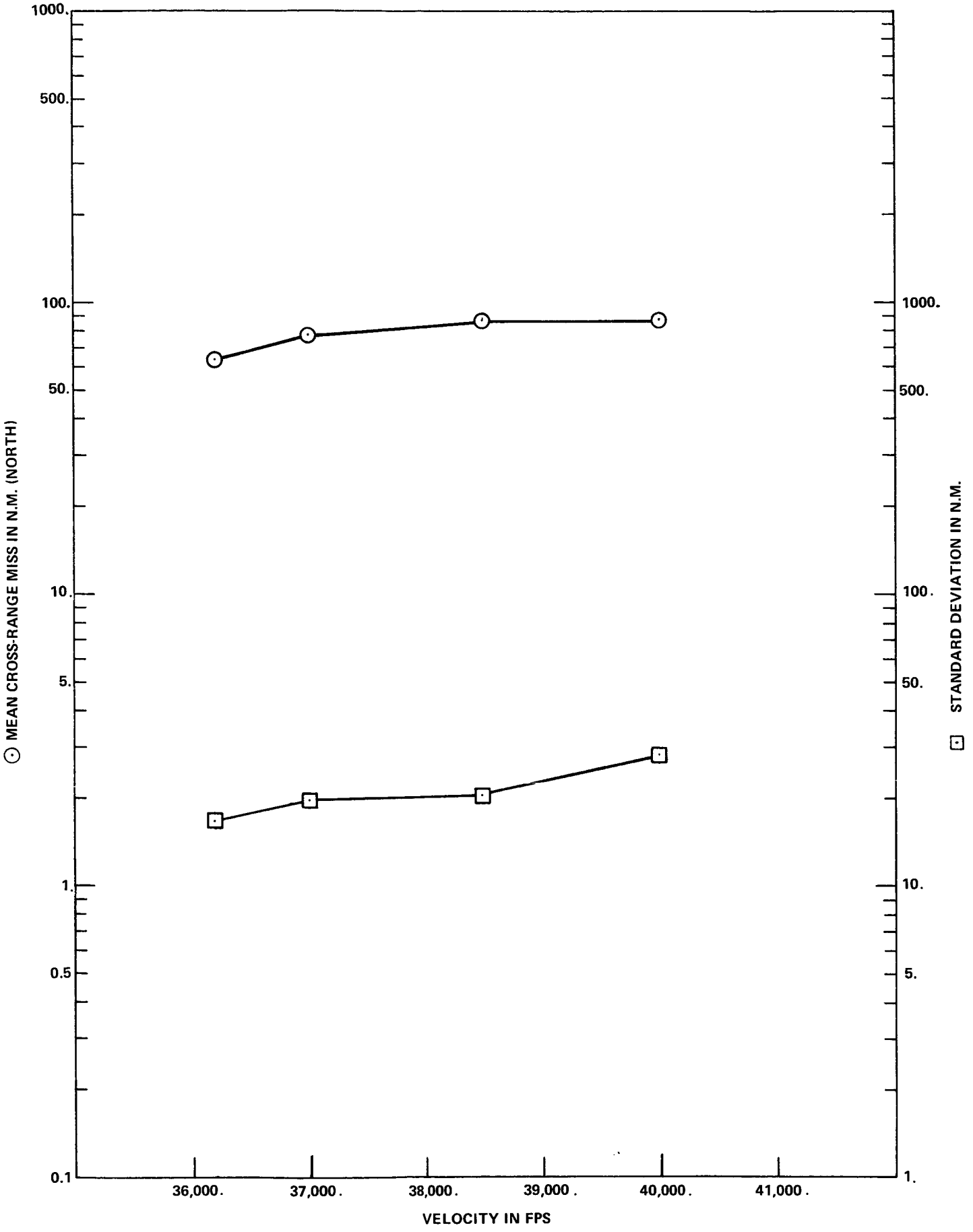

FIGURE 2c - MEAN AND STANDARD DEVIATION OF CROSS-RANGE MISS VS. VELOCITY

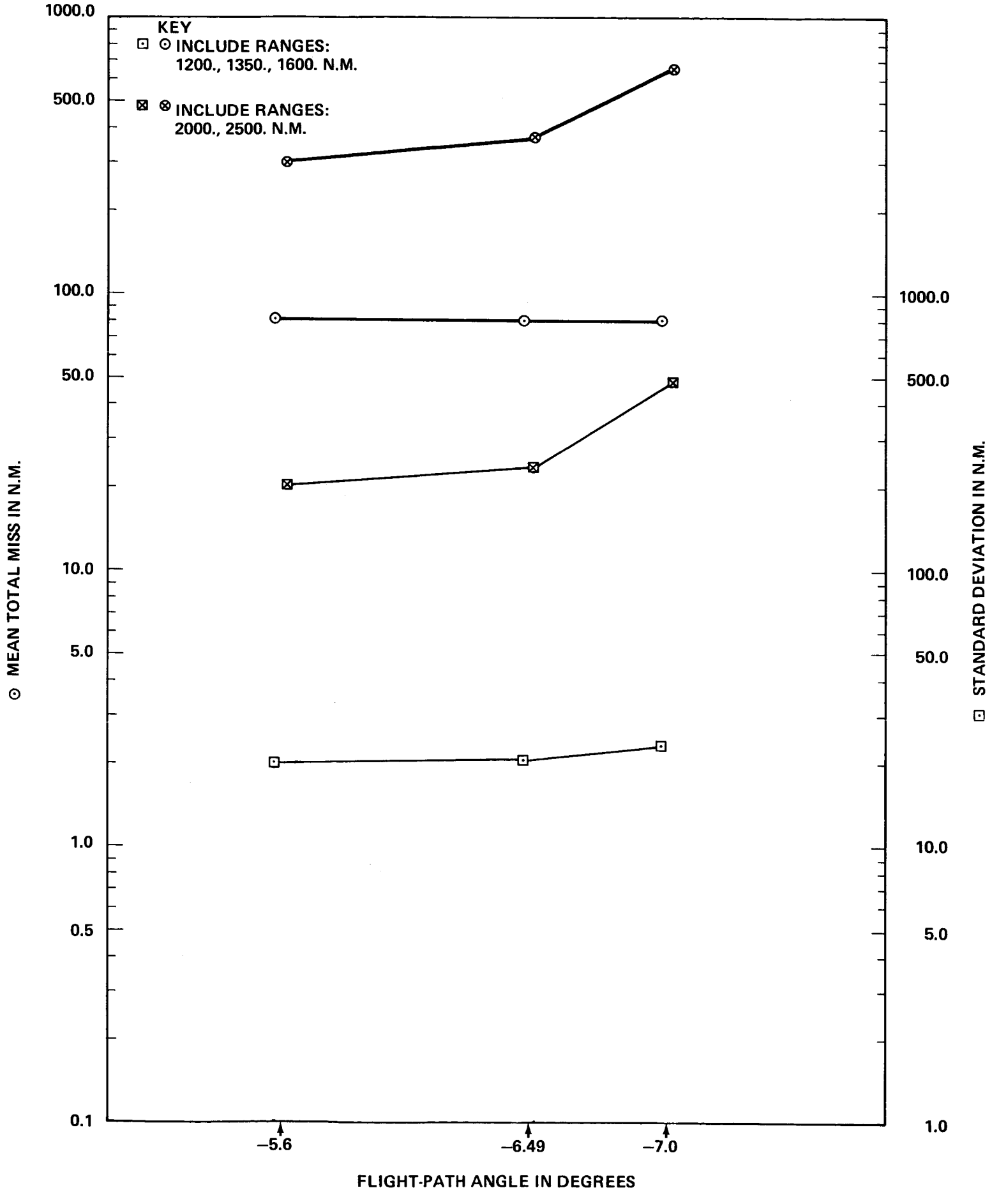

FIGURE 3a - MEAN AND STANDARD DEVIATION OF TOTAL MISS VS. FLIGHT-PATH ANGLE

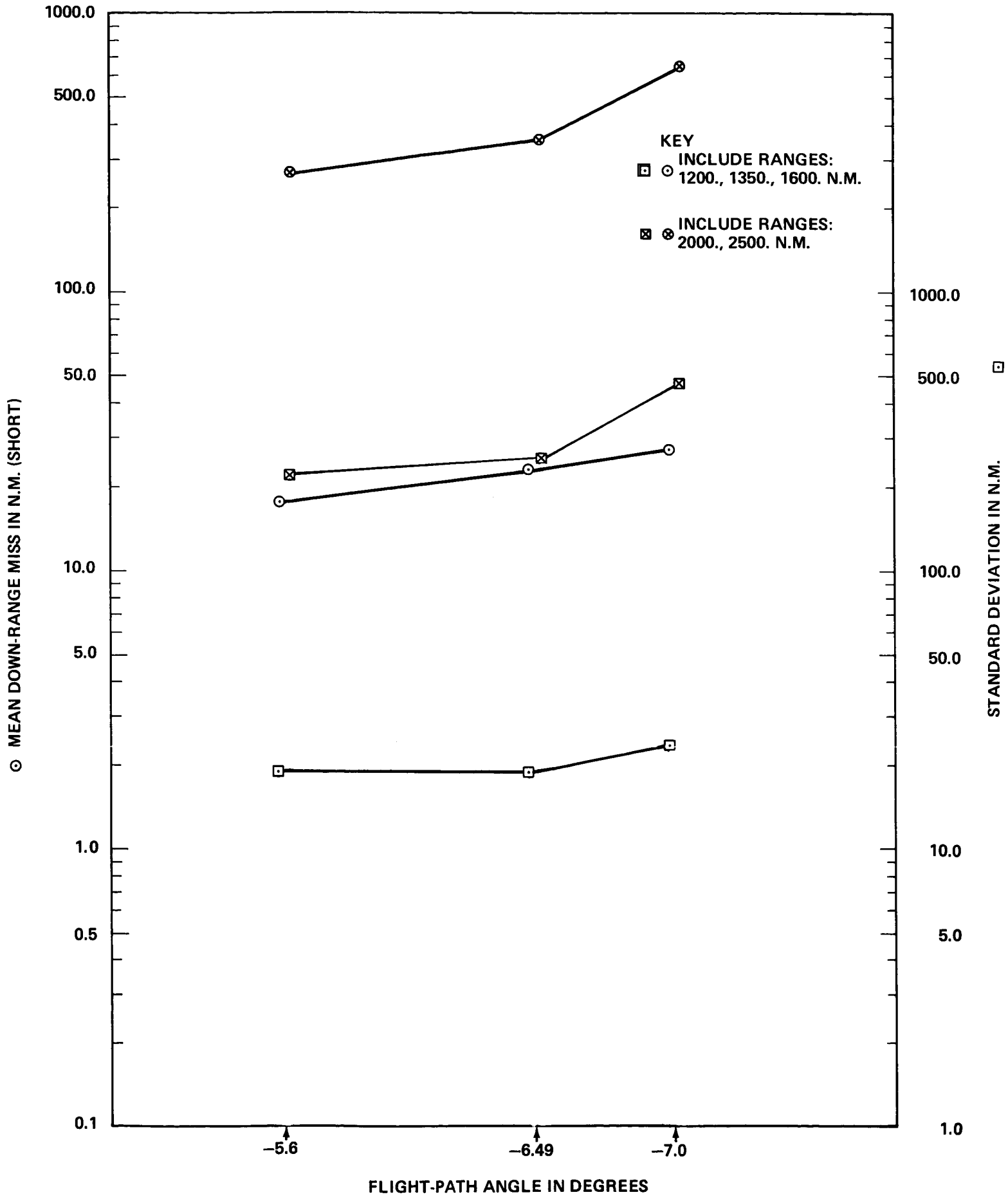

FIGURE 3b - MEAN AND STANDARD DEVIATION OF DOWN-RANGE MISS VS. FLIGHT-PATH ANGLE

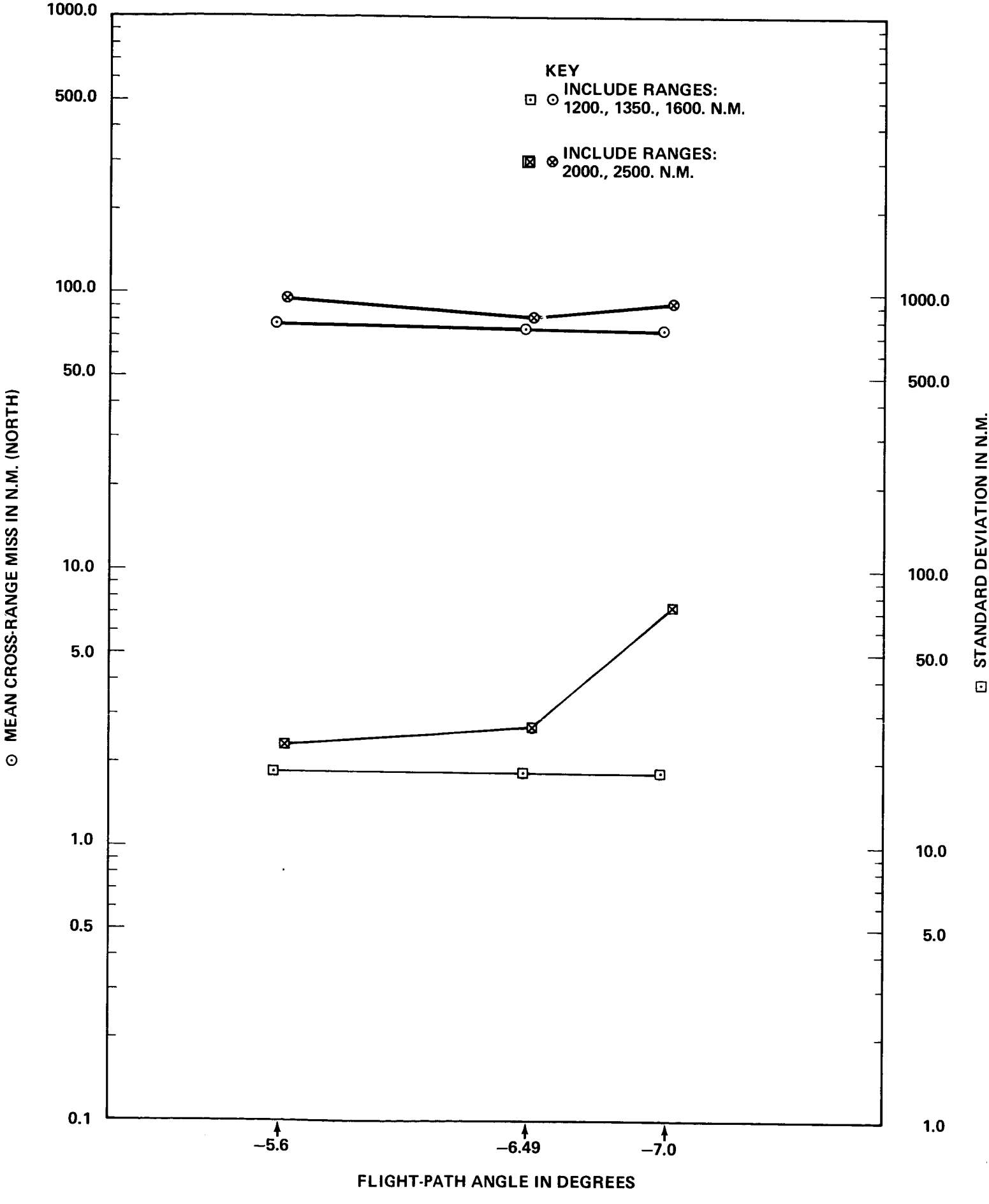

FIGURE 3c - MEAN AND STANDARD DEVIATION OF CROSS-RANGE MISS VS. FLIGHT-PATH ANGLE

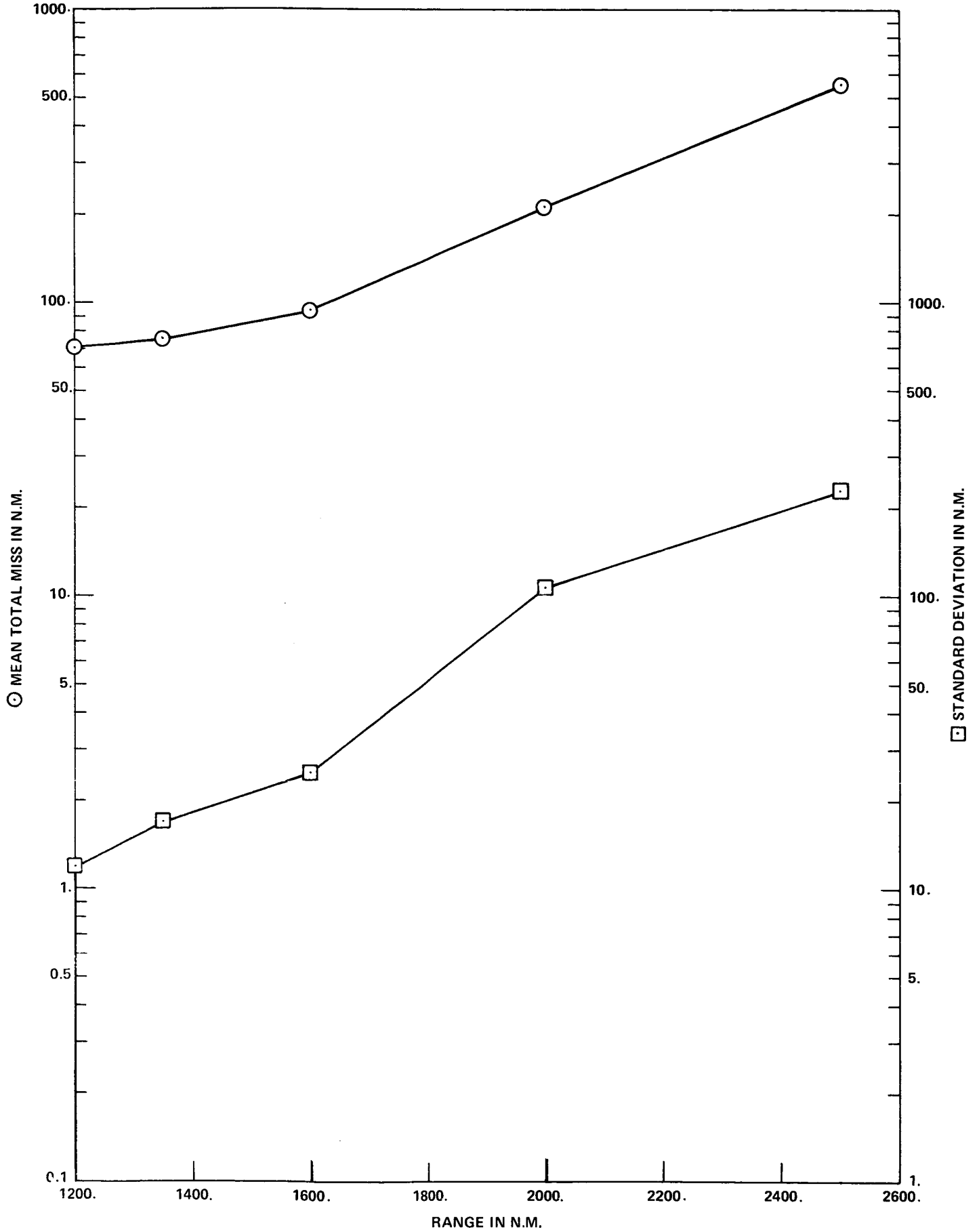

FIGURE 4a - MEAN AND STANDARD DEVIATION OF TOTAL MISS VS. RANGE

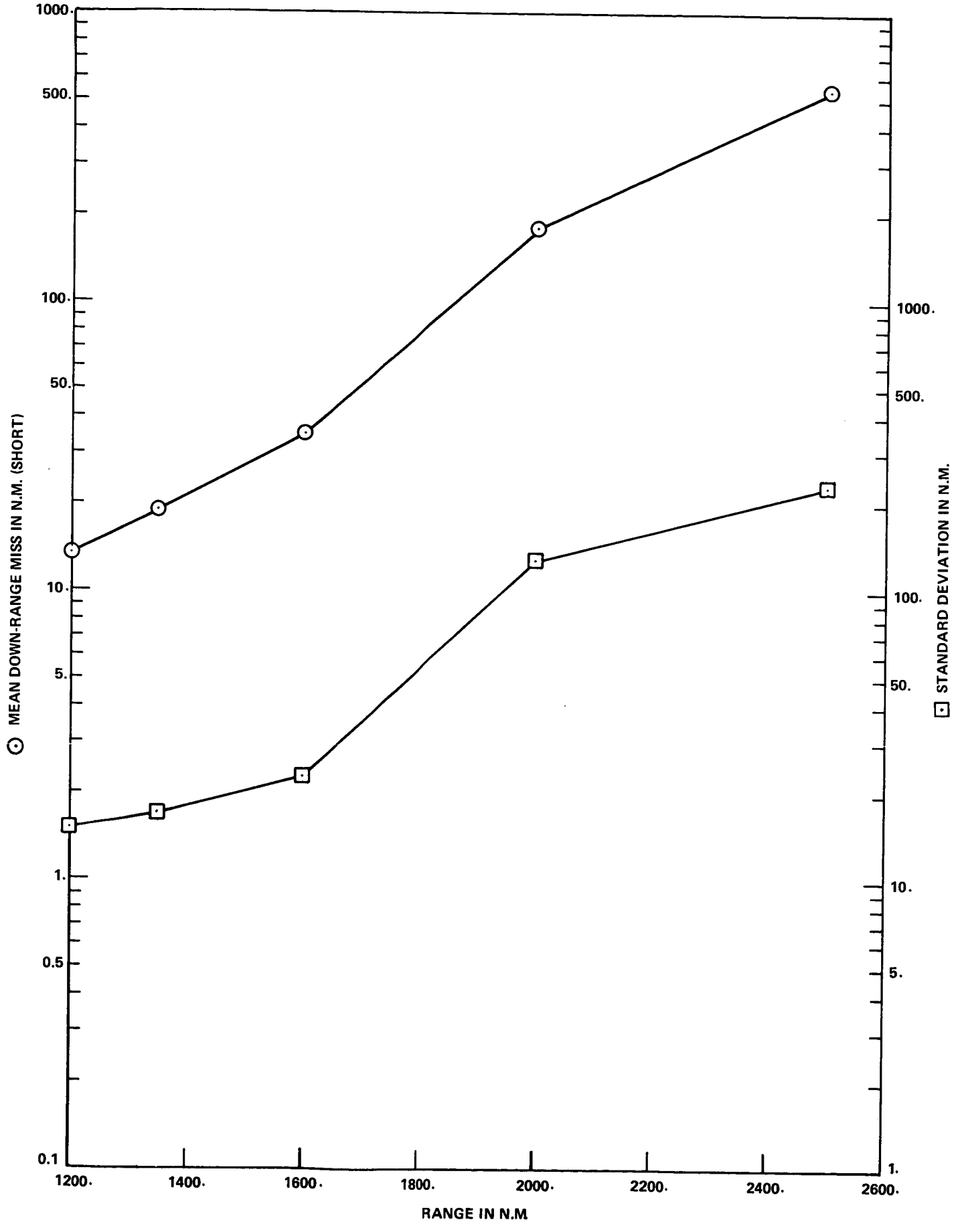

FIGURE 4b - MEAN AND STANDARD DEVIATION OF DOWN-RANGE MISS VS. RANGE

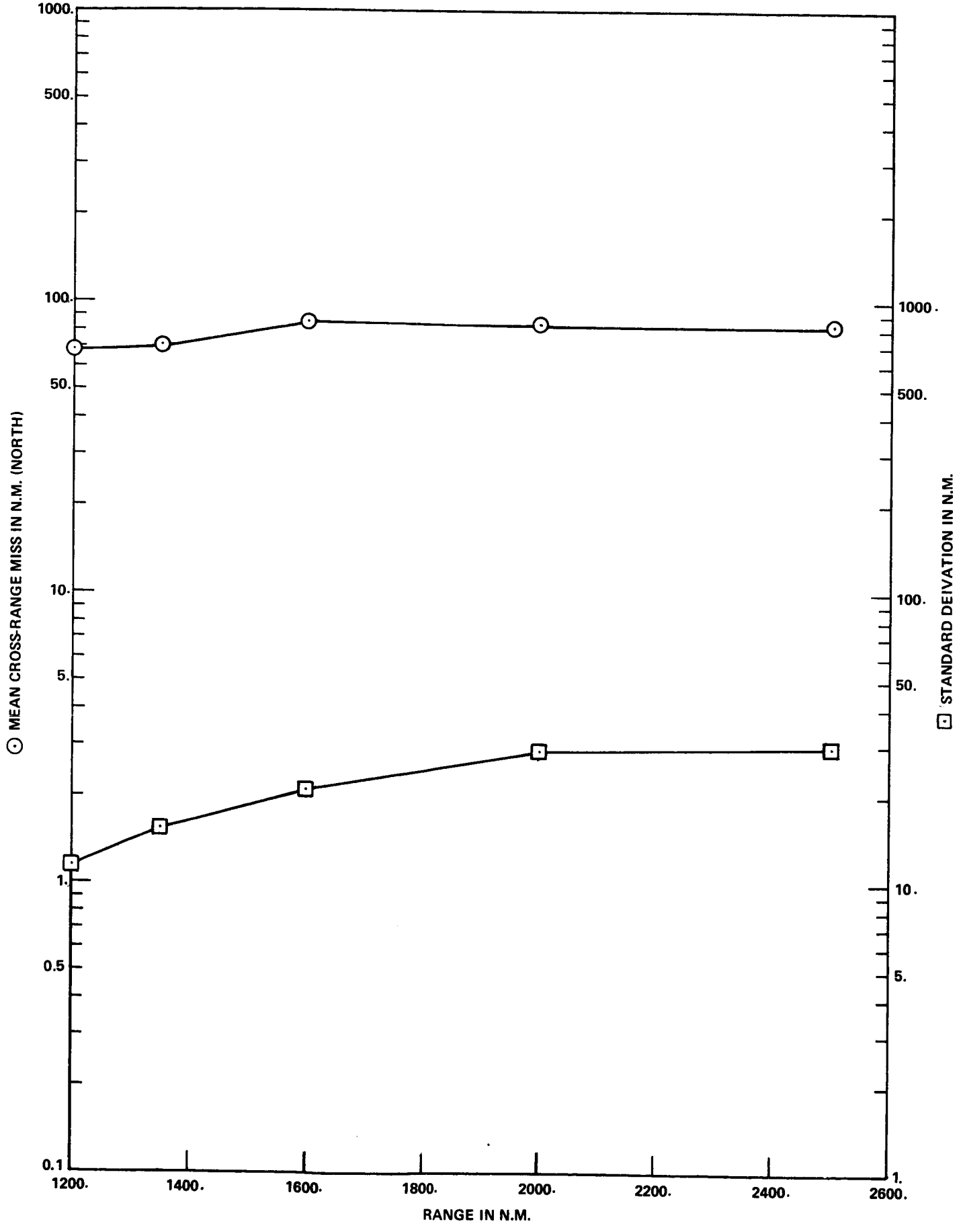

FIGURE 4c - MEAN AND STANDARD DEIVATION OF CROSS-RANGE MISS VS. RANGE

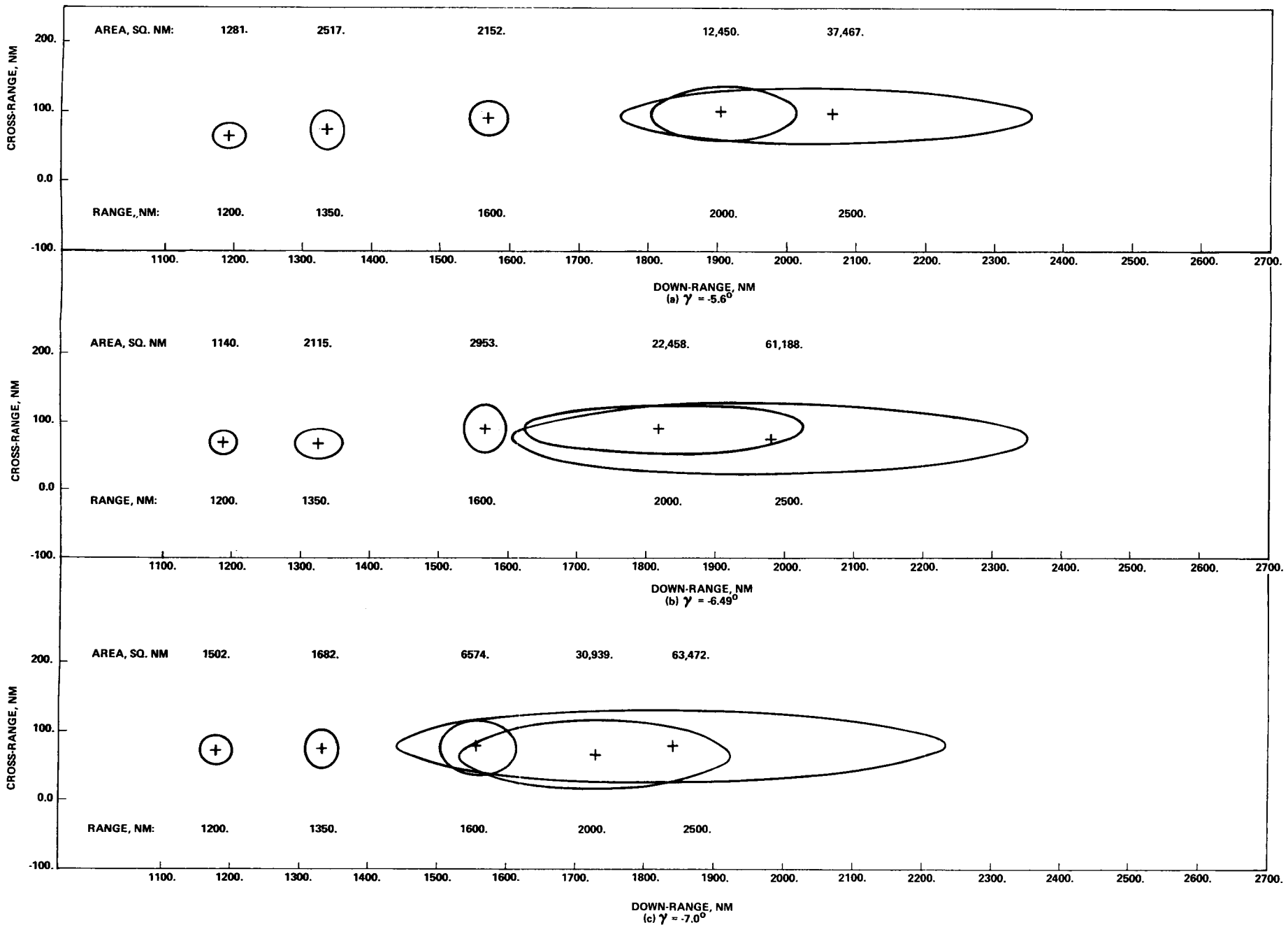

FIGURE 5 - EMS 75% PROBABLE LANDING AREAS

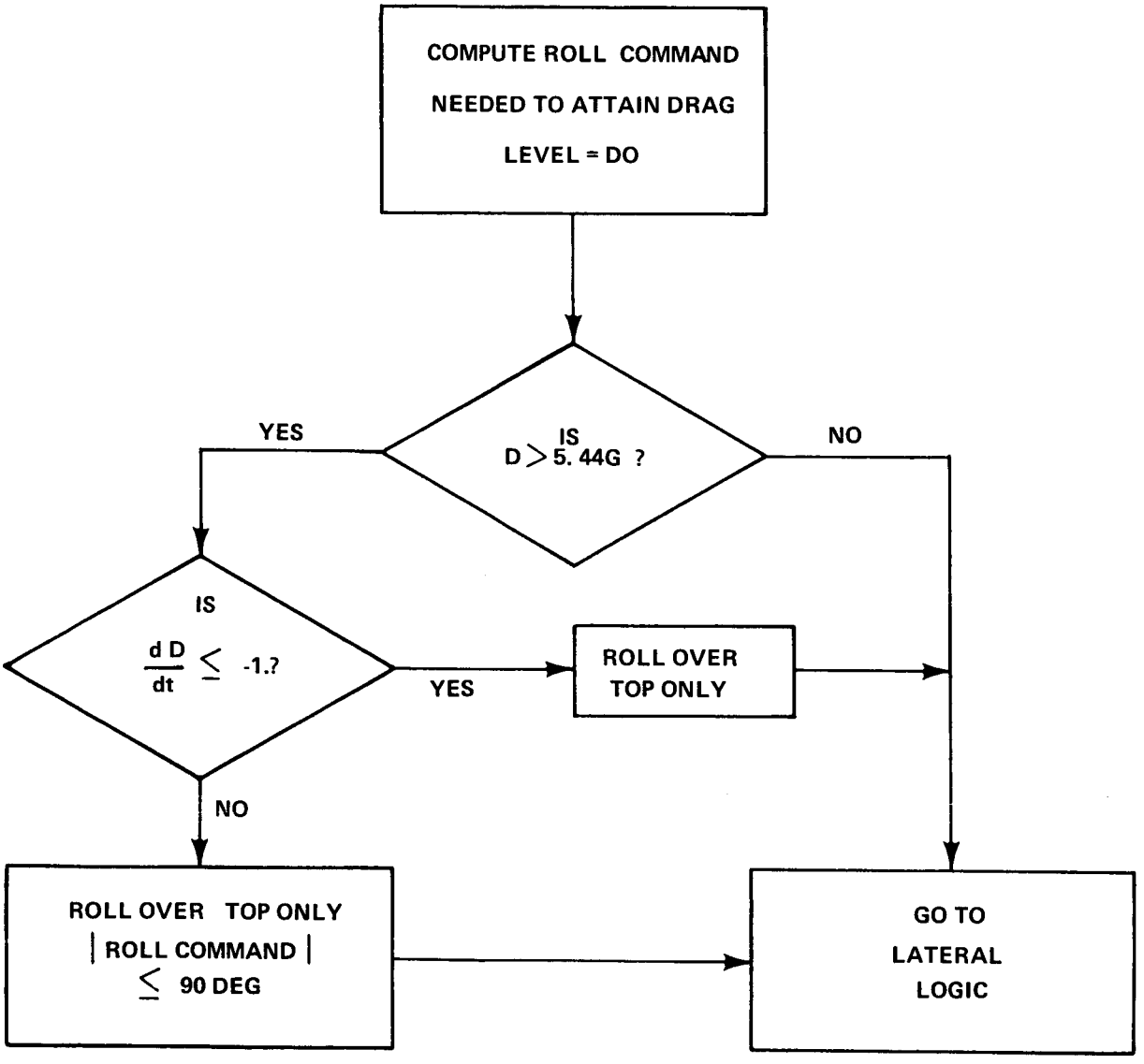

FIGURE 6 - REVISED CONSTANT DRAG LOGIC

V = 38,500. FPS
γ = -6.49°
RANGE = 1350. N. M.

A) USING COLOSSUS 2

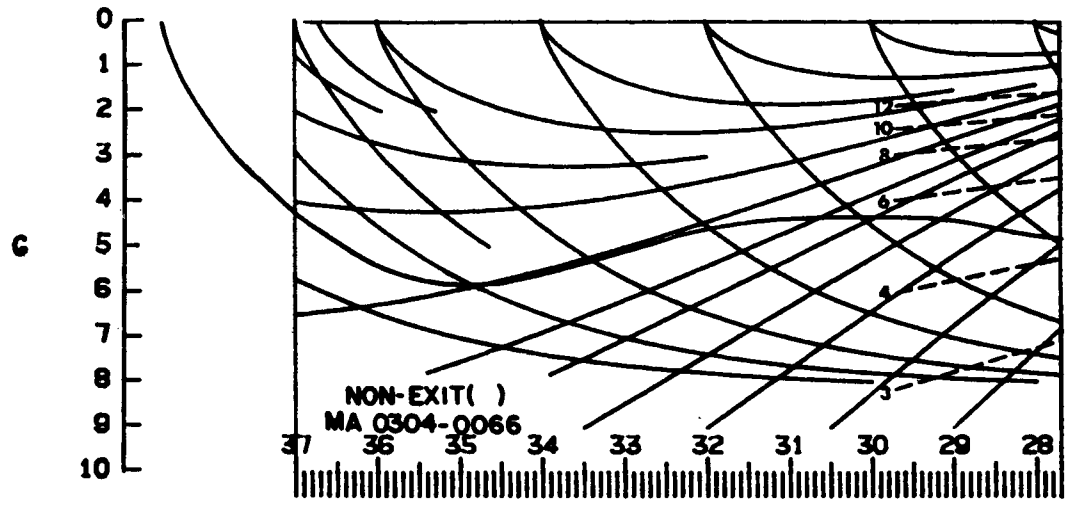

B) USING REVISED COLOSSUS 2

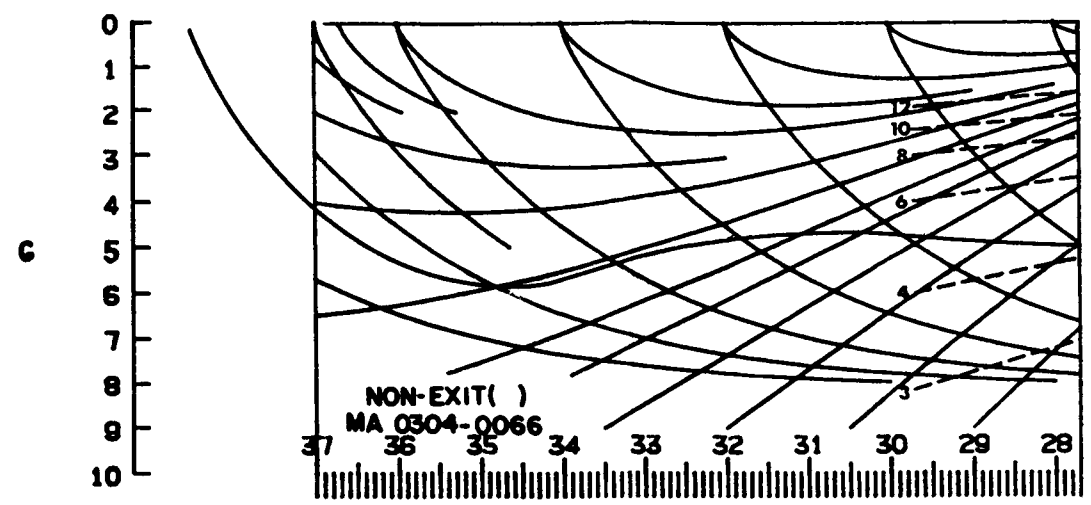

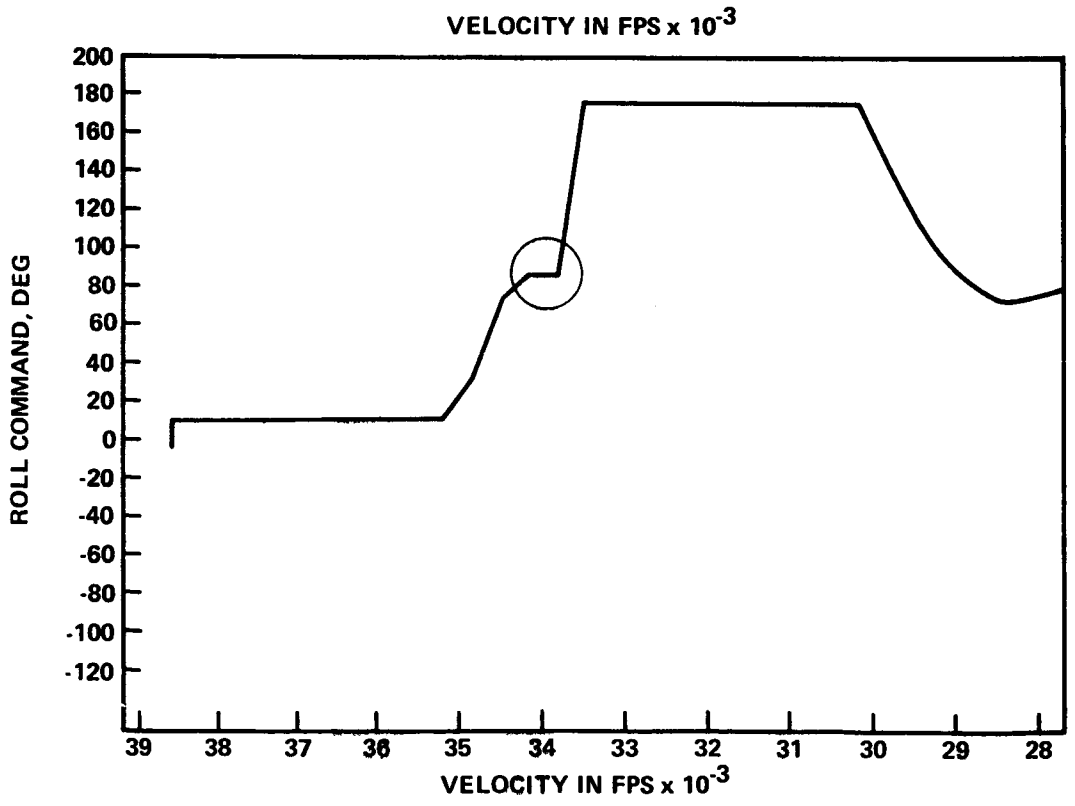

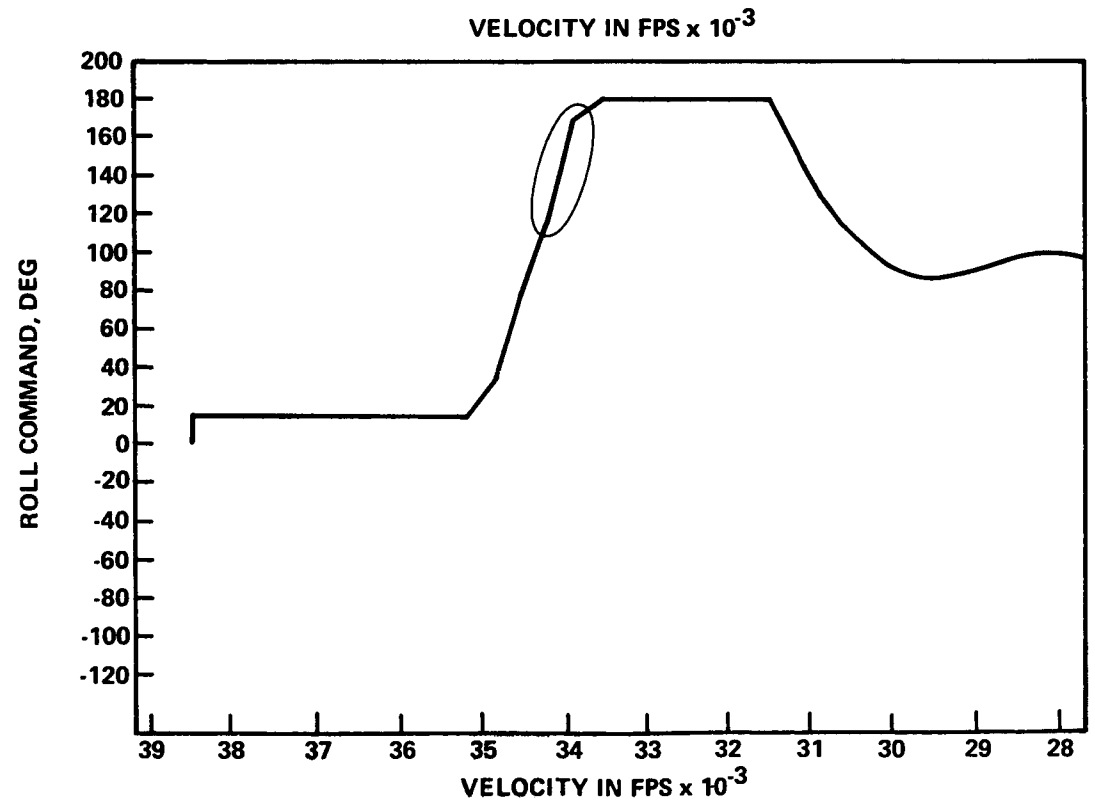

FIGURE 7 - COMPARISON OF COLOSSUS II AND REVISED CONSTANT DRAG LOGIC

FOLDOUT FRAME 1

FOLDOUT FRAME 2

BELLCOMM, INC.
Washington, D. C. 20024

APPENDIX 1

ENTRY GUIDANCE BACKGROUND

APPENDIX 1

TABLE OF CONTENTS

APPENDIX 1

TABLE OF CONTENTS (CONTINUED)

Appendix 1

LIST OF TABLES

APPENDIX 1

LIST OF ILLUSTRATIONS

APPENDIX 1

LIST OF ILLUSTRATIONS (CONTINUED)

Appendix 1

Entry Guidance Background

A1.0 THE ENTRY PROBLEM

A1.1 Guidance Objectives

Apollo entry guidance meets two objectives: crew safety and landing point control, in that order of importance. (1)(2) The spacecraft may not experience aerodynamic decelerations exceeding 10.g, nor -- in an attempt to reach a long range -- may it re-exit the atmosphere at super-circular velocity. Weather and land-mass avoidance capability require that the spacecraft be guided from the entry interface (EI), the point the spacecraft first reaches the 400,000.ft altitude, to any preselected impact point having a ground range between 1200.nm and 2500.nm. Accuracy requirements on the primary guidance are specified at 10.nm CEP.

A1.2 Spacecraft Control

Axially symmetric, as shown in Figure A1-1, the spacecraft has its center of gravity displaced from its axis of symmetry. The resulting trim angle of attack α -- a function of the center of gravity offset -- produces a lift-to-drag ratio (L/D) of between 0.25 and 0.33. Rotation of the lift vector about the drag or velocity vector by means of reaction jets provides desired trajectory control.

A1.3 Control Problem

Insight into the control problem is provided by Wingrove.(3) In Figure A1-2 he illustrates the relationship between the controlling force, the lift, and the controlled states, the drag and the range. To increase the range the vehicle is rolled about the velocity vector to increase the vertical component of lift. In time the altitude increases, decreasing the drag and consequently increasing the range.

In addition to designing a control for the fourth-order system of Figure A1-2, the designer is confronted with a number of other challenges. Segments of communication blackout require the guidance to be self-contained, dictating an inertial system. Range and g level are sensitive to initial V and γ, atmospheric changes, vehicle aerodynamics and measurement errors. In the case of V and γ, Figure A1-3 depicts the

entry corridor at the interface. Transearth midcourse maneuvers must place the spacecraft within this corridor if the guidance is to execute a safe entry. If the spacecraft finds itself on the shallow side, the guidance cannot prevent an overshoot; on the steep side, it cannot prevent excessive loading. One portrayal of the sensitivity of range to flight-path angle is shown is Figure A1-4.

A2.0 APOLLO ENTRY GUIDANCE SYSTEMS

A2.1 Primary System

A2.1.1 Hardware

Apollo guidance and control tasks are performed by the Primary Guidance, Navigation, and Control System (PGNCS or GNCS) and the Stabilization and Control System (SCS). Pictured in Figure A1-5, they provide spacecraft attitude reference, attitude control and acceleration measurement and control. A gimballed, gyro-stabilized platform, maintaining an inertially fixed orientation, provides the attitude reference. Referred to as the Inertial Measurement Unit (IMU), the reference provides the pilot with spacecraft attitude through a display, the Flight Director Attitude Indicator (FDAI). Attitude errors and angular rates also appear on the FDAI.

The IMU platform is the base for three orthogonally-mounted pulsed-integrating pendulous accelerometers (PIPA's). Sensing changes in velocity, the PIPA's provide data to the Command Module Computer (CMC), enabling the computer to generate current velocity and position. Based upon sensed data, the CMC executes the guidance program, supplies the autopilot with the roll command, and provides the data for the pilot display. CMC erasable memory contains mission and system programs wired in during assembly. Data storage and telemetered information are located in the erasable section.

A Rotation Hand Controller (RHC), the FDAI, Gyro-Assembly (GA), and the electronics necessary to control the reaction jets form the Stabilization and Control System. In response to a CMC generated deflection of the roll error needle, the pilot moves the hand controller off center, turning on the roll jets. As a roll rate builds up, a gyro-sensed roll rate signal is fed back to null the hand controller signal.

If he wishes, the pilot removes himself from the guidance loop, switching the CMC roll command to the entry Digitial Autopilot (DAP).

A2.1.2 Primary Guidance Logic, Colossus II

A 1870.nm entry trajectory is presented in Figure A1-6. Names along the trajectory refer to specific sections of the guidance logic which exercise control.(4)

A2.1.2.1 Initialization, Navigation, Targeting. Figure A1-7

Entry initialization, is performed once at the start of entry. Included are: insertion of target coordinates, setting switches, setting guidance constants peculiar to the vehicle, and computing the initial roll -- North or South -- to reduce initial cross-range error. At two second intervals state vector update occurs: PIPA counts are integrated using an average-g algorithm to yield a new velocity and position. New vehicle and revised target coordinates are then used to compute revised range-to-go and cross-range miss.

A2.1.2.2 Initial Roll. Figure A1-8

Prior to entry the roll is full up. At 0.05g, the start of the sensible atmosphere, this logic section determines lift -- full up or full down -- depending upon the position of the entry in the V-γ corridor in Figure A1-3. For entry speeds less than 27,000.fps the guidance bypasses much of the logic, going to Kepler and Final Phase. KA, approximately 1.5g, and DO a drag acceleration of approximately 4.g, both functions of initial velocity, are computed for subsequent use.

If the altitude rate RDOT, initially on the order of -4100.fps, is more negative than -700.fps the guidance shifts to Lateral Logic until the drag level builds to KA ($\sim$1.5g). At this level it passed to Constant Drag. The intent with capture assured (g>1.5), is to reach a safe constant g (DO$\sim$4.g). The sequence of Initial Roll-Constant Drag is maintained during each 2-second pass until just before pullout, RDOT equal to -700.fps, when the Mode Selector steps to Huntest.

A2.1.2.3 Huntest. Figure A1-9

Key trajectory shaping, with range to the target as the dependent variable, is based upon guiding the spacecraft along a computed reference trajectory to exit, a ballistic lob and finally guidance along an internally-stored reference trajectory. Huntest performs the following:

1. Predicts pullout drag level, pullout velocity, and both altitude rate and atmosphere exit velocity VL, at the end of the first guided phase. For a VL <18,000.fps the guidance transfers to the final guided phase.

2. If the predicted VL of the first guided phase is greater than circular speed (VSAT = 25,766.fps), indicating a skip, the guidance is recycled to the Constant Drag Phase. This is repeated at each guidance cycle until the VL, now safely below VSAT, permits an estimate of range capability. Range prediction is based upon an L/D of 0.15 for the first guided phase, a Keplerian lob for the ballistic portion and half full lift for the final guided phase. If predicted range agrees with the required range within 25.nm the planned trajectory is accepted; if the prediction is for an overshoot, the guidance reverts to Constant Drag and recomputes the Huntest prediction 2-seconds later.

For short range targets i.e., 1350.nm, the repeated cycling through Constant Drag causes VL to drop below 18,000.fps. Control then shifts to the final phase.

A2.1.2.4 Upcontrol. Figure A1-10

Assuming the range sufficiently long to require this phase, i.e., greater than 1400.nm, the guidance attempts to fly the Command Module to the computed VL. Two checks are made on the drag level:

1. To prevent cross-range logic from adversely affecting down-range performance, roll reversals are barred from drag levels above 4.35g.

2. Roll commands greater than 90.°, i.e., negative lift, are not permitted for aerodynamic decelerations greater than 5.44g. This logic, the source of the incompatability between the primary and backup guidance, is discussed in Section 9 of the text.

If the drag drops below approximately 0.2g, guidance transfers to the ballistic phase. If the drag is greater than 0.2g but the altitude rate is negative and the velocity is within 500.fps of VL, the guidance concludes that there is no need for a ballistic phase and moves to the final phase.

A2.1.2.5 Kepler. Figure A1-11

Assuming the range is sufficiently long, e.g. >1800.nm, a ballistic phase is necessary following Upcontrol. The last roll command prior to 0.2g is maintained, however should the drag fall below 0.05g, roll is set to full up (heads down) to permit a horizon check. Attitude hold is maintained until 0.2g when control shifts to the final phase.

A2.1.2.6 Final Phase. Figure A1-12

Approximately 500.nm from the landing, terminal guidance starts, based upon a stored reference trajectory. Sensitivities of range with respect to altitude rate and drag are used to compute the down-range capability. With the range partial as a function of L/D, the difference between range capabilities and actual range-to-go is used to compute the L/D necessary to null the range-to-go error. This is the only phase where range-to-go error is continuously nulled.

A2.1.2.7 Constant Drag. Figure A1-13

Prior to trajectory planning by the computer, this phase tries to maintain a safe drag level DO ($\sim$4.g). During and following planning, this guidance eliminates excess energy, thus avoiding target overshoot. Commanded roll is based upon L/D balancing gravity and centrifugal force, and then nulling the drag deviation from DO. If drag exceeds 5.44g only zero or positive lift is permitted, with all rolls for lateral control going over the top.

A2.1.2.8 G Limiter. Figure A1-14

If acceleration is between 4. and 8.g, altitude rate is compared to a computed rate which, with full lift up, results in 8.g peak acceleration. If the sensed or predicted acceleration is 8.g or more, full up lift is commanded.

A2.1.2.9 Lateral Logic. Figure A1-15

A conservative lateral range capability is computed and compared with present cross-range error. Should the error exceed the capability during the guidance cycle, the lift vector is reflected about the vertical plane. In the specific situation when the roll angle command is 0.° (full up) or 180.° (full down), the command is modified to $\pm$15.° or $\pm$165.°. While having little influence on down-range capability, the change materially affects lateral ranging.

A2.2 BACKUP SYSTEMS

A2.2.1 Entry Monitoring System

Similar to the primary system, the EMS has as its objectives safe entry and landing point control.(5) While making no compromise on safety, the EMS has no specification on ranging accuracy. The EMS sensor, shown in Figure A1-16, is a single strapped-down accelerometer mounted with its sensitive axis along the spacecraft axis of symmetry. EMS inertial velocity and range are calculated as:

$$VEMS = V_o - 0.948 \int_o^t A \, dt, \text{ fps}$$

V_o = initialized velocity, fps

A = sensed acceleration, fps^2

$$R = R_o - 0.00162 \int_o^t VEMS \, dt, \text{ nm}$$

R_o = initialized range, nm

A2.2.1.1 Threshold Indicator

As a visual indication of when the vehicle is in the atmosphere, an indicator lamp lights at 0.05g and is extinguished if the sensed acceleration falls below 0.02g.

A2.2.1.2 Corridor Verification and Roll Attitude Indicator

Ten seconds after 0.05g the measured acceleration is compared to a preset level (0.262g). If the sensed g is lower, indicating a shallow entry angle, the lift-vector down light is illuminated. A sensed acceleration greater than the 0.262g calls for a lift up command.

Vehicle roll attitude supplied by body mounted gyros is a part of the corridor verification assembly. The pilot, via the SCS, manually rolls the spacecraft to the desired orientation.

A2.2.1.3 Flight Monitor

Illustrated in Figures A1-16, A1-17, and A1-18a, the key display is a real-time scroll recording of sensed acceleration G against EMS velocity V. Preprinted on the scroll are two patterns: a 3500.nm Range Limit Pattern, premitting g levels below 0.2g, intended to limit range to 3500.nm, and a Non-exit Pattern intended to limit minimum g to 0.2 and range to 3500.nm, whichever is most constraining. For ranges under 1500.nm the Non-exit Pattern is used; for ranges over 2100.nm the pilot uses the 3500.nm pattern. Between these ranges pattern selection is a function of the position of V and γ in the corridor.

Prior to entry and based upon data supplied from the ground, the G-V scroll is initialized by aligning the inertial velocity expected at 0.05g with the stylus. By comparing the generated G-V trace with the preprinted scroll, the pilot monitors the performance of the automatically guided entry. If necessary, he flies the entry using only the EMS. On the scroll the g-onset pattern corresponds to the limiting state of g, $\frac{dg}{dV}$, and V. If the G-V trace becomes parallel to or steeper than the onset lines with CM lift down, the spacecraft may experience greater than 10.g during pullout. Thus if the G-V trace violates the onset lines and the spacecraft roll is anything but 0.° ±15.°, the pilot rolls to a full up condition. Similarly, if the G-V trace is parallel to or steeper than the g-offset lines and the spacecraft has lift full up, the spacecraft may skip out, violating the range-limit or the minimum g constraint or both. When the G-V trace violates the offset lines and the roll is anything but 180.° ±15.°, the pilot rolls full down. Onset and offset lines do allow for a 2-second crew-response time and for the time necessary for a 180.° roll maneuver.

Of current interest is the scroll of Figure A1-18b which shows the PGNCS entry trace as monitored by the crew of the Apollo 11 Lunar Landing Mission.

A2.2.1.4 Range-to-go Counter

The pilot initializes the counter with a ground-supplied range, computed either by a simulated EMS in a digitial simulation of the anticipation automatically-guided entry, or by the flight computer. Following the start of entry, the EMS range -- the time integral of computed velocity -- is subtracted from the initial range-to-go. Using the continuous display of range-to-go and the stylus path across Range Potential lines on the scroll, the pilot modulates the roll to null the range difference. The numbers on the lines indicate range capability, in hundreds of nautical miles, if the spacecraft maintains a constant g. As the pattern moves across the scribe, the pilot compares range-to-go with range capability. Should he be in danger of landing short of the target, he rolls lift up to a lower g region increasing vehicle range capability. In practice, once safe entry is achieved through the avoidance of excessive g at pullout and later the avoidance of skipout, the pilot maneuvers the CM into a low g region to achieve an excess of range capability. He maintains this condition until the G-V trace nears the end of the scroll. He then rolls to a higher g region matching range capability with requirements through to the end of the trajectory.

A2.2.2 Constant g Entry

Should both primary guidance and the EMS fail prior to entry, the pilot can execute a safe entry by flying a constant g on his G-meter. Completely separate from the EMS, his sensor, an accelerometer with sensitive axis parallel to the spacecraft axis of symmetry, displays g-level via a mechanical pointer against a scale. One of two guidance methods is used depending upon the availability of ground information. With normal communications, a ground-computed g level, between 3. and 5.g, a function of range, is voiced to the pilot. With the voice link out the pilot flies a preselected, probably 4.g, entry.

A3.0 HYBRID ENTRY SIMULATION (HES)

A3.1 Computer System-General Description

The form of the required simulation may be visualized with the aid of the block diagram in Figure A1-19. Spacecraft behavior as described by the real world differential equations of motion, is controlled by either the primary guidance loop or the backup guidance. Each loop contains sensors, navigation, guidance philosophy and a means for executing a change in roll attitude.

Selection of the type of simulation was resolved by first itemizing the simulation requirements:

1. Real-time simulation to interface with the pilots.

2. Slowly varying translational dynamics where accuracy -- and more important, repeatability, to approximately 5.nm in latitude and longitude -- is important.

3. Rotational dynamics of moderate accuracy and repeatability: equipment primarily necessary to provide the pilot with the correct feel, i.e., speed of response.

4. Computer equipment necessary to provide the analog display and digital control of the primary system.

5. Computer equipment necessary to provide the digital and analog displays and the analog control of the backup system.

There followed considerations of cost, availability of equipment in the hands of experienced personnel, and experience by others in real-time engineering simulations of entry. A review of all factors led to the selection of a hybrid computer system.(6)

The computational factors are emphasized when one looks at the diagrams of Figures A1-20 and A1-21. Translation equations are performed digitally. Requiring more in the way of speed and response, rotational computations are performed on the analog. Translation sensor data is used in the digital guidance computer to produce a roll command which is fed to the Digital Autopilot. Analog rotational data is transformed for use in the DAP.

Backup system sensors consist of two accelerometers -- digitally simulated -- and roll and yaw rates from the analog. Rotational rates, combined and integrated, produce EMS roll. Digital acceleration, converted to analog for the G-meter and G-V display, is integrated twice on the analog to produce EMS velocity and range. Simulated on the analog, the backup attitude control system compares roll rate to hand controller deflection in providing the control signals to the roll jet logic. In summary then, the broad capability of hybrid was put to good use in meeting the diverse needs of the entry simulation.

A3.2 Six-Degree of Freedom Simulation

In the digital half, shown in Figure A1-20, aerodynamic forces and gravity are integrated twice to yield translational velocity and position. Aerodynamic velocity, combines with Euler angles from the analog to produce aerodynamic coefficients. These coefficients, a function of the orientation of the aerodynamic velocity in body axes, determine the aerodynamic forces, thus closing the loop.

Aerodynamic torques about the spacecraft center of gravity are converted to analog for use in the rotation equations of Figure A1-21. Here they are combined with jet torques to provide total moments. The rotation rate computation in principal coordinates saves computing equipment in spite of the coordinate transformations. Body rates, combined to form Euler angle rates, are integrated and converted to digital form for use in the aerodynamic coefficient calculation described previously.

A3.3 Simulation Hardware

An EAI (Electronic Associates, Inc.) 690 Hybrid Computer, supplemented by an EAI TR-48 Analog Computer were programmed to perform the entry simulation. The 690 consisted of a 680 Analog Computer, a 640 Digital Computer and a 693 Interface System. Equipment characteristics are as follows:

640 Digital Computer

- 16,184 words of 16 bit storage.
- Add time 3.3 microseconds.
- High speed paper tape punch and reader.
- Teletypewriter.
- Card Reader.
- Line Printer.

680 Analog Computer

- 156 amplifiers, 500 khz bandwidth.
- 30 integrators and 24 multipliers.
- 132 Potentiometers.
- 1 X-Y plotter.
- 2 eight channel recorders.

693 Interface System

- Control interface for monitoring component and setting potentiometers.
- 20 channels of analog to digital conversion.
- 16 channels of digital to analog conversion.

TR-48 Analog Computer

- 58 Amplifiers.
- 16 integrators and 6 multipliers.
- 60 potentiometers.

Equipment listed is presented in the photographs of Figures A1-22 through A1-25. The 680 Analog Computer with the patch panel in place is shown in the right in Figure A1-22. In the background from right to left are the two eight-channel recorders, the 693 Interface, the 640 Digital Computer and the TR-48. Shown in Figure A1-23 supplemented by logic and relay circuitry built for the simulation, the TR-48 serves to

interface between the 690 hybrid and the displays and controls in the spacecraft mockup. A partial view of the mockup is shown in the room at the left of the figure. In the foreground of Figure A1-23 are the various digital input and output devices listed above.

Located on top of the recorders in Figure A1-22, and repeated in Figure A1-24, is the EMS G-V display generator. A standard plotter was modified to permit the mounting of a television camera on the X-translation carriage. The resulting G-V trace on the preprinted pattern is transmitted to the picture tube on the EMS panel in the CM mockup. CM mockup displays and controls are shown in Figure A1-25. The EMS display includes the G-V display picture tube, lift vector indicator, and range-to-go counter. The G-meter, FDAI and an event timer are directly below the EMS. A number of inactive switches are provided to add realism to the pilots display area of interest. Scaling switches for the FDAI and mode and control switches needed for entry are active. The FDAI and the hand controller, are Block I flight hardware.

A3.4 Simulation Model

There are various characteristics such as atmospheric variations and L/D ratio which under a broader study might be parameters. For this study they remained constant.

A3.4.1 PGNCS Control

In the automatic guidance mode rotation control was via the digital autopilot (7), a bang-bang controller in roll, designed around an acceleration of $4.55°/sec^2$ and a speed of 20.°/sec.

A3.4.2 SCS/EMS Control

Hand-controller roll deflection produced a signal in the roll and yaw channels. Rate feedback in both channels combined to produce a coordinated roll rate about the aerodynamic velocity vector. Maximum rate was approximately 20.°/sec in roll and 7.°/sec in yaw.

A3.4.3 Vehicle Configuration

Moment Table: Table A1-1

Aerodynamic Table: Table A1-2

Aerodynamics included a pitch and yaw damping coefficient of -0.3.

Lift to Drag Ratio: 0.291

L/D was set by location of the center of gravity.

Weight: 12,121.5 lbs.

Inertial Tensor: slug-ft^2

$$\begin{bmatrix} 6250. & -60.2 & 446.1 \\ & 6434. & -51.9 \\ & & 5851.2 \end{bmatrix}$$

A3.4.4 Environment

Atmosphere: U.S. Standard Atmosphere, 1962.

Gravity Model: Based on Fisher Ellipsoid with first harmonic term.

Earth Model: Spherical.

A3.5 Simulation Validation

The Hybrid Entry Simulator was compared to four simulations associated with the Apollo Project.(8)(9) They included a Bellcomm 4-degree-of-freedom digital simulation, two similar to Bellcomm's digital entry simulator, and a hybrid 6-degree-of-freedom system. Test run parameters included speed, flight-path angle, weight and atmosphere. The lifting profiles comprised rolling at 20.°/sec, zero lift (90.° roll), and full lift up. Comparison was in terms of state variables as a continuous function of time and state varaiables at termination. The table below, with standard deviation and mean based upon the three non-Bellcomm simulations, provides a basis for comparison.

Case	1	2	3	4	5
Latitude*					
Standard Deviation (σ_1).	0.01°	0.03°	0.09°	0.06°	0.22°
HES deviation from mean.	$0.8\sigma_1$	$1.5\sigma_1$	$1.0\sigma_1$	$1.4\sigma_1$	$0.4\sigma_1$
Longitude					
Standard Deviation (σ_L).	0.11°	0.13°	0.52°	0.12°	0.74°
HES deviation from mean.	$2.5\sigma_L$	$1.8\sigma_L$	$0.1\sigma_L$	$0.8\sigma_L$	$0.1\sigma_L$

*All terminal latitudes were between 29.8° and 33.0°.

As described in Reference 8, a comparison of the results led to the conclusion that the Hybrid Entry Simulation was acceptable for generating data.

APPENDIX I: REFERENCES

1. Likely, D. J., H. R. Morth, B. S. Crawford, Apollo Reentry Guidance, MIT/SL, Report R416, August 1963.

2. Apollo Program Specification, Office of Manned Space Flight, Document SE 005-001-1 Revision B, Paragraphs 3.5.1.22 and 3.5.2.5.2, May 1969.

3. Wingrove, R. C., A Survey of Atmosphere Reentry Guidance and Control Methods, IAS Paper Number 63-86.

4. Entry Monitoring and Backup Control Procedures for Lunar Return Trajectories, NASA/MSC Internal Note Number 69-FM-22, January 31, 1969.

5. Frank, A. J., E. F. Knotts, B. C. Johnson, An Entry Monitoring System for Maneuverable Vehicle, Journal of Spacecraft, Volume 3, Number 8, August 1966.

6. Hybrid Entry Simulation of the Apollo Vehicle, Electronic Associates Washington Analysis and Computation Center Report.

7. Heiber, A., R. Singers, Classification of Entry DAP for Entry Monitoring System Hybrid Simulation, Bellcomm Internal Document, January 18, 1968.

8. Bogner, I, S. B. Watson, Reentry Simulation Comparison, Bellcomm Technical Memorandum Number TM-69-2014-1, January 28, 1969.

9. Voybeck, V. W., J. MacParks, Reentry Simulation Comparison, NASA Action Document Number AD 30-617-20.

TABLE A1-1

COMMAND MODULE REACTION JET MOMENTS (ft - lbs) - SINGLE SYSTEM

AXIS	ROLL MOMENT	PITCH MOMENT	YAW MOMENT
+Roll	+480.2	+067.5	-012.5
-Roll	-452.5	-002.8	+068.6
+Pitch	-000.2	+515.6	+031.3
-Pitch	+007.1	-341.3	+037.7
+Yaw	-029.6	+061.5	+485.3
-Yaw	+029.6	+002.6	-473.5

TABLE A1-2

COMMAND MODULE REENTRY AERODYNAMIC COEFFICIENTS

PITCH PLANE DATA

Alpha	C_L	C_D	L/D	C_N	C_A	C_{M_A}
			HYPERSONIC MACH RANGE			
110.1365	0.0495	0.4107	0.1206	0.3686	-0.1879	-0.2099
115.1365	0.1643	0.4286	0.3833	0.3182	-0.3308	-0.1610
120.1365	0.2710	0.4706	0.5760	0.2709	-0.4706	-0.1178
125.1365	0.3704	0.5328	0.6952	0.2225	-0.6095	-0.0770
130.1365	0.4330	0.6244	0.6934	0.1983	-0.7335	-0.0547
135.1365	0.4801	0.7403	0.6485	0.1819	-0.8634	-0.0410
140.1365	0.4983	0.8599	0.5795	0.1687	-0.9794	-0.0328
145.1365	0.5021	0.9699	0.5177	0.1424	-1.0828	-0.0194
150.1365	0.4815	1.0799	0.4458	0.1202	-1.1763	-0.0103
155.1365	0.4457	1.1901	0.3745	0.0960	-1.2672	-0.0016
160.1365	0.3867	1.2906	0.2997	0.0748	-1.3452	0.0033
165.1365	0.3118	1.3800	0.2259	0.0526	-1.4138	0.0083
170.1365	0.2202	1.4447	0.1524	0.0305	-1.4611	0.0114
175.1365	0.1144	1.4797	0.0773	0.0115	-1.4840	0.0129
180.1365	0.0000	1.4900	0.0000	-0.0035	-1.4900	0.0137
185.1365	-0.1144	1.4797	-0.0773	-0.0185	-1.4840	0.0144
190.1365	-0.2202	1.4447	-0.1524	-0.0375	-1.4609	0.0158

Note:

Moment reference center is at X_A = 1141.25 inches, Y_A = 0.0 inch, Z_A = 0.0 inch (CM theoretical apex).

Reference length (d) = 154.0 inches. Reference area = 129.4 square feet.

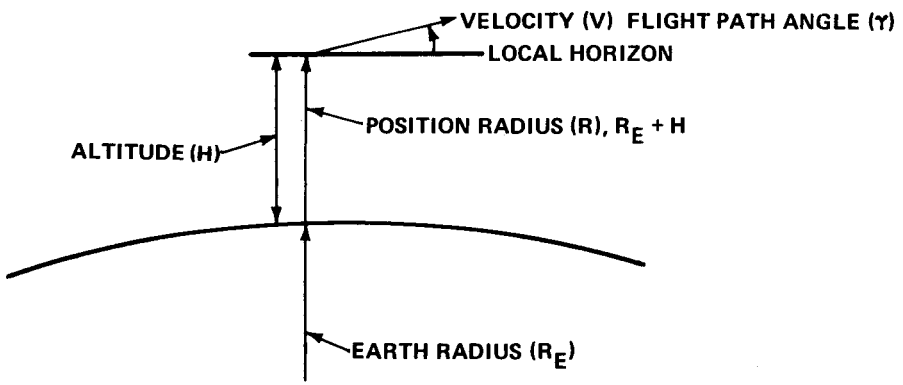

FIGURE1a VERTICAL PLANE OF MOTION TRAJECTORY PARAMETERS

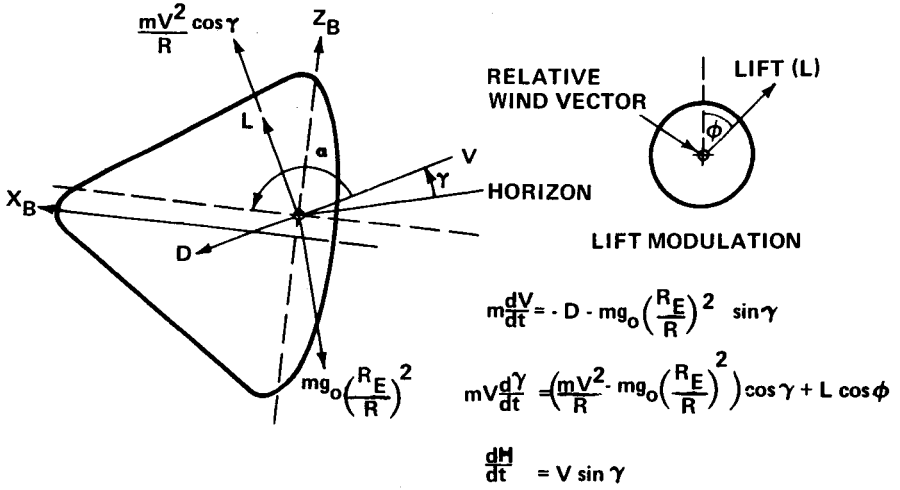

FIGURE 1b VERTICAL PLANE POINT MASS EQUATIONS OF MOTION

FIGURE AI-1 - ENTRY GEOMETRY

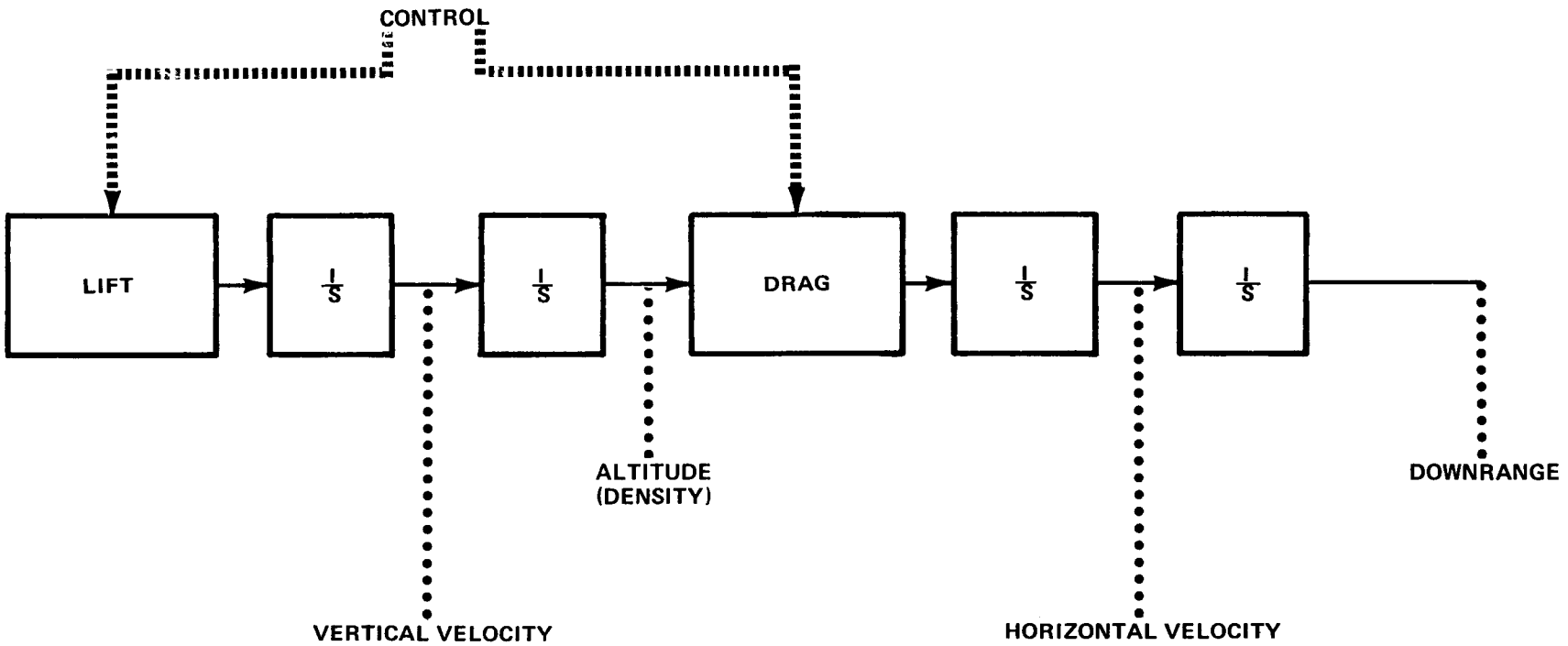

FIGURE AI-2 - RELATIONSHIP BETWEEN CONTROL AND DYNAMICS.

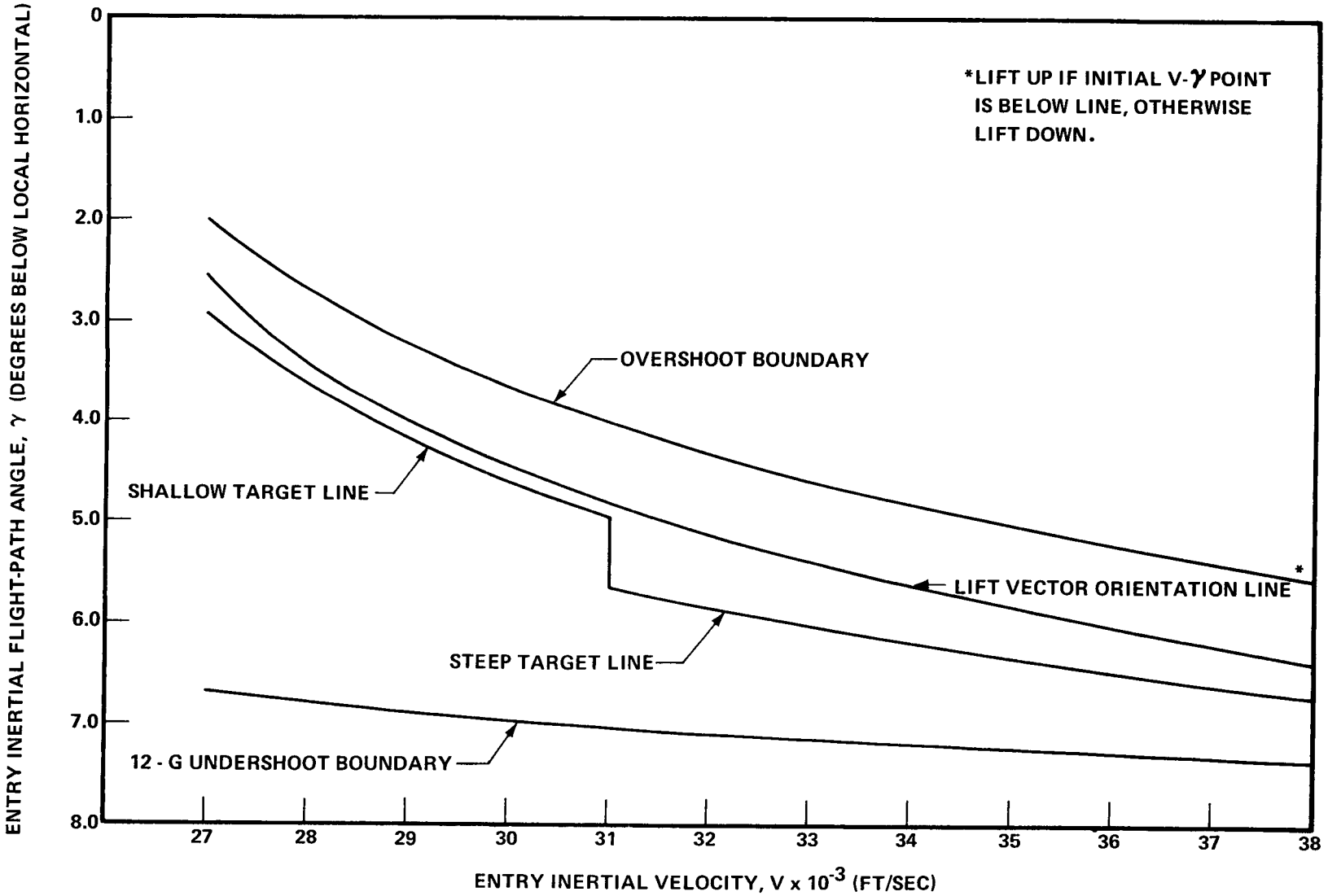

FIGURE AI-3 - MOST RESTRICTIVE ATMOSPHERIC ENTRY CORRIDOR FOR MISSION C'.

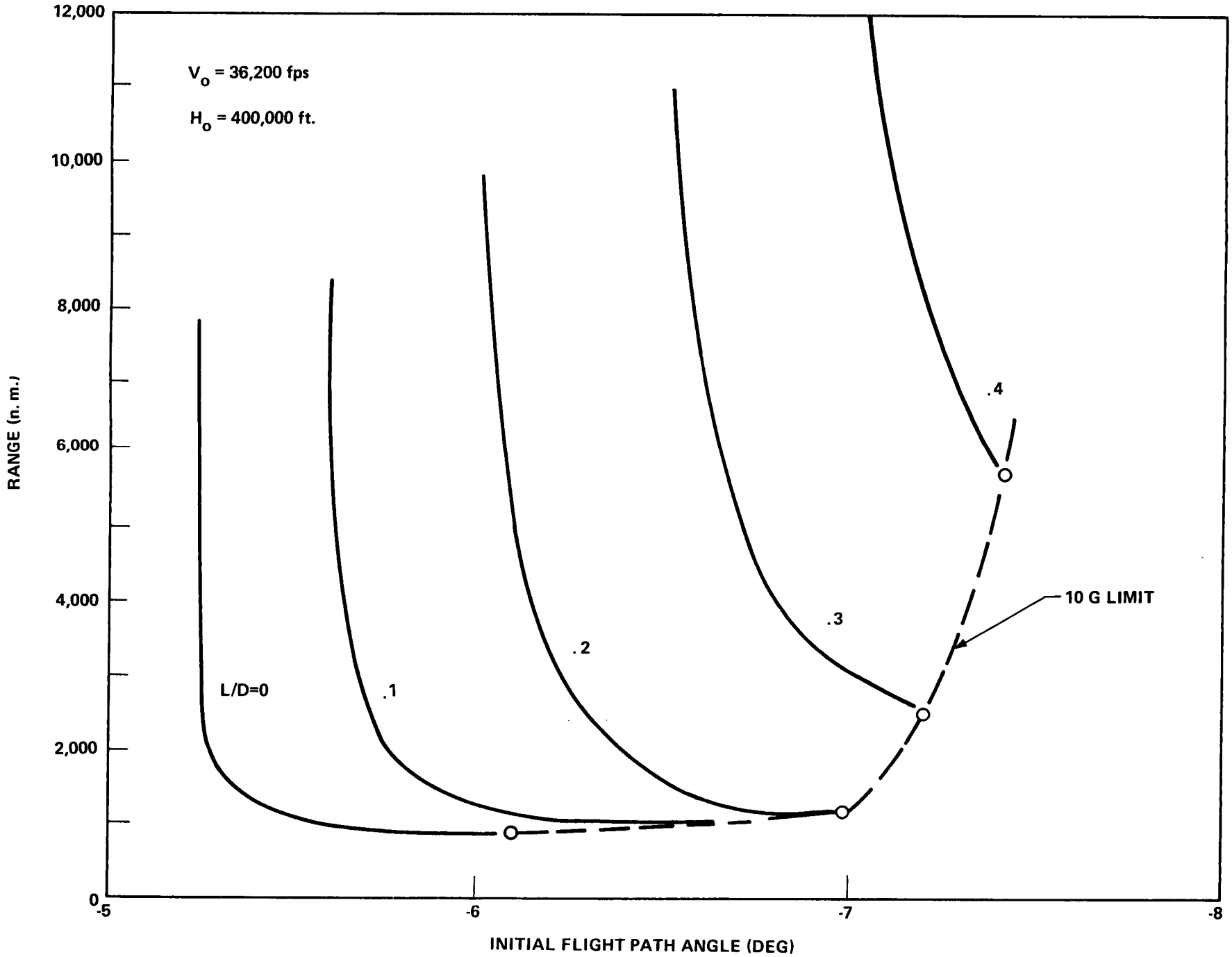

FIGURE AI-4 - RANGE CAPABILITIES

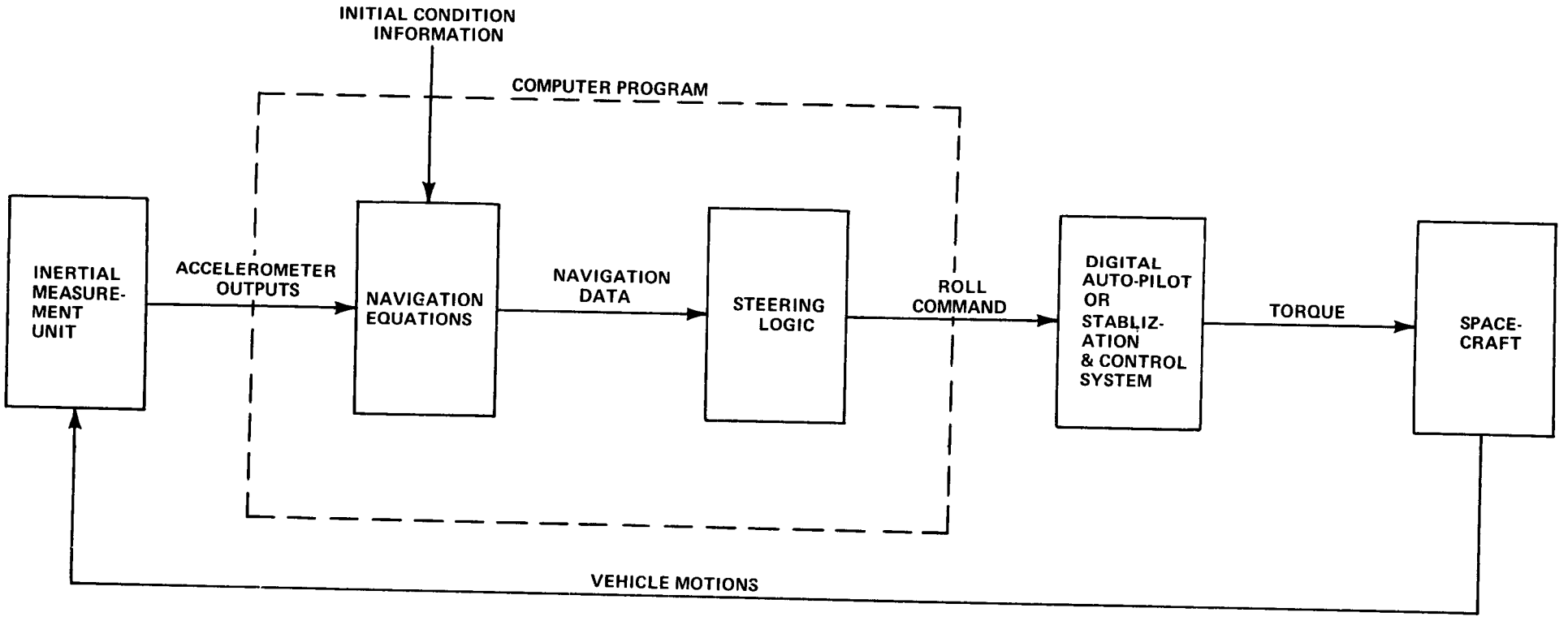

FIGURE AI-5 - PRIMARY SYSTEM BLOCK DIAGRAM

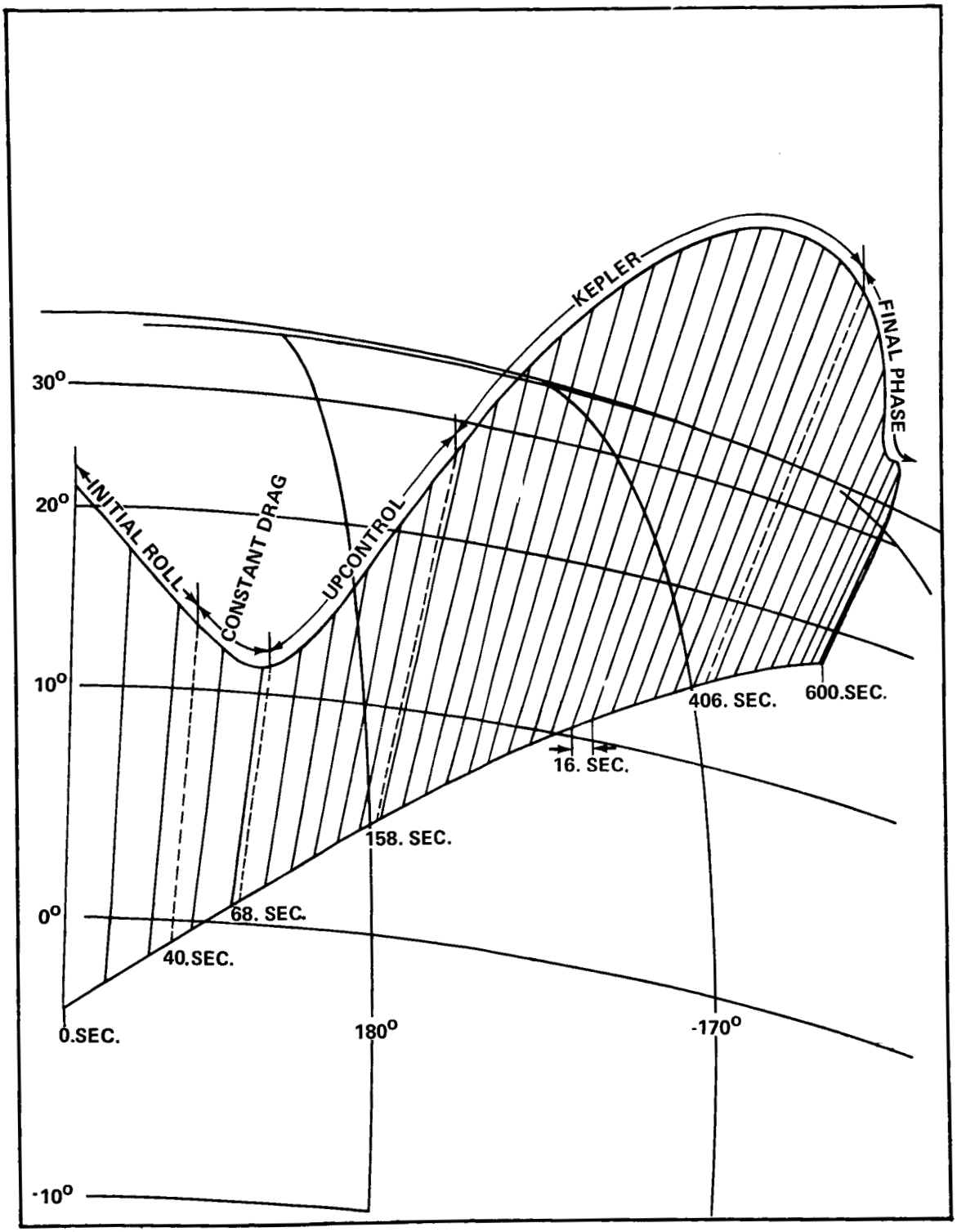

RANGE = 1866.N.M.
ALT = 20x

FIGURE AI-6a - PICTORIAL VIEW OF ENTRY TRAJECTORY-EXPANDED SCALE

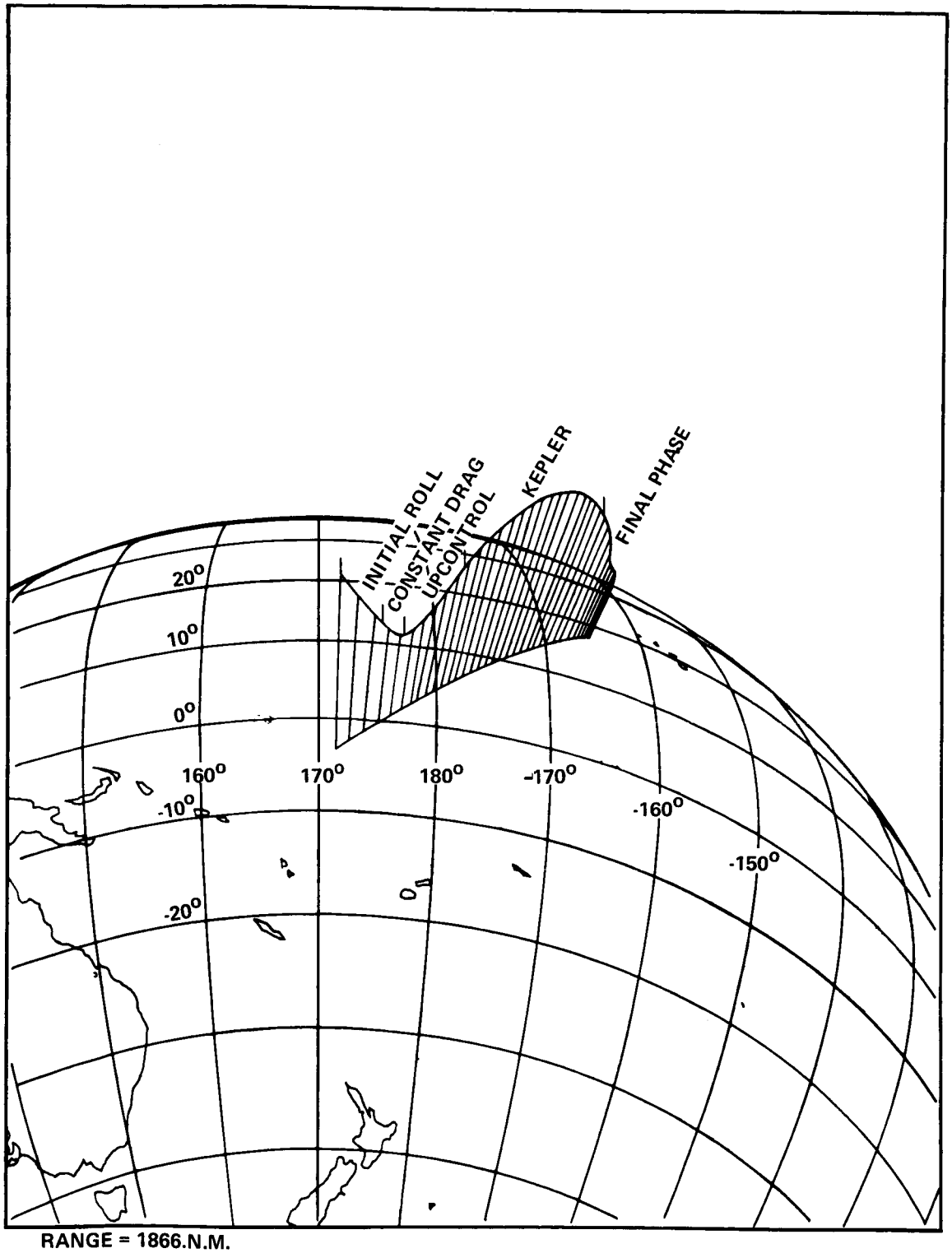

RANGE = 1866.N.M.
ALT = 20x

FIGURE AI-6b - PICTORIAL VIEW OF ENTRY TRAJECTORY - COMPRESSED SCALE

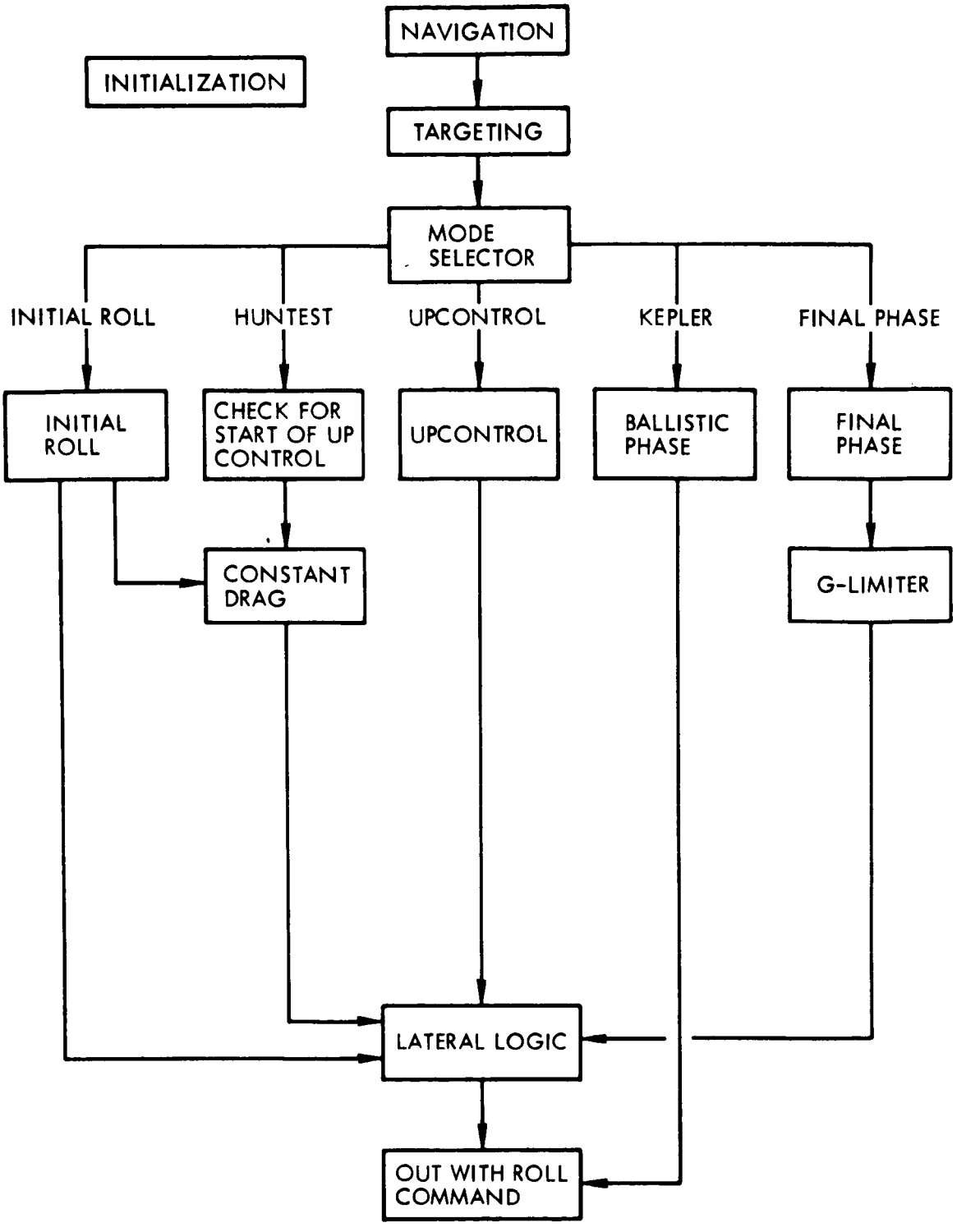

FIGURE AI-7 - PRIMARY GUIDANCE BLOCK DIAGRAM

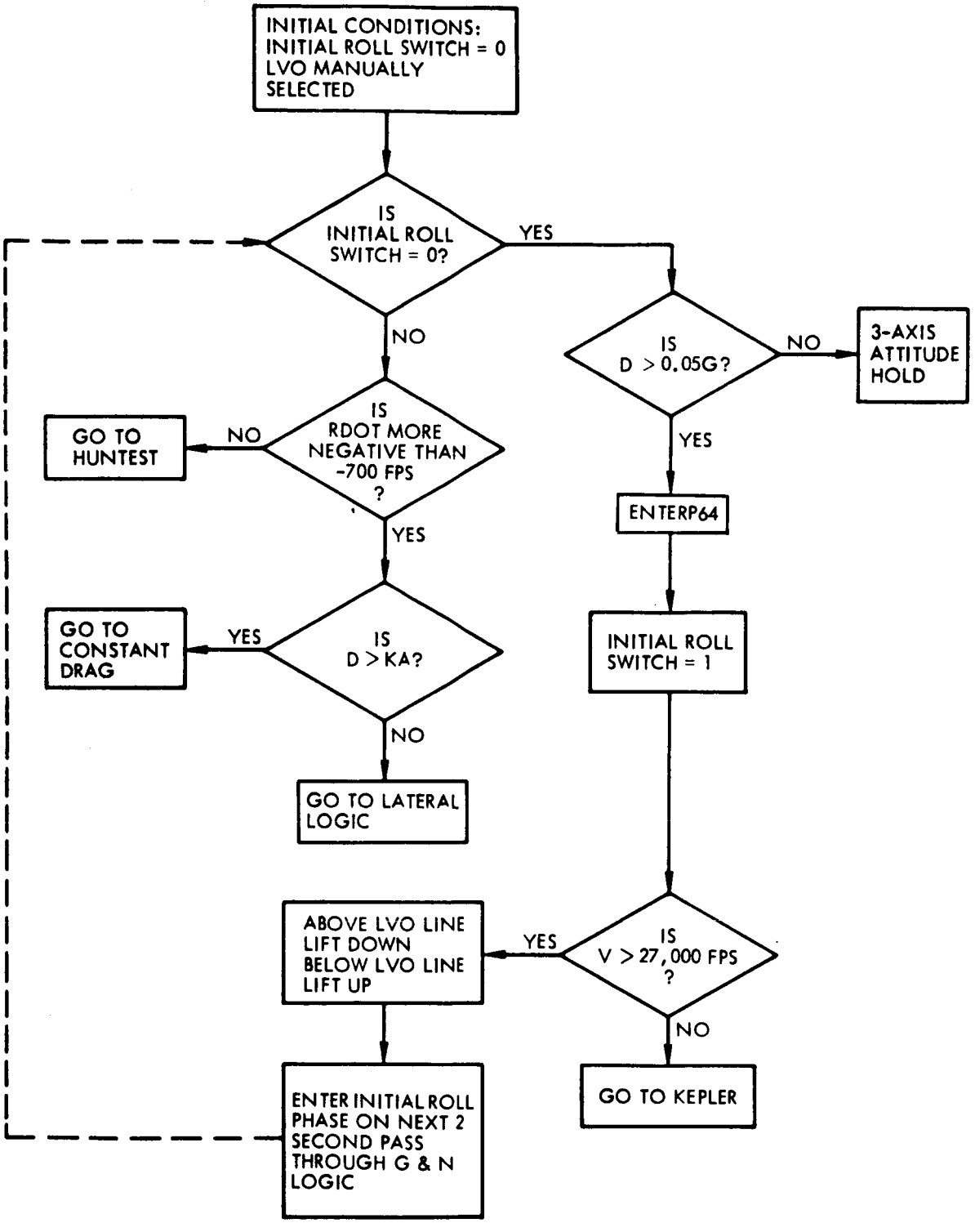

FIGURE AI-8 - INITIAL ROLL PHASE (P63 AND 64)

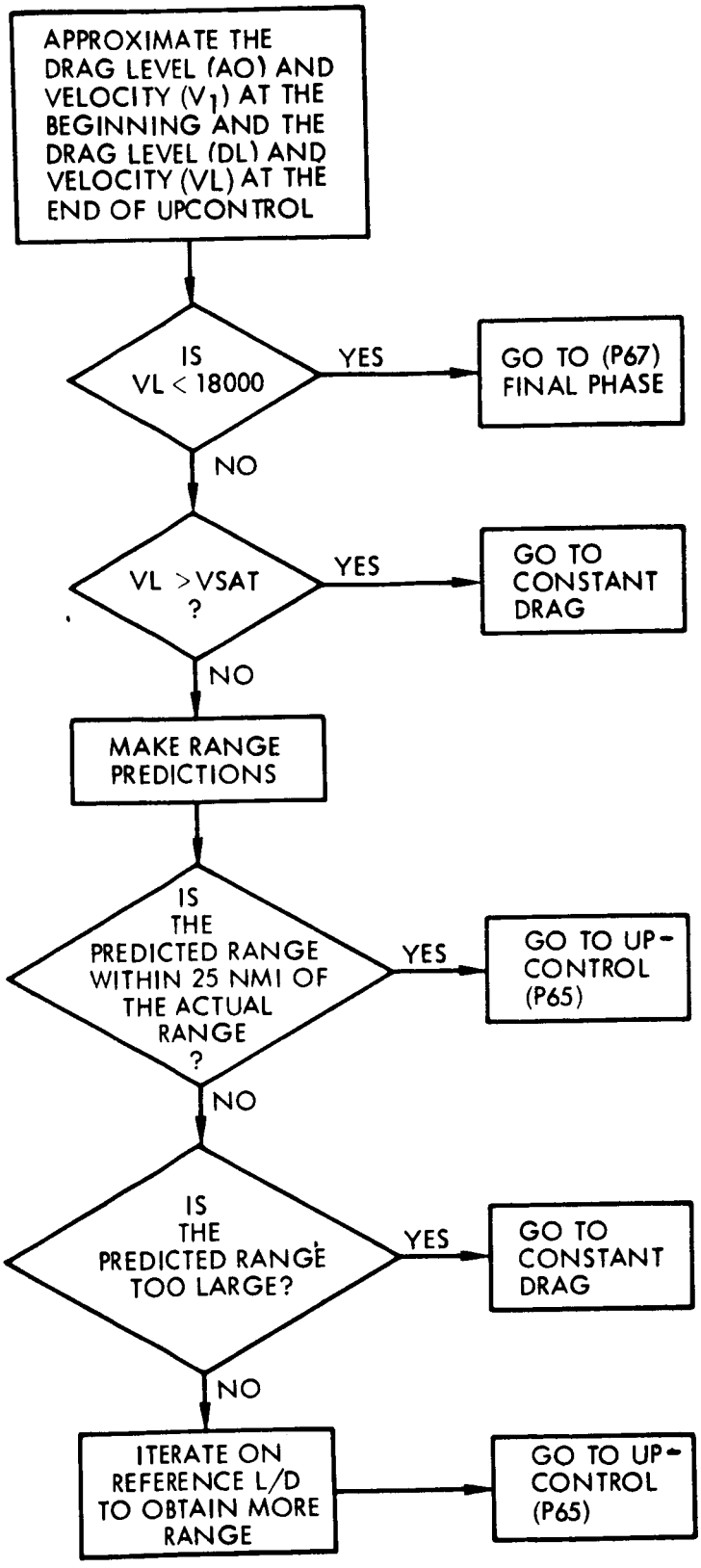

FIGURE AI-9 - HUNTEST PHASE (P64)

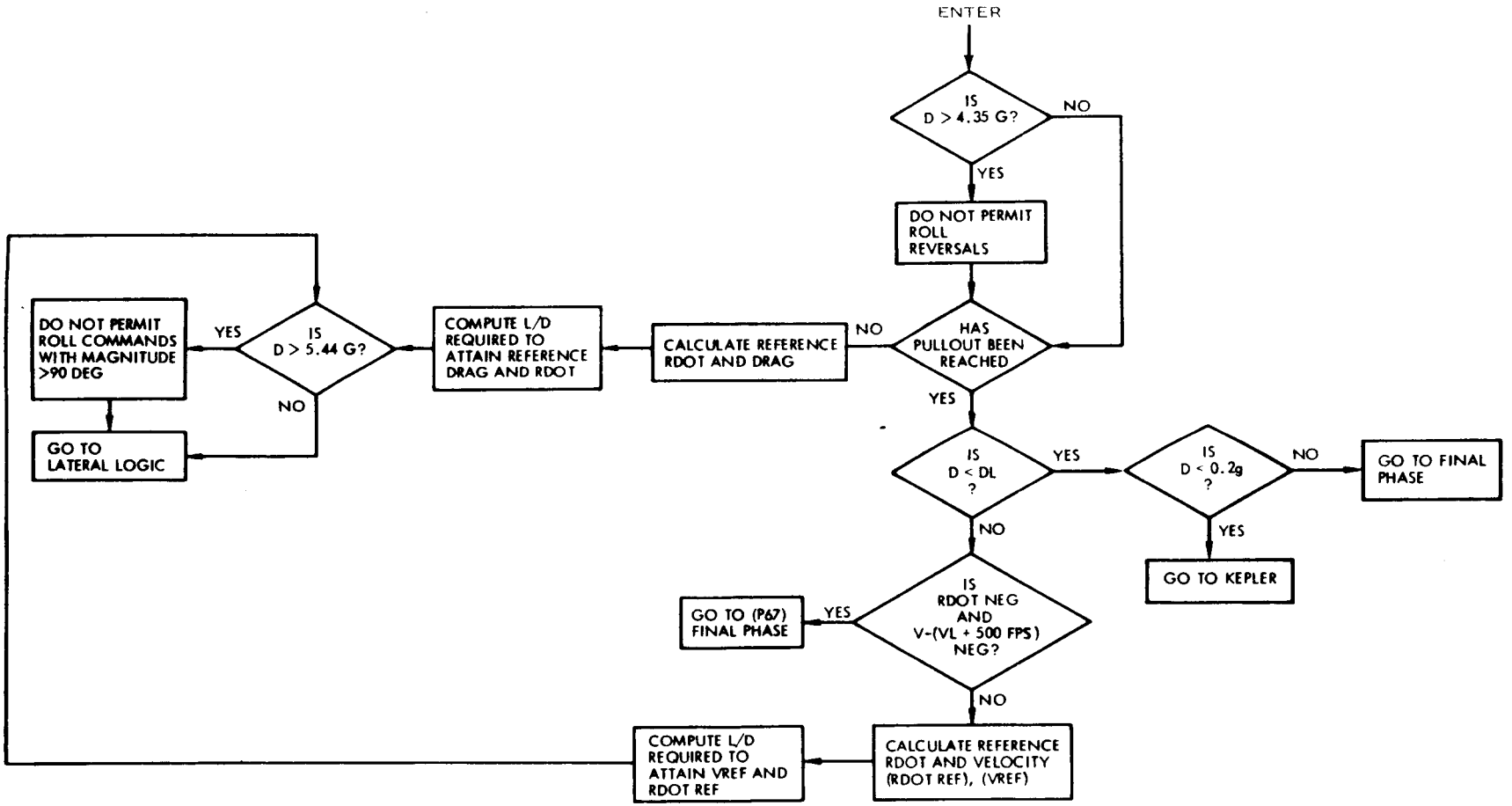

FIGURE AI-10 - UPCONTROL PHASE (P65)

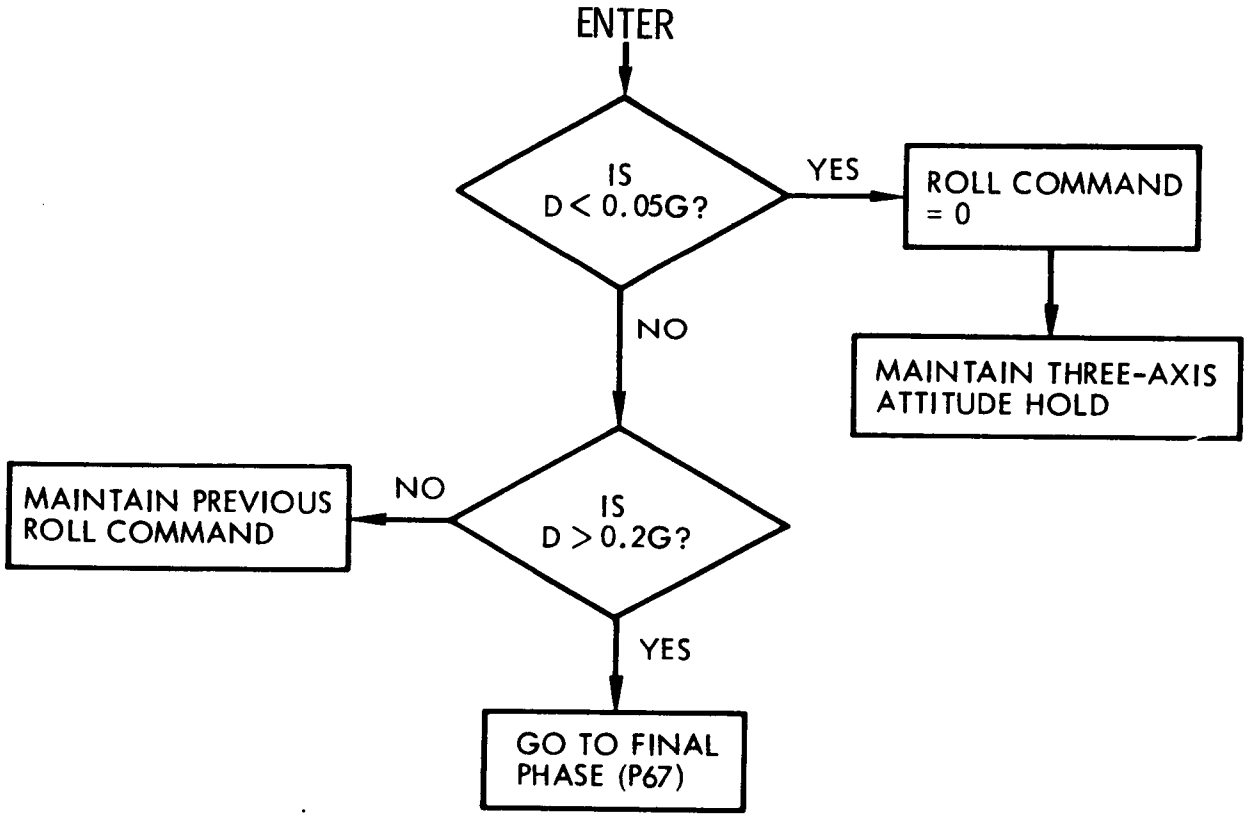

FIGURE AI-11 - BALLISTIC (KEPLER) PHASE (P66)

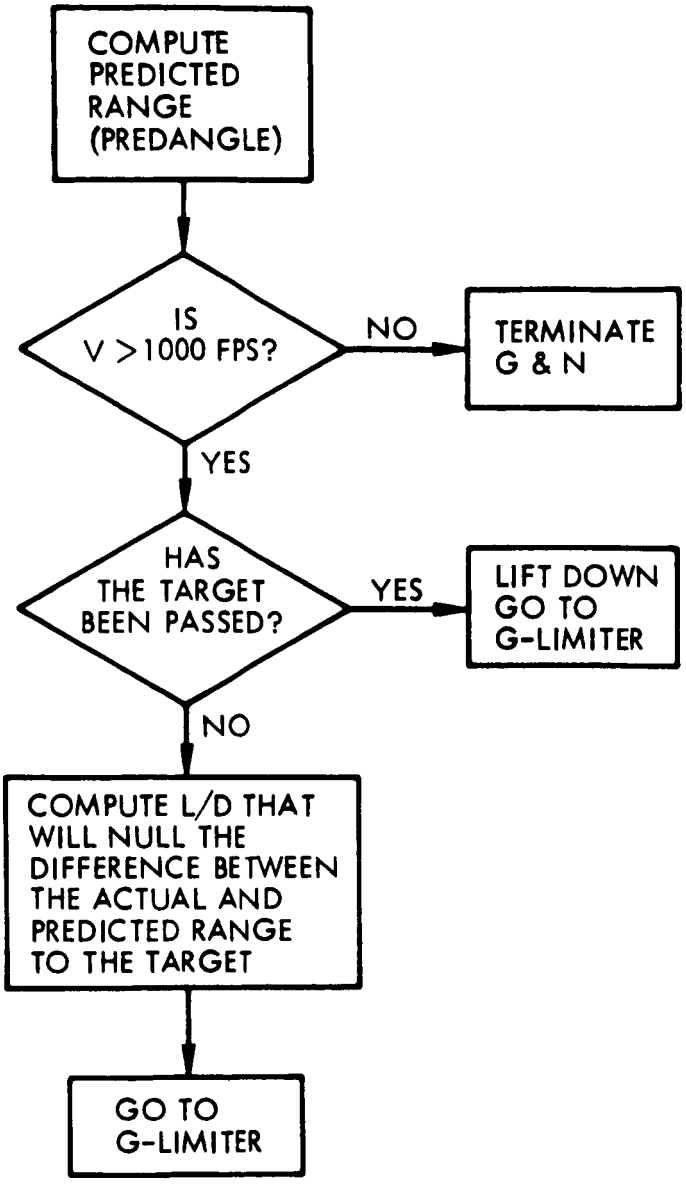

FIGURE AI-12 - FINAL PHASE (P67)

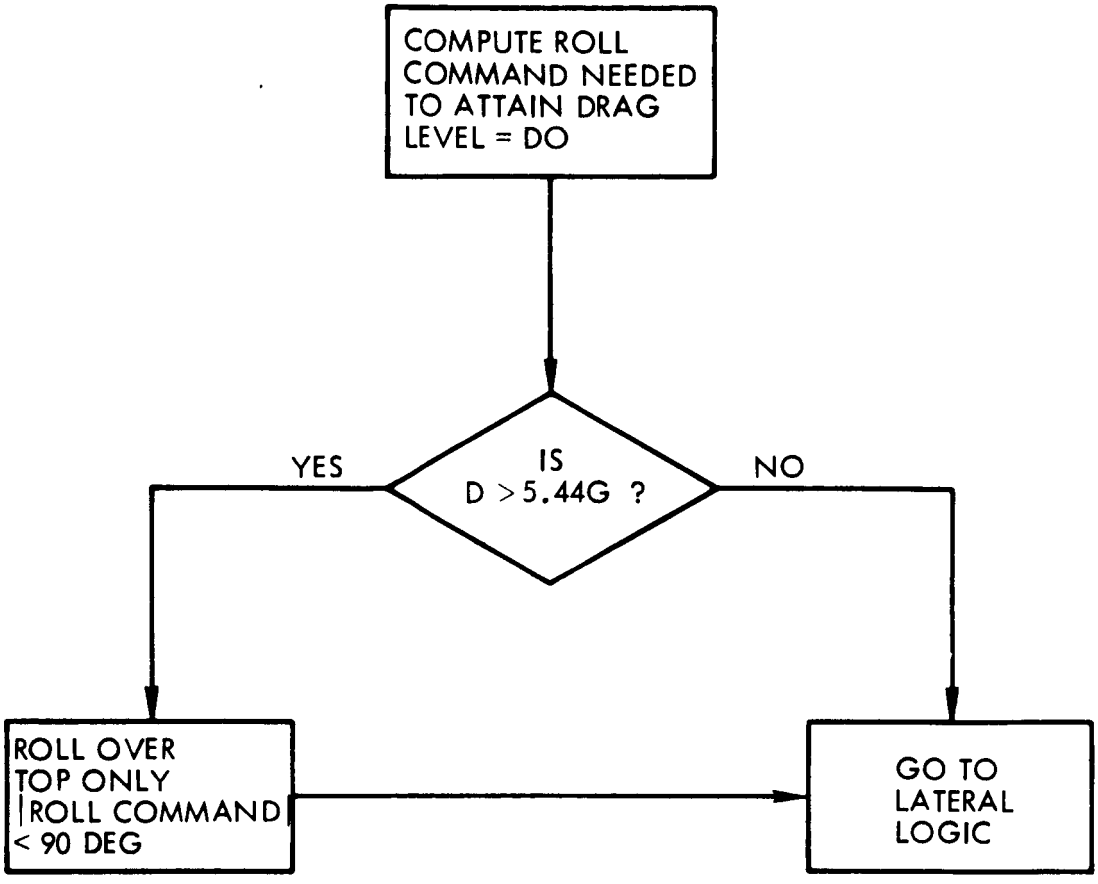

FIGURE AI-13 - CONSTANT DRAG LOGIC (P64)

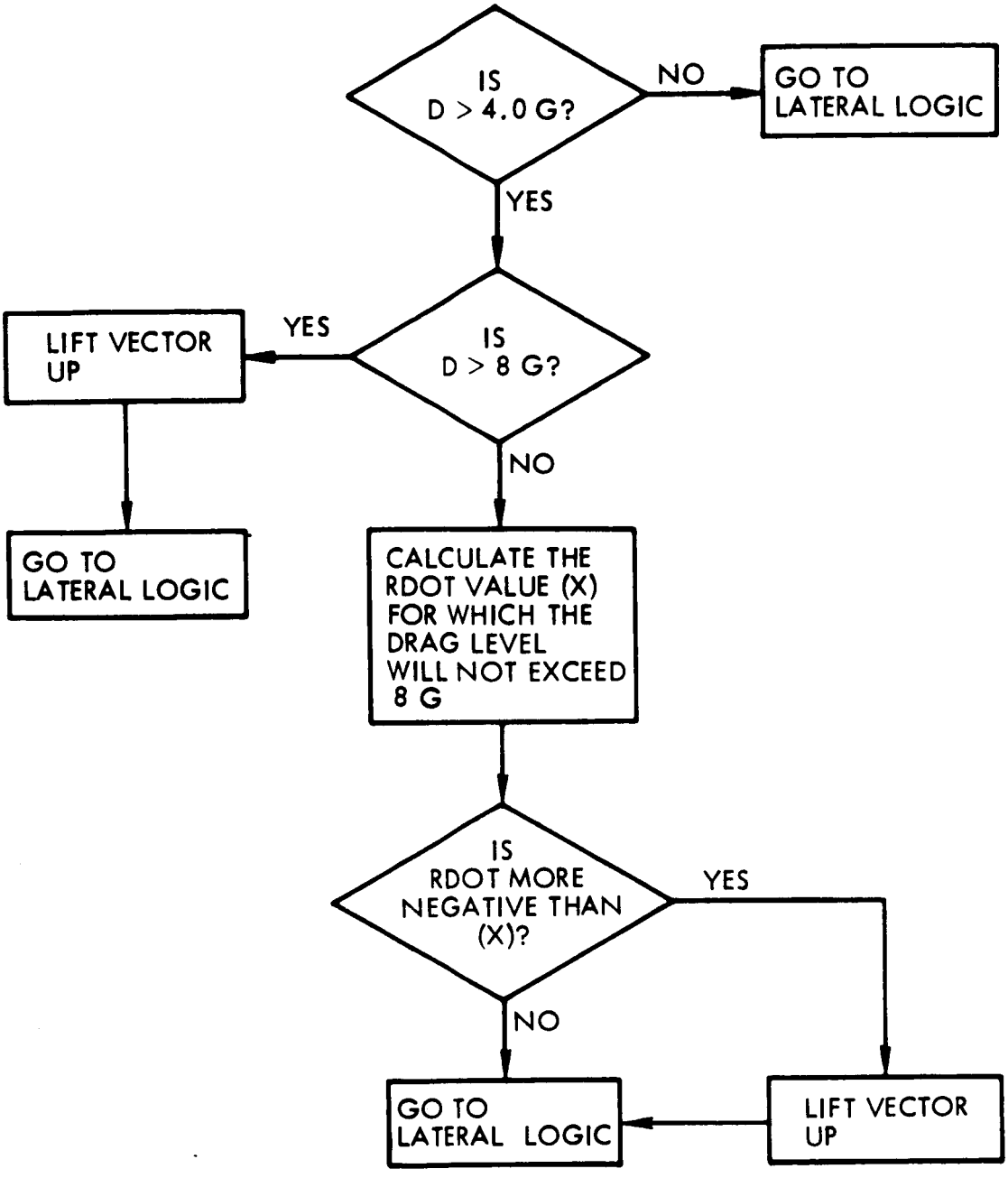

FIGURE AI-14 - G – LIMITER (P67)

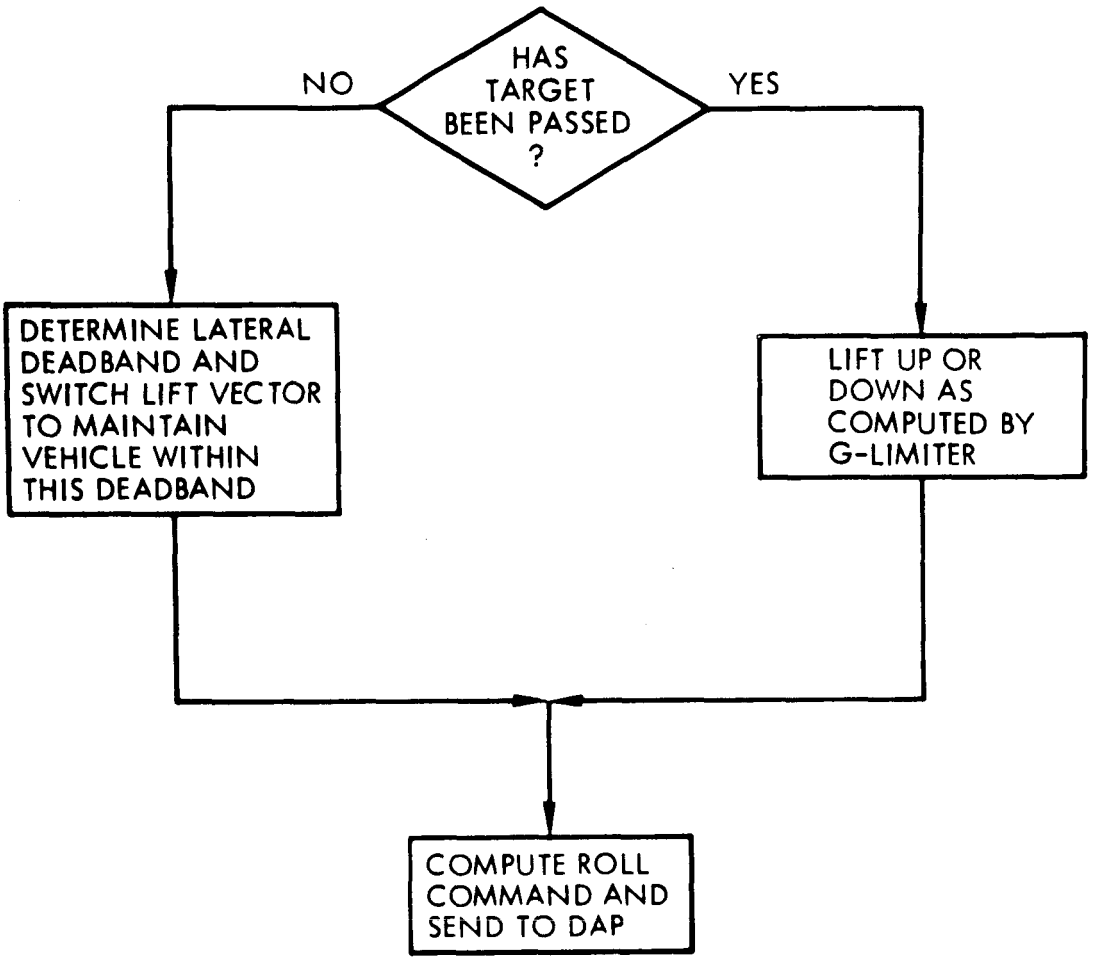

FIGURE AI-15 - LATERAL LOGIC

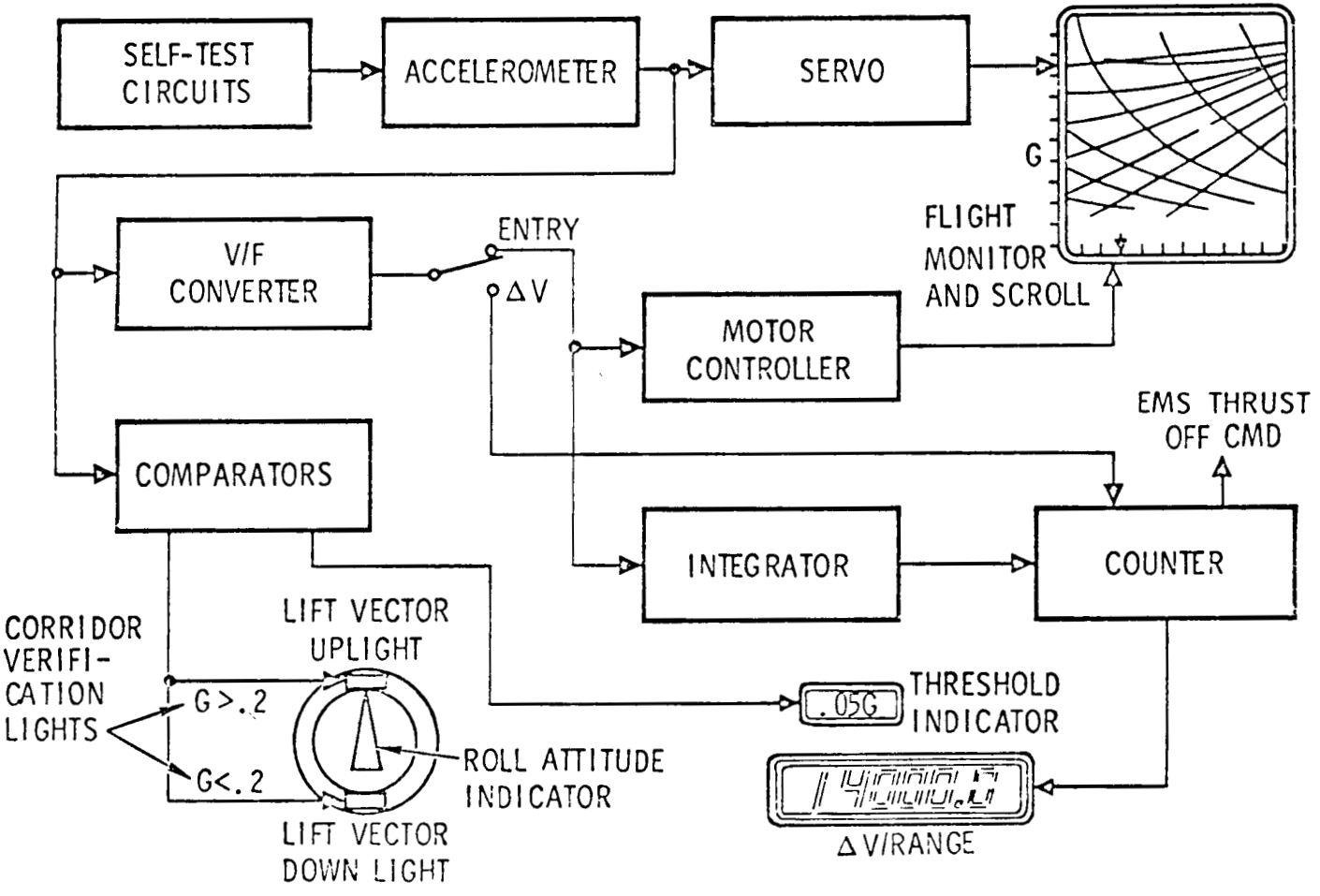

FIGURE AI-16 - EMS BLOCK DIAGRAM

1 ROLL ATTITUDE INDICATOR

2 .05g LIGHT

3 CORRIDOR VERIFICATION LIGHTS

4 FLIGHT MONITOR

5 RANGE-TO-GO COUNTER

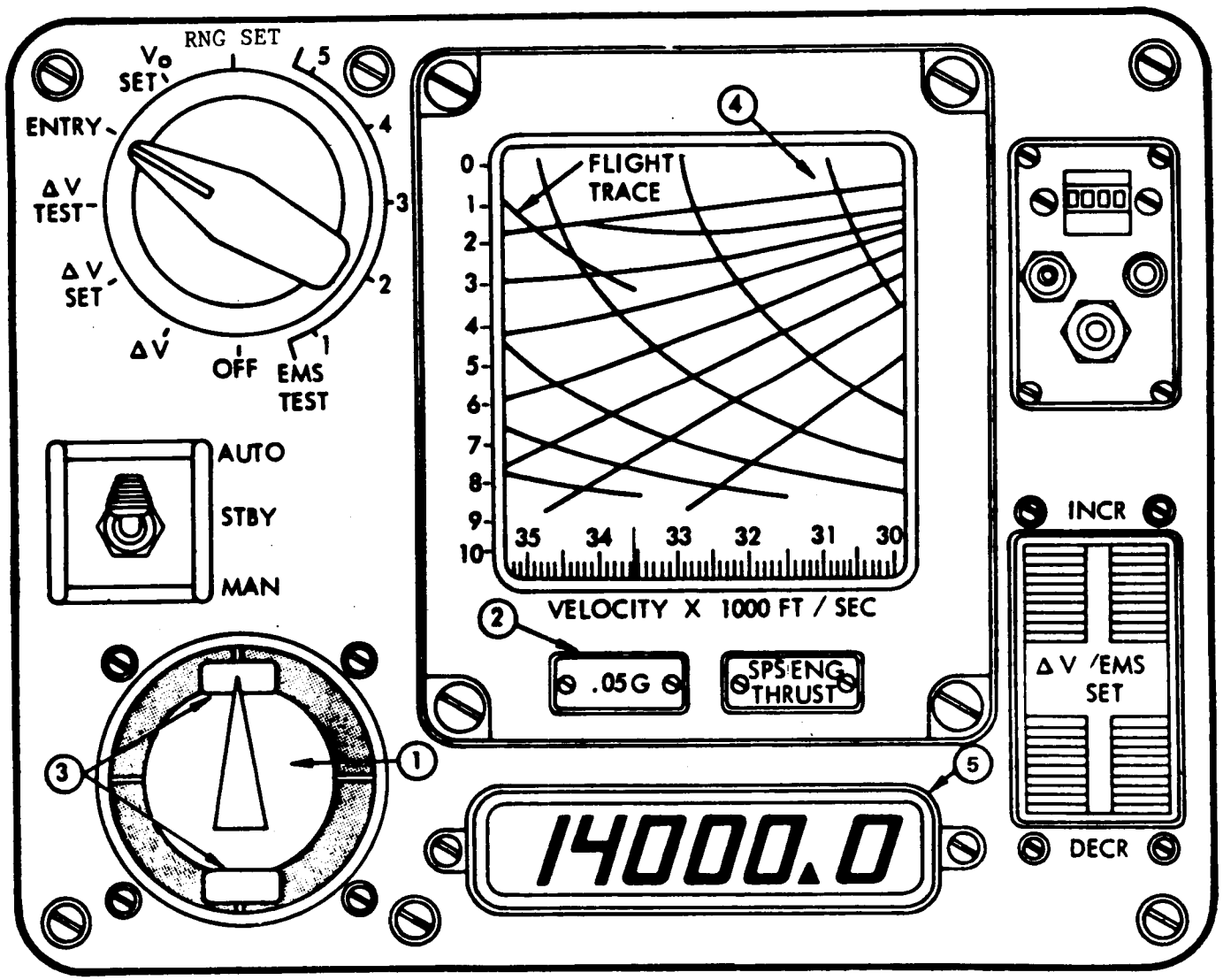

FIGURE AI-17 - EMS FRONT PANEL LAYOUT

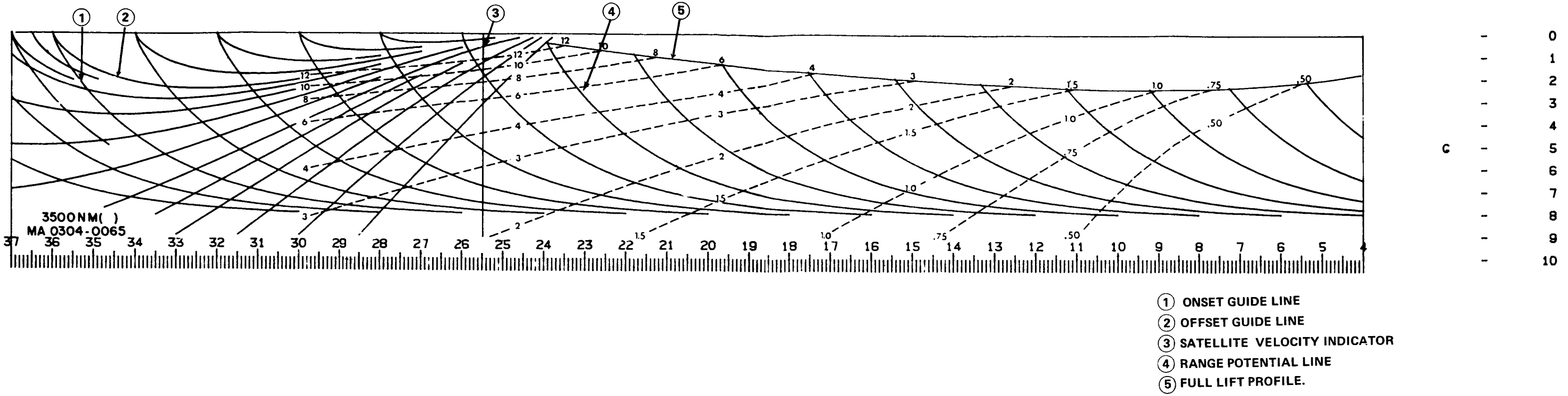

1. ONSET GUIDE LINE
2. OFFSET GUIDE LINE
3. SATELLITE VELOCITY INDICATOR
4. RANGE POTENTIAL LINE
5. FULL LIFT PROFILE.

FIGURE A1-18a - EMS LUNAR NON-EXIT RANGE LIMIT PATTERN (7/22/68)

VELOCITY 36,194.4 FPS
FLIGHT-PATH ANGLE -6.483°
EMS RANGE-TO-GO 1403.3 NM

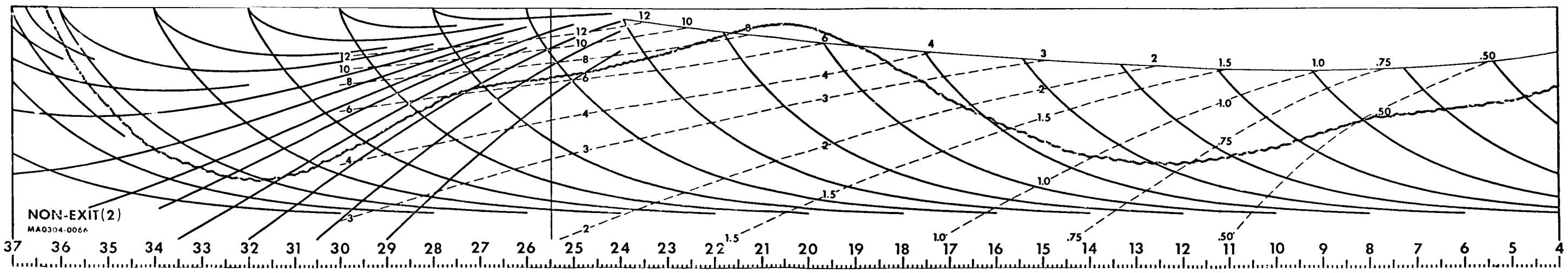

FIGURE A1-18b EMS TRACE GENERATED DURING APOLLO 11 REENTRY

FOLDOUT FRAME 1

FOLDOUT FRAME 2

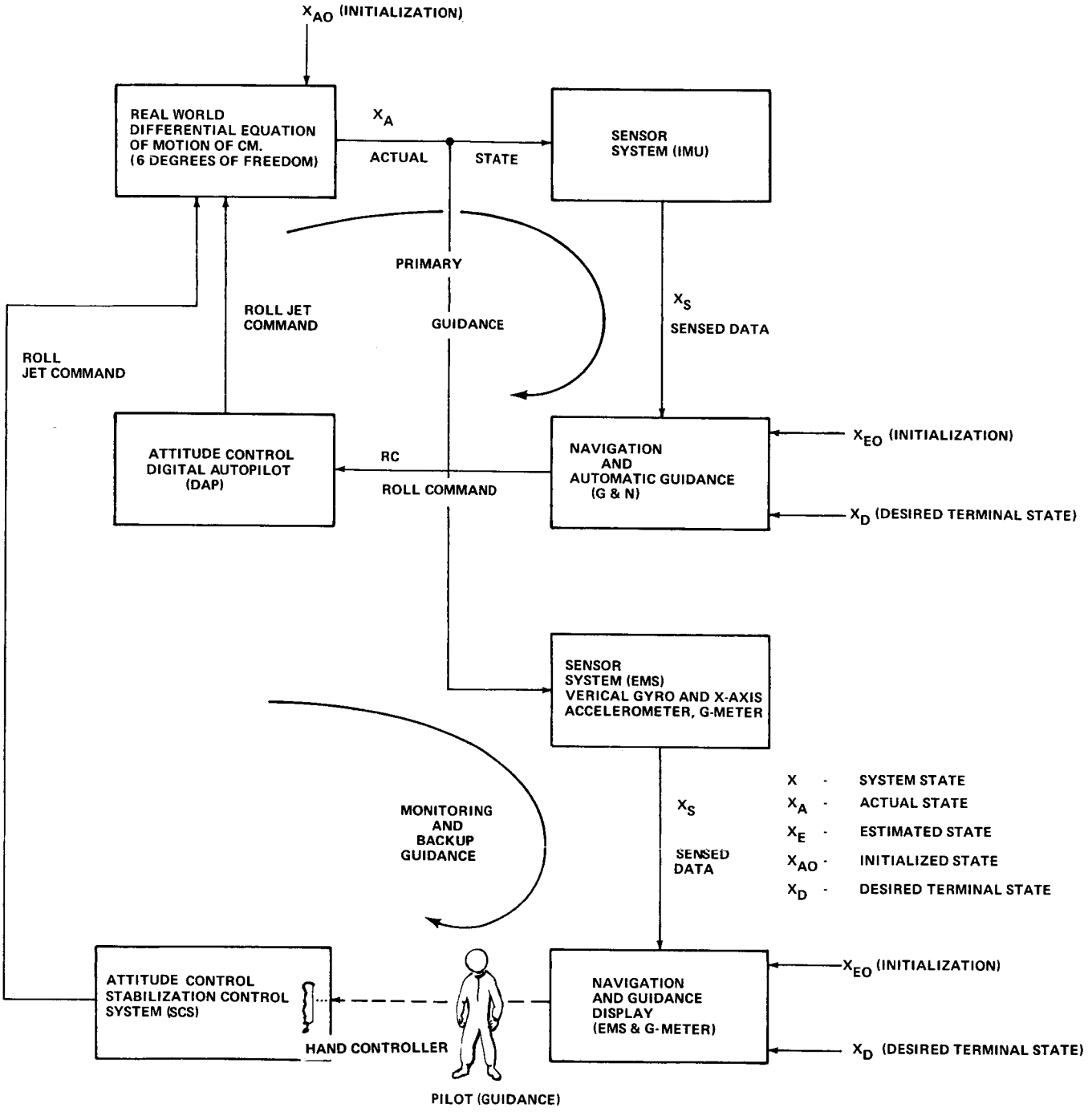

FIGURE A1-19 - SIMULATION SYSTEM BLOCK DIAGRAM

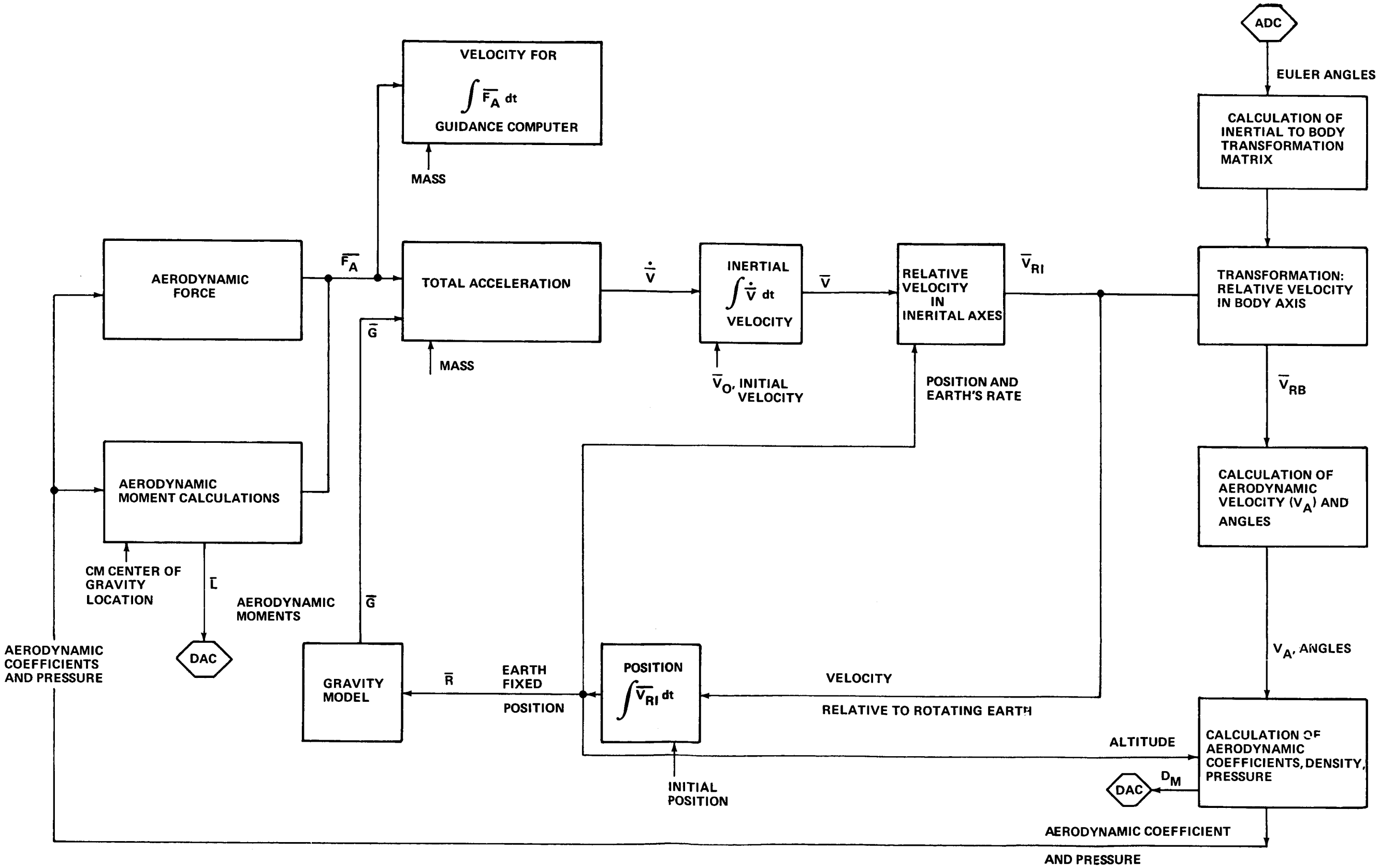

ADC ANALOG TO DIGITAL CONVERTER
DAC DIGITAL TO ANALOG CONVERTER
DM ROTATIONAL DAMPING COEFFICIENT

FOLDOUT FRAME 1

FIGURE AI-20 - DIGITAL SIMULATION OF SPACECRAFT TRANSLATION EQUATIONS OF MOTION

FOLDOUT FRAME 2

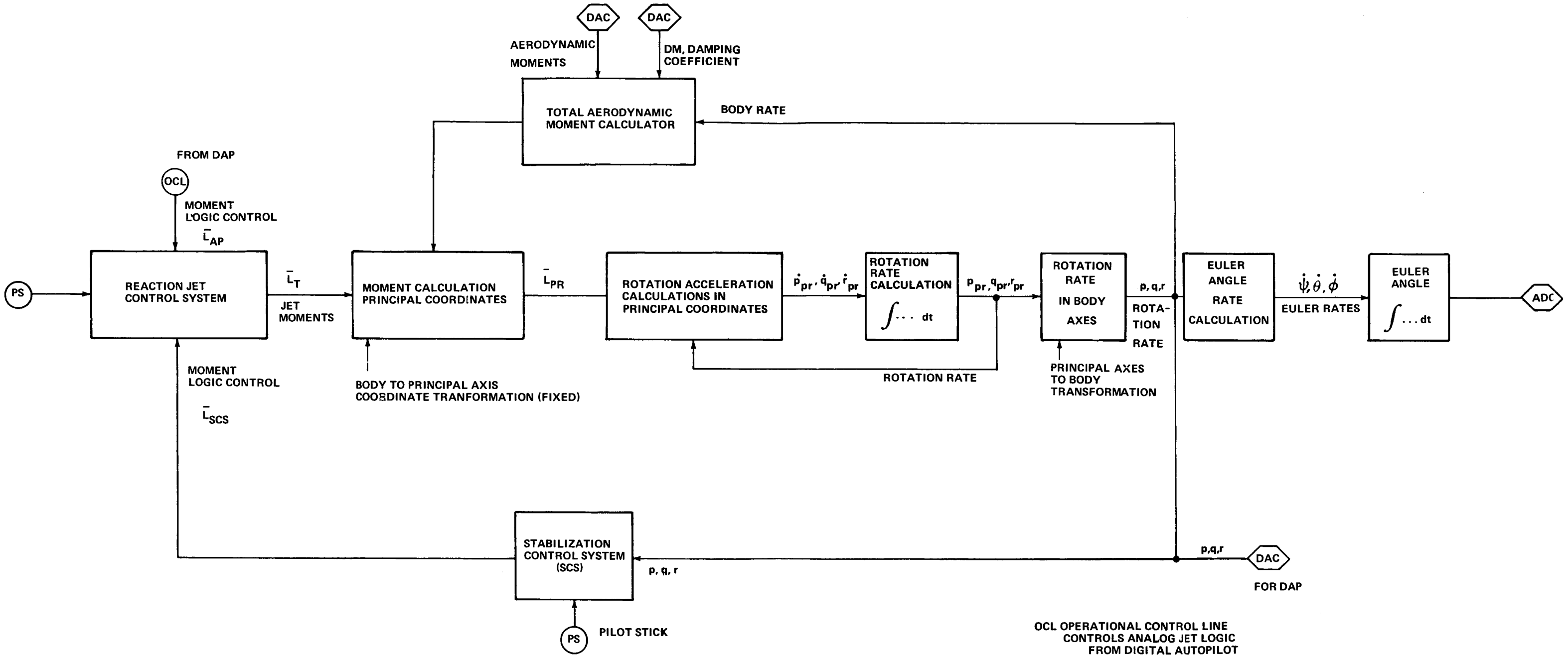

FIGURE AI-21 - ANALOG SIMULATION OF SPACECRAFT ROTATIONAL EQUATIONS OF MOTION

FOLDOUT FRAME 1

FOLDOUT FRAME 2

FIGURE AI-22 - RIGHT SIDE OF HYBRID COMPUTATION CENTER

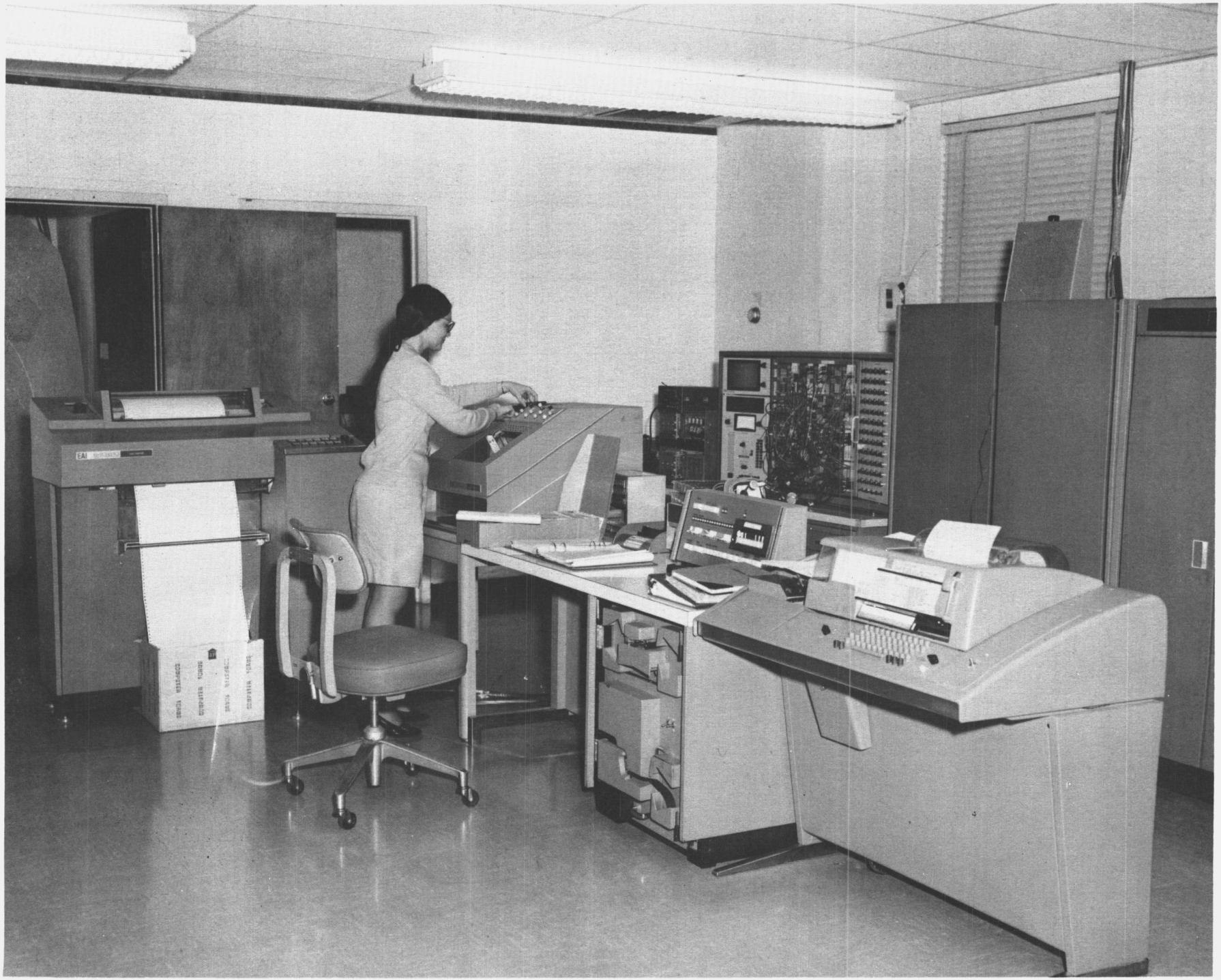

FIGURE AI-23 - LEFT SIDE OF HYBRID COMPUTATION CENTER

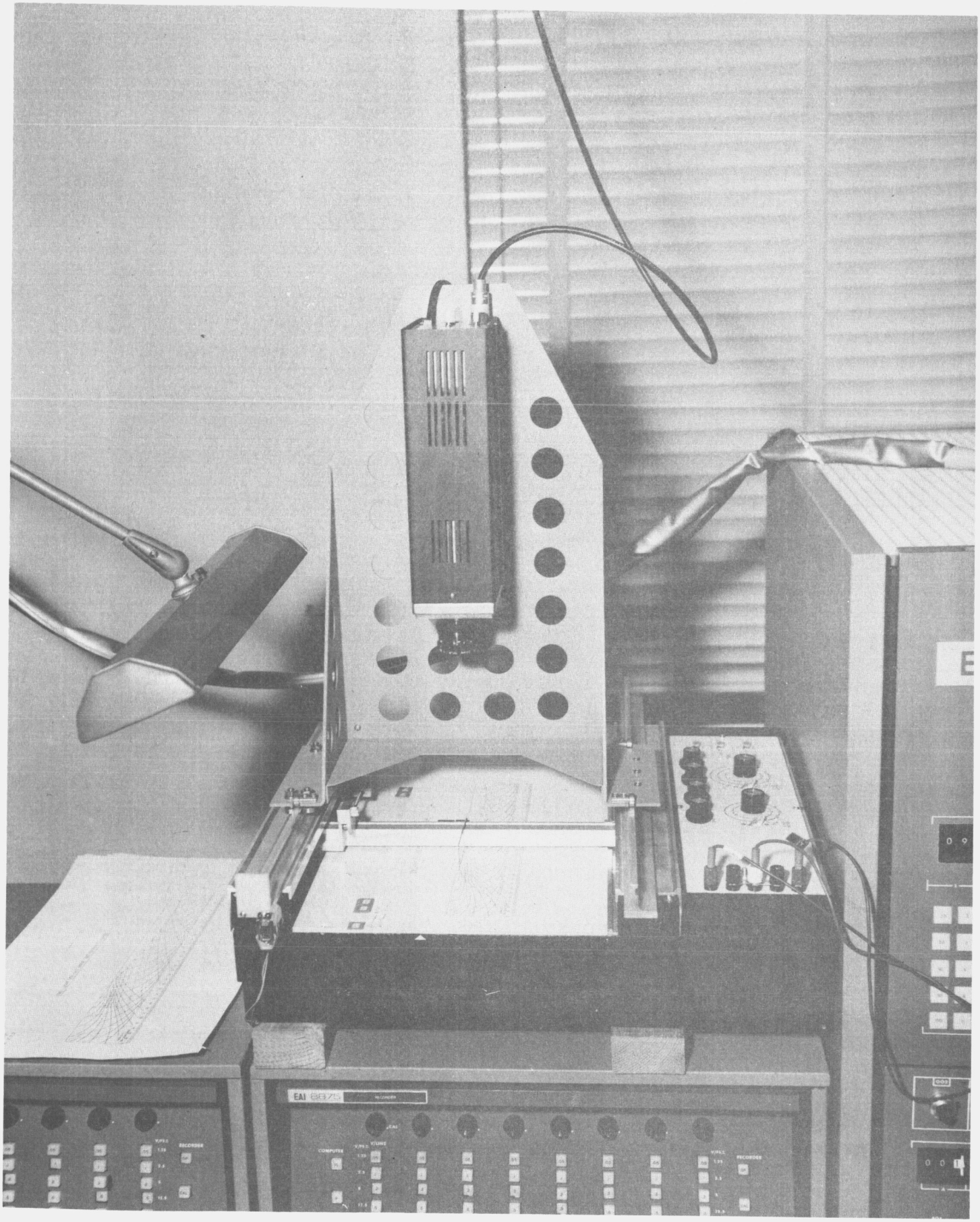

FIGURE AI-24 - ENTRY MONITORING SYSTEM G-V DISPLAY GENERATOR

FIGURE AI-25 - EMS STUDY COCKPIT MOCKUP VIEW OF DISPLAY AND CONTROLS

Appendices 2 and 3

Phase 2 and Phase 3 Results

Appendix 2 contains the G-V traces, trajectory data and pilot comments for each of 60 different entries simulated in Phase 2. Appendix 3 contains similar data for the 44 entries of Phase 3. Because of the quantity of material involved, the appendices are bound separately. What follows are a set of manual SCS/EMS entries and a set of PGNCS entries for nominal lunar return initial conditions. The reader can receive the complete appendices by submitting his request to Mrs. S. B. Watson, Department 2014, Bellcomm, Inc.

PILOT 1

EMS LUNAR NON-EXIT RANGE LIMIT PATTERN (7/22/68)

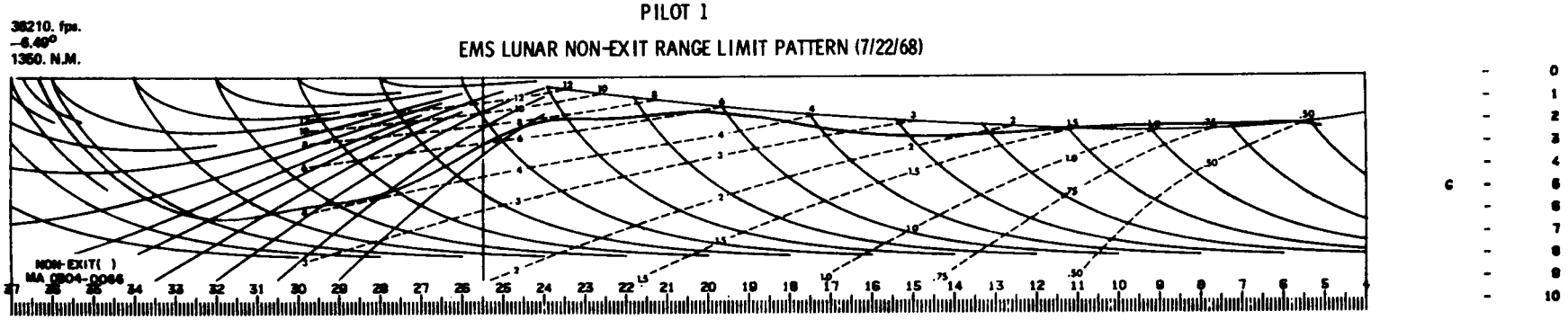

PILOT 2

EMS LUNAR 3500 NM RANGE LIMIT PATTERN (7/22/68)

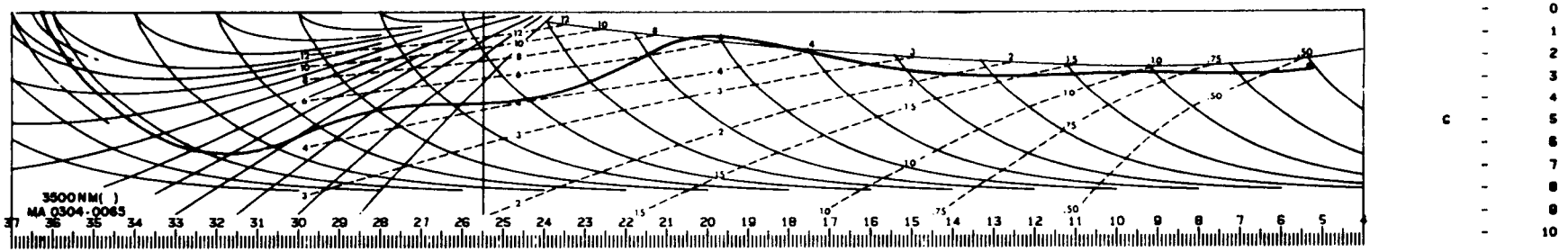

PILOT 3

EMS LUNAR NON-EXIT RANGE LIMIT PATTERN (7/22/68)

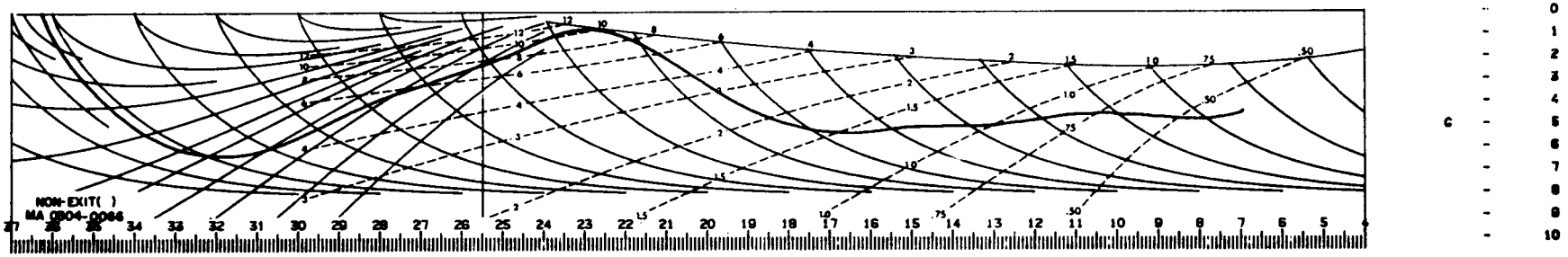

FIGURE A2-6a - PHASE 2 CASE I7

CASE-PILOT	CONTROL MODE	VELOCITY FPS	FLIGHT-PATH ANGLE DEG.	TARGET COORDINATES		DOWN-RANGE ERROR NM	CROSS-RANGE ERROR NM	TOTAL RANGE ERROR NM	EMS RANGE-TO-GO NM	G_{MAX}	G_{MIN}	G AT V_{SAT}	TIME OF FLIGHT .05 G TO 100,000 FT.
		AT 400,000 FT.		LATITUDE DEG.	LONGITUDE DEG.	AT 100,000 FT.							
17-1	SCS/EMS	36210.	-6.49	0.2	22.5	-21.3	-61.6	65.1	38.	6.3	1.9	2.9	407.
17-2	SCS/EMS	36210.	-6.49	0.2	22.5	-28.1	-63.1	69.1	28.	6.3	1.1	4.0	397.
17-3	SCS/EMS	36210.	-6.49	0.2	22.5	-1.2	-54.3	54.3	1.	6.3	0.7	2.3	347.
					MEAN	-16.9	-59.7	62.9					
					RMS	11.4	3.8	6.2					

FIGURE A2-6c - TRAJECTORY DATA

PILOT 2

EMS LUNAR 3500 NM RANGE LIMIT PATTERN (7/22/68)

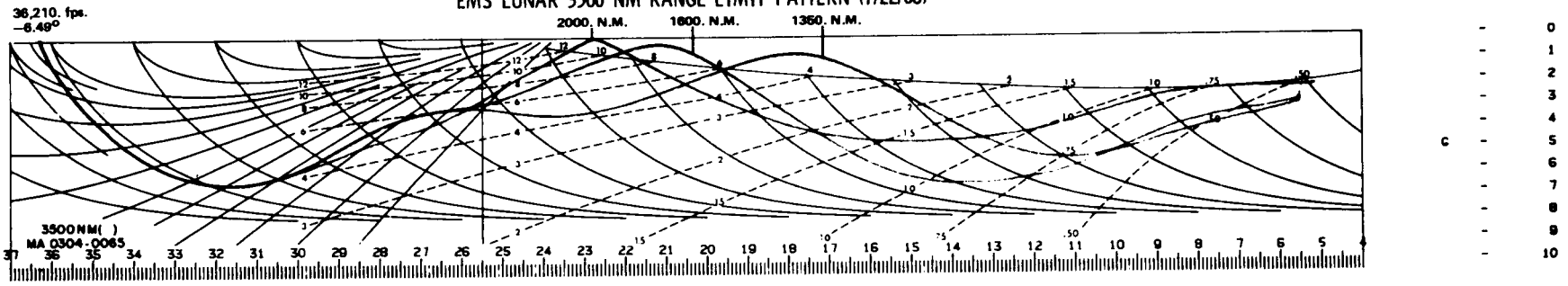

FIGURE A3-Ia - PHASE 3 GUIDED ENTRIES

Appendix 4

Some Comments on Testing a Hypothesis

In testing a hypothesis a wrong decision can be made in two ways: i.) The hypothesis might be rejected when it is true.

ii.) The hypothesis might be accepted when it is false.

In statistical literature i.) is called a type I error and ii.) a type II error. Each of these errors has a probability of occurring associated with it. When a hypothesis is rejected, it is often mentioned that it was rejected at the p level of significance. P is the probability of committing a type I error. The smaller the value of p is, the more confidence we can place in a decision to reject the hypothesis. In the tests performed here, a hypothesis was rejected if $p<.05$. This is an arbitary but commonly accepted level for rejecting a hypothesis. If serious consequences could result from a type I error, an experimenter would not reject a hypothesis unless p had a much smaller value such as $p<.01$ or .001.

Although the probability of a type I error can be given when a hypothesis is rejected (this is actually the criterion for rejection), it is not always possible to give the probability of a type II error for the case of a hypothesis being accepted. This is due to lack of knowledge of an alternative hypothesis if the hypothesis being tested is false. Thus there is generally more confidence that a correct decision has been made when a hypothesis is rejected than when it is accepted.

The Wilcoxon Matched-Pairs Signed-Ranks Test

The Wilcoxon test is useful in determining whether values from one set of data are greater than those of another related set. This test has two attractive features.

a. It does not depend on the underlying distribution of data. Hence even if the data is not normal, the test is still valid.

b. It can test two data sets for differences related to one factor while disregarding effects of other factors. This is done by pairing points of data from each set, keeping all irrelevant factors constant within each pair. For example, in testing

for differences in miss between a range of 1200. and 1350.nm, each miss for the 1200. range is paired with that miss from the 1350. range which has the same pilot, velocity, and flight-path angle. By calculating the signed difference of misses within each of these pairs, it is possible to detect a difference between the distribution of misses for the two ranges.

In this report the Wilcoxon test was slightly modified. It was not used to test for a difference in misses between two ranges, but to test whether this difference exceeded 10.nm. This involved testing the following hypothesis: An increase in range is accompanied by an increase in miss of less than or equal to 10.nm. Rejection of this hypothesis at low p-value gives us good reason to believe that miss increases by more than 10.nm. In the two cases in which this hypothesis was rejected p was less than $10.^{-4}$. Acceptance does not imply that miss does not increase with range. It simply means that it could not be shown statistically that the increase exceeded 10.nm.

The Kolmogorov-Smirnov Test

This test is commonly used in testing hypotheses concerning the underlying distribution of the data. In applying this test for normality, the mean and variance of the assumed normal distribution must generally be known. Because in this report, the mean and variance were estimated from the data, the standard tables could not be used. Fortunately, a recent paper by Lilliefors* gives tables for the case in which estimates may be used in place of the unknown distribution parameters.

A good discussion of the above test requiring a minimum of statistical background can be found in Siegel.**

Plots of the Cumulative Distribution

In addition to applying the Kolmogorov-Smirnov test, the cumulative distributions of down-range and cross-range misses were plotted on probability paper. Examples are presented in

---

*Lilliefors, W. H., "On the Kolmogorov-Smirnov Test for Normality with Mean and Variance Unknown," Journal of the American Statistical Association, Vol. 62, No. 318, pp. 399-403, 1967.

**Siegel, S., Nonparametric Statistics for Behavioral Sciences, McGraw-Hill, 1956.

Figures A4-1a,b and A4-2a,b. Probability paper has the property that plots of the theoretical normal distribution appear as a straight line. Because the plots shown here do not markedly deviate from the straight lines, the data may be assumed to be approximately normal. Using a linear scale for the ordinate, the lines were obtained by performing a least-squares fit on all but the two extreme data points. In a probability plot it is not unusual for the two extreme points to deviate from linearity even when the population is normal.

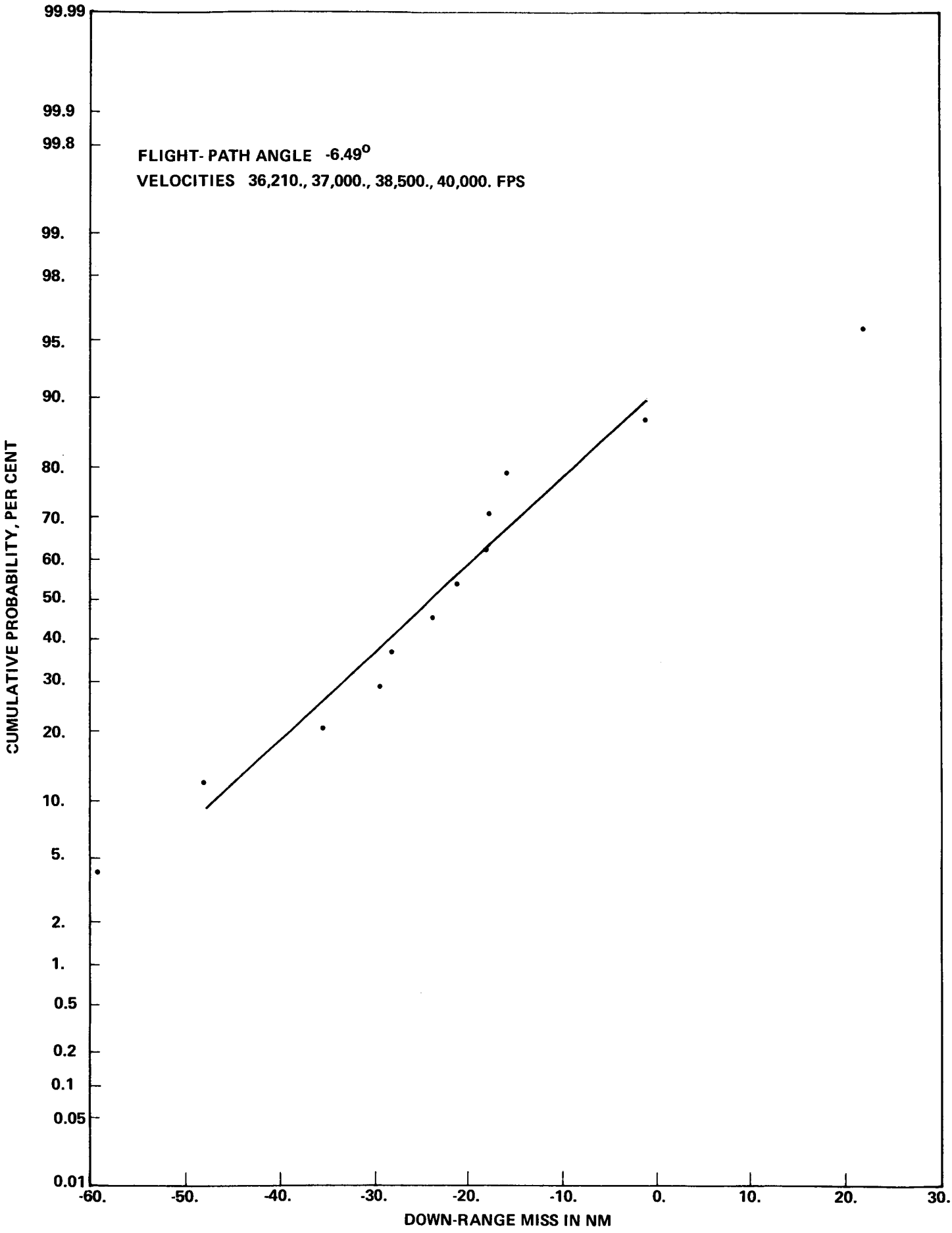

FIGURE A4-1a - CUMULATIVE PROBABILITY DISTRIBUTION FOR DOWN-RANGE MISS FOR A 1350.NM ENTRY (PLOTTED ON NORMAL PROBABILITY PAPER)

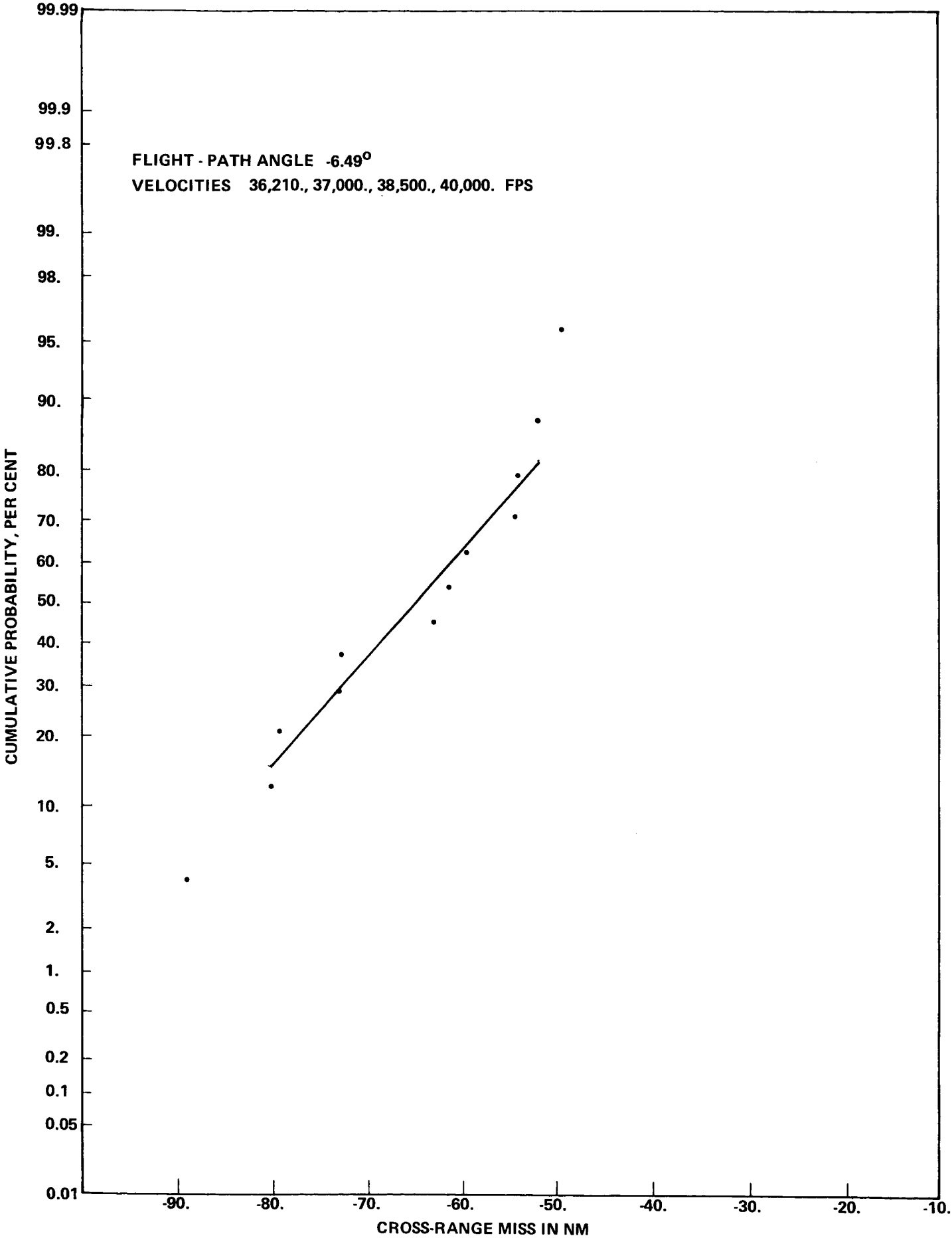

FIGURE A4-1b - CUMULATIVE PROBABILITY DISTRIBUTION FOR CROSS-RANGE MISS FOR A 1350. NM ENTRY (PLOTTED ON NORMAL PROBABILITY PAPER)

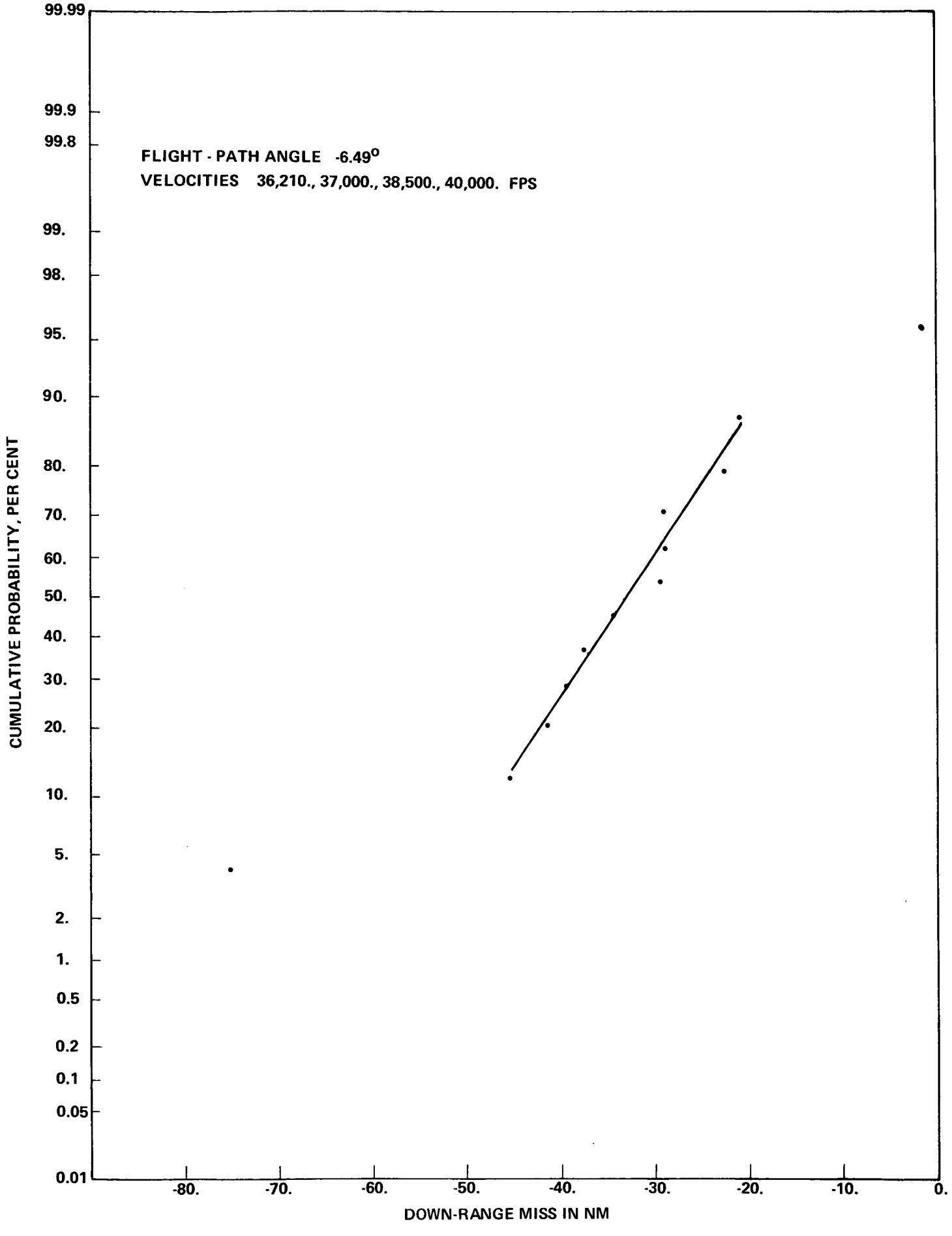

FIGURE A4-2a - CUMULATIVE PROBABILITY DISTRIBUTION FOR DOWN-RANGE MISS FOR A 1600. NM ENTRY (PLOTTED ON NORMAL PROBABILITY PAPER)

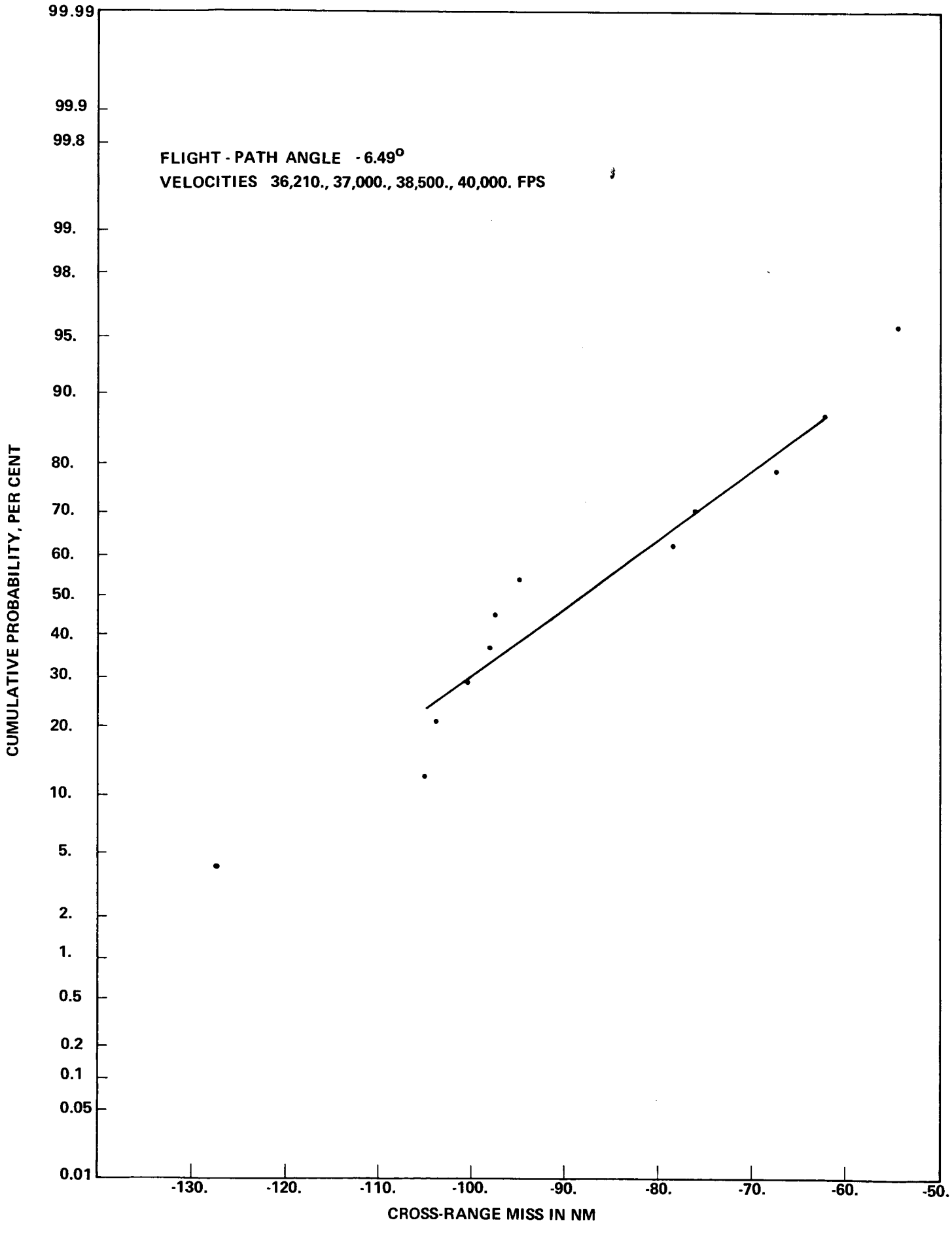

FIGURE A4-2b - CUMULATIVE PROBABILITY DISTRIBUTION FOR CROSS-RANGE MISS FOR A 1600. NM ENTRY (PLOTTED ON NORMAL PROBABILITY PAPER)

BELLCOMM, INC.

DISTRIBUTION LIST

Complete Memorandum to

NASA Headquarters

T. A. Keegan/MA-2
R. A. Petrone/MA

Manned Spacecraft Center

J. W. Bilodeau/CF2
J. K. Burton/FM2
D. C. Cheatham/EG2
C. M. Duke/CB
R. M. Edwards/FM2
R. E. Ferland/FM2
D. W. Gilbert/EG27
R. F. Gordon/CB
C. A. Graves/FM2
J. C. Harpold/FM2
D. W. Heath/FM2
J. E. I'anson/FC
P. C. Kramer/CF24
M. K. Lake/CF131
W. J. North/CF
H. G. Patterson/EG27
C. H. Paulk, Jr./EG27
J. Rogers/FM2
D. K. Slayton/CA

Bellcomm, Inc.

A. P. Boysen, Jr.
W. G. Heffron
J. Z. Menard
R. L. Wagner
M. P. Wilson
Department 1024 File
Central Files
Library

Memorandum to without Appendices

Bellcomm, Inc.

D. R. Anselmo
W. L. Berger
H. J. Bixhorn
J. O. Cappellari, Jr.
K. R. Carpenter
D. A. Corey
T. H. Crowe
D. A. DeGraaf
J. P. Downs
D. R. Hagner
C. M. Harrison
T. B. Hoekstra
B. T. Howard
D. B. James
V. S. Mummert
B. G. Niedfeldt
I. M. Ross
F. N. Schmidt
R. V. Sperry
A. W. Starkey
W. Strack
J. W. Timko